Acta Universitatis Szegediensis

Acta Biologica Szegediensis

Volume 59, Suppl. 3, 2015

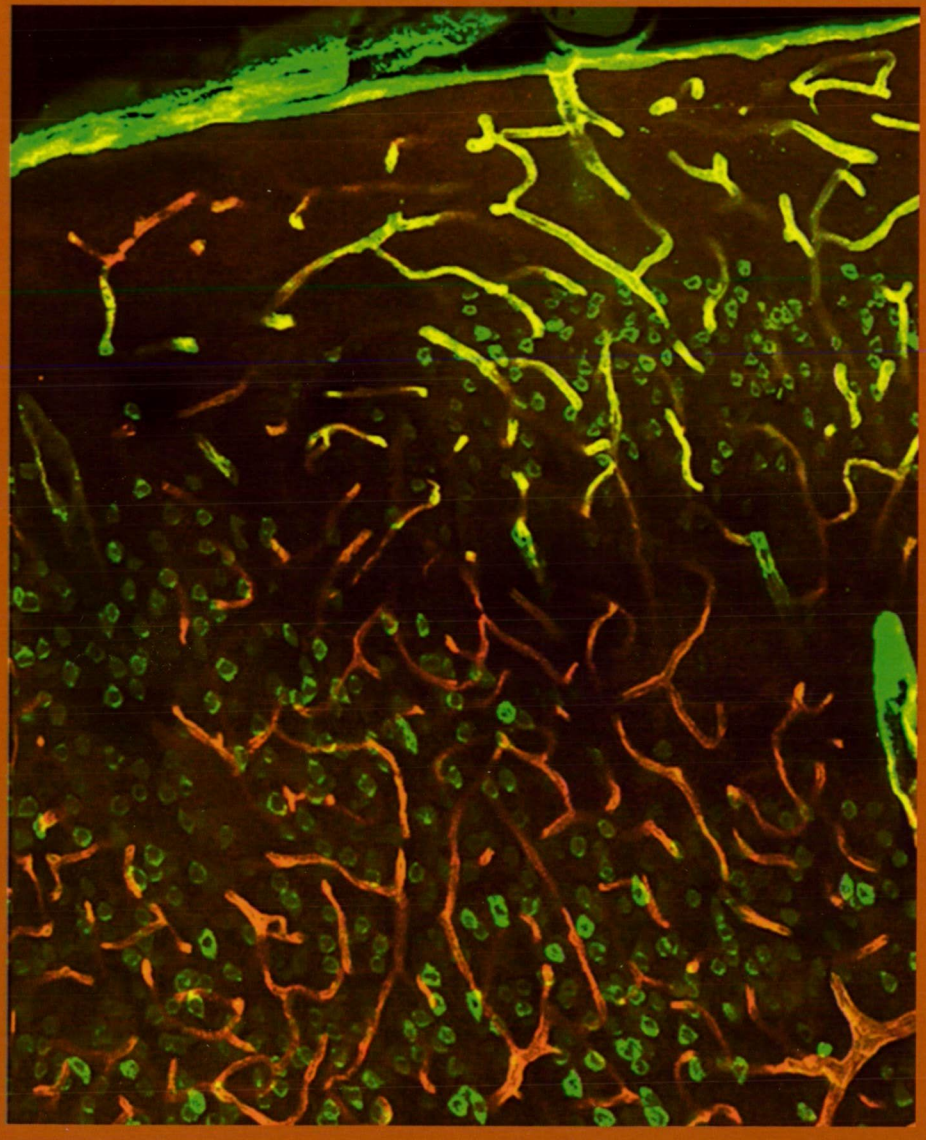

University of Szeged, Szeged, Hungary

ACTA BIOLOGICA SZEGEDIENSIS

VOLUME 59(SUPPL. 3), 2015

Table of Contents

Articles

On the cover: A merge picture of double labeling for laminin and β-dystroglycan following immediate post-lesion fixation (see: Tóth et al. in this issue).

Volume 59(Suppl.3):341-343, 2015
Acta Biologica Szegediensis
http://www2.sci.u-szeged.hu/ABS

ARTICLE

Congenital external auditory canal atresia and methods of rehabilitation

Ádám Perényi*, Attila Nagy, József Géza Kiss, László Rovó

Department of Otorhinolaryngology, Head and Neck Surgery, Albert Szent-Györgyi Clinical Center, University of Szeged, Hungary

ABSTRACT Congenital external auditory canal atresia is a disorder with a prevalence of one in 10 000-20 000 live births and is bilateral in one third of the patients. With a conductive hearing loss of 60 dB, even unilateral atresia restricts hearing related social skills. The degree of middle ear deformity may make reconstruction surgery impossible or too hazardous, thus bone-conduction hearing aids have become the first-line therapy. Children with unilateral cartilaginous and bony external auditory canal atresia were enrolled. High-resolution computed tomography with three dimensional reconstructions were made. Reconstruction surgery from retroauricular approach comprised maximal enlargement of the tympanic and mastoid cavities and their closure with adapted conchal cartilage. Hearing improvement reached the level above the social threshold. The auditory canal remained stable and widely patent and facial nerve function was unremarkable. The authors highlight that surgical reconstruction of the external auditory canal is possible in selected cases. The procedure is safe and effective with a reasonably short surgical time, if it is supported by deep anatomical knowledge, careful preoperative imaging and intraoperative facial nerve monitoring. Stable audiological benefits improve patients' satisfaction and quality of life. If reconstruction surgery is not possible, bone-conduction hearing aids are beneficial.
Acta Biol Szeged 59(Suppl.3):341-343 (2015)

KEY WORDS

bone-conduction hearing aids
external auditory canal atresia
reconstruction
3D imaging

Introduction

Congenital external auditory canal atresia is a disorder with a prevalence of one in 10 000-20 000 live births and is bilateral in one third of the patients. It is characterized by complete or incomplete bony atresia of the external auditory canal. Being a complex developmental disorder of the temporal bone, it can be associated with malformations (*e.g.,* malformation of the ossicles, hypoplasia of the tympanic and mastoid cavities, malformation of the temporomandibular joint, and microtia) (Jahrsdoerfer 1978). The facial nerve may be variable in structure and position (Tasar et al. 2007). Conductive hearing loss of 60 dB is typical. If unilateral, hearing and speech development is usually normal or near normal. In bilateral atresia, speech development is compromised and this condition requires therapy in an early age.

A preferable therapy is surgical repair of the missing external auditory canal. Due to the developmental degree of the mastoid and tympanic cavities, the absence of anatomical landmarks, the variety in the shape and position of the anatomical structures, abnormal position of the facial nerve and structural deformities of the ossicles, reconstruction surgery is difficult and hazardous (Kesser 2010). Because of the good cost-benefit ratio, bone-conduction hearing aids have become the first-line therapy in very low age and in those cases in which the surgical outcome is doubtful. Bone-conduction hearing aids include non-implantable and implantable, percutaneous and transcutaneous, active or passive systems.

Surgical repair of the missing external auditory canal has some fundamental requirements. When planning surgery one has to pay attention to the position of the facial nerve and the tympanic tegmen, the anatomy of ossicles (stapes and malleus-incus complex), the pneumatisation and spatial development of the tympanic and mastoid cavities, the development of the oval and round windows (Kesser 2010). Jahrsdoerfer et al. (1992) published a scoring system which helps to predict postoperative hearing outcome and assist in determining surgical candidacy (Shonka et al. 2008). During the removal of excess bone with a burr, the normal anatomical landmarks are missing, thus injury to the facial nerve is a real danger. Even experienced surgeons need long time to visualize and avoid the structures at risks. Meticulous preoperative assessment of the shape and position of the facial

Submitted June 15, 2015; Accepted July 30, 2015
*Corresponding author. E-mail: perenyi.adam@med.szote.u-szeged.hu

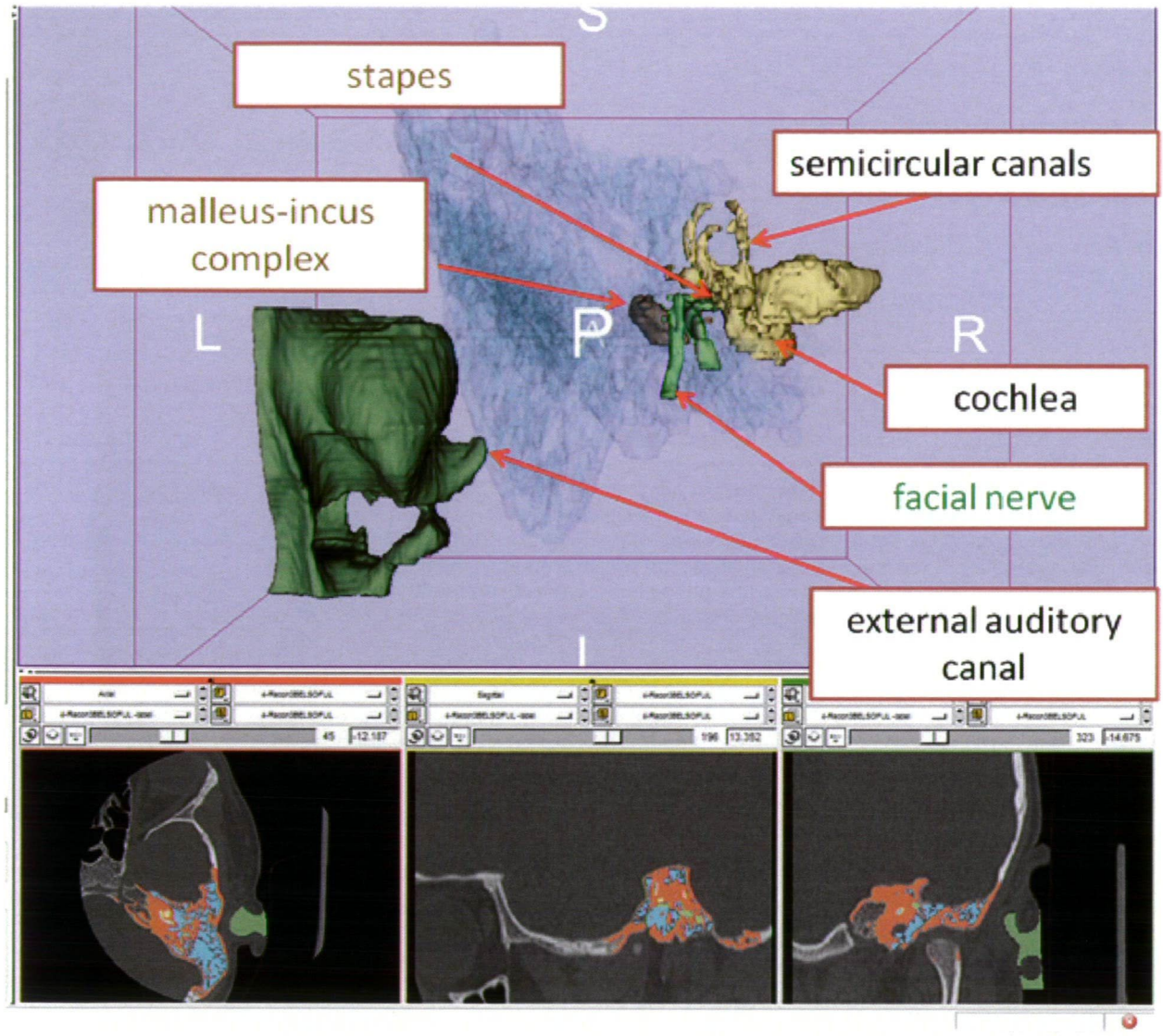

Figure 1. Three dimensional CT reconstruction of the external, middle, and inner ear of the ear with external auditory canal atresia. 3D Slicer 4.3.

nerve with imaging diagnostics is crucial, because the facial nerve has been reported to be abnormal in position in 25 to 52% of atresia patients, its bony canal can be dehiscent and abnormal bifurcation has also been seen (Chang et al. 1994; Jahrsdoerfer and Lambert 1998).

Materials and Methods

Two 6-year-old subjects with unilateral congenital external auditory canal atresia have been enrolled. Apart from minor anomalies of the pinna, the external ears were unremarkable. Unilateral conductive type hearing loss of 60 dB with normal contralateral hearing level was seen in both subjects. Both subjects were trained by speech therapists due to minor articulation issues.

In order to make successful surgical planning, reconstruction images were made, in that the preoperative CT reconstructions were generated with 3D Slicer (a free and open-source imaging software from high resolution, non-enhanced axial CT images (DICOM) of the head with ear protocol. 3D Slicer was used in visualizing anatomical structures by three-dimensional reconstructions of the trachea and this was successfully applied in the surgical reconstruction of a critical case (Furák et al. 2011; Perényi et al. 2014).

By showing the structures of the external, middle, and inner ear we aimed to provide the ear surgeon with inevitable information about the anatomical landmarks, the absolute and relative three-dimensional anatomy of the anatomical structures with focus on the facial nerve and the ossicles (Fig. 1) (Perényi et al. 2014).

Surgical repair from retroauricular approach comprised maximal enlargement of the tympanic and mastoid cavities and their closure with adapted conchal cartilage. Hearing improvement reached the level above the social threshold. The auditory canal remained stable and widely patent and facial nerve function was preserved. Stable audiological benefits improved the patients' quality of life.

Results

Both patients had congenital external auditory canal atresia. Reconstruction surgery was predicted to be effective based on the Jahrsdoerfer grading system (Jahrsdoerfer et al. 1992). Preoperative CT reconstructions demonstrated slight hypoplasia of the mastoid cavities in both cases. The mastoid and tympanic cavities were air-containing. Bony atresia was found in both cases. The tympanic membrane and handle of the malleus were absent, but the rest of the ossicular chain, although malformed (malleus-incus complex and stapes) were present. The inner ear was unremarkable and the round window was open. The position of the facial nerve was near normal in both cases, although bifurcation in the mastoid section was seen in case 2. The position of tympanic section of the facial nerve (slightly but always medial to the malleus-incus complex) allowed for straightforward and quick surgical preparation until the malleus-incus complex was reached without putting the facial nerve into risk. The latter was assisted with a facial nerve monitoring system.

Discussion

Careful selection of candidates for surgery is paramount. In the authors' opinion when considering surgical repair of external auditory canal atresia it is inevitable to have high quality, high resolution CT scans of the ears, which enable accurate reconstructions in each conventional (axial, coronal, and sagittal) and any non-conventional plane. Three-dimensional reconstructions give further important information about the spatial relationship of the anatomical structures at risk. By applying the appropriate criteria (*e.g.*, the Jahrsdoerfer grading system) together with thorough imaging the result of surgery can be predicted and an individual surgical plan can be set up. This method renders straightforward visual information to the surgeon, thus, based on the preoperative plans, the surgical procedure can be conducted quickly and with low risk.

References

Chang SO, Min YG, Kim CS, Koh TY (1994) Surgical-management of congenital aural atresia. Laryngoscope 104:606-611.

Furák J, Szakács L, Nagy A, Rovó L (2011) Multiple costal cartilage graft reconstruction for the treatment of a full-length laryngotracheal stenosis after an inhalation burn. Interact Cardiovasc Thorac Surg 13:453-455.

Jahrsdoerfer RA, Lambert PR (1998) Facial nerve injury in congenital aural atresia surgery. Am J Otol 19:283-287.

Jahrsdoerfer RA, Yeakley JW, Aguilar EA, Cole RR, Gray LC (1992) Grading system for the selection of patients with congenital aural atresia. Am J Otol 13:6-12.

Jahrsdoerfer RA (1978) Congenital atresia of the ear. Laryngoscope 88:1-48.

Kesser BW (2010) Repair of congenital aural atresia. Oper Techn Otolaryngol 21:278-286.

Perényi A, Nagy A, Kiss JG, Rovó L (2014) Képi rekonstrukciók szerepe fülműtétekben, fülfejlődési rendellenesség esetében. In Bari F, Almási L, eds., Orvosi Informatika 2014: A XXVII Neumann Kollokvium Konferenciakiadványa, 127-130 [*in Hungarian*].

Shonka DC, Livingston WJ, Kesser BW (2008) The Jahrsdoerfer grading scale in surgery to repair congenital aural atresia. Arch Otolaryngol Head Neck Surg 134:873-877.

Tasar M, Yetiser S, Yildirim D, Bozlar U, Tasar MA, Saglam M, Ugurel MS, Battal B, Ucoz T (2007) Preoperative evaluation of the congenital aural atresia on computed tomography; an analysis of the severity of the deformity of the middle ear and mastoid. Eur J Radiol 62:97-105.

Volume 59(Suppl.3):345-352, 2015
Acta Biologica Szegediensis
http://www2.sci.u-szeged.hu/ABS

ARTICLE

Histological structure of the human and rodent periodontium

András Mihály[1]*, Eszter Mihály[2]

[1]Department of Anatomy, Histology and Embryology, Faculty of Medicine, University of Szeged, Szeged, Hungary
[2]Medicover Eiffel Dental Clinic, Budapest, Hungary

ABSTRACT Adult human dental tissue and young rat jaws with developing teeth were investigated. The tissues were fixed by immersion in 4% buffered paraformaldehyde. Decalcified tissues were embedded into paraffin or sectioned on a freezing microtome. Paraffin sections were stained with hematoxylin and eosin. Frozen sections were stained with calcitonin gene-related peptide (CGRP) antibodies using avidin-biotin systems and peroxidase labelling. The histology of the acellular cement and the histology of the periodontal ligament were analyzed and the course of the Sharpey-fibers and the epithelial rests of Malassez were described in human samples. The epithelial sheath of Hertwig in developing rat maxillae and mandibles (postnatal days 1-11) were depicted. The layers of the Hertwig-sheath were described. We observed the numerical increase of CGRP-stained nerve fibers during these postnatal days. The CGRP-stained nerve fibers appeared before the development of the dental root indicating the presence of growth factors which guide the sensory axons. We hypothesize that the epithelial sheath of Hertwig plays essential role in the development of cementoblasts, periodontal fibroblasts and alveolar osteoblasts. Furthermore, the growth factors secreted by the Hertwig-sheath may stimulate the axonal growth, too. **Acta Biol Szeged 59(Suppl.3):345-352 (2015)**

KEY WORDS
dental cement
Hertwig-sheath
immunohistochemistry
periodontal ligament
sensory nerve

Introduction

The periodontium or tooth-bed is a complex structure of hard- and soft tissues supporting the teeth. It consists of the cement covering the tooth, the periodontal ligament, the alveolar bone and the gums or gingiva. The periodontium participates in the fixation of the teeth, participates in the absorption of the root of the deciduous teeth, in the regeneration of the cement and in sensory reflexes which regulate masticatory movements, just to mention the most important functions (Gera 2005). The diseases of the periodontium are manyfold, affecting every structural element and they are treated in clinical subject of periodontology (Gera 2005).

The cement is modified bone tissue, containing cells called cementocytes. The upper part of the cement, close to the tooth neck, does not contain cells: this is the acellular cement. The acellular cement is mainly for the anchorage of the Sharpey-fibers originating from the periodontal membrane. The cellular cement is a layered tissue: according to the layers the collagen fibers of the matrix are arranged circularly and/or longitudinally (Yamamoto et al. 2010). The cellular cement increases in thickness with age: generally it is thickest at the apex of the root. The periodontal ligament/membrane fills the gap between the cement and the alveolar bone. It is rich in cells some of which are undifferentiated stem cells (Volponi et al. 2010). The periodontal membrane is richly vascularized and contains several sensory nerve endings (Hattyasi 1982). The alveolar bone has fine, lamellar structure and a cell-rich periosteum with osteoblasts and osteoclasts (Harokopakis-Hajishengallis 2007). The bone is traversed by minute openings for blood vessels and nerves. The gingiva is a special mucous membrane covered by stratified squamous epithelium which may show parakeratosis. The gingival connective tissue is rich in sensory nerve endings. The periodontal tissues constitute a morphological and functional unit – their diseases often lead to teeth loss (Gera 2005). We illustrate the main morphological-histological components of the periodontium on Figure 1.

The periodontium has a multiple, rich blood supply. Blood vessels originate from the sublingual artery (branch of the lingual artery), from the inferior alveolar artery and the superior alveolar arteries (branches of the maxillary artery), from the descending palatine artery and from the facial artery. Veins are draining into the facial vein, lingual vein and retromandibular vein (Liebgott 2001). The sensory nerves of the periodontium originate from the maxillary- and mandibular divisions of

Submitted June 15, 2015; Accepted July 30, 2015
*Corresponding author. E-mail: mihaly.andras@med.u-szeged.hu

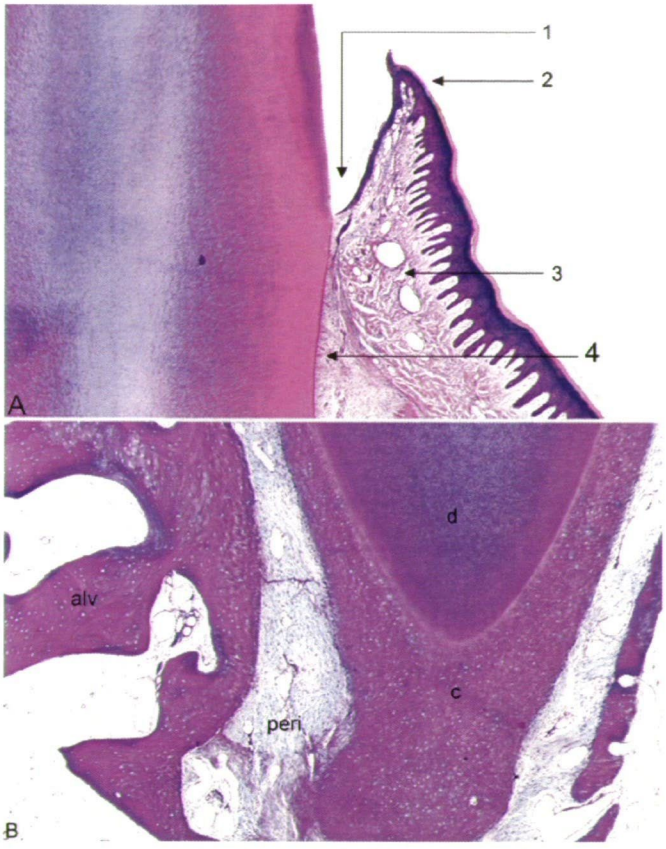

Figure 1. Histological section of an incisor tooth of a Rhesus monkey (from the histological collection of the Department of Anatomy, Histology and Embryology (Faculty of Medicine, University of Szeged, Szeged, Hungary), displaying the elements of the periodontal apparatus. Decalcificated tissue, hematoxylin-eosin staining. A: the gingiva at the neck of the tooth. The enamel was dissolved during the decalcification, therefore, the gingival sulcus (1) is larger, than *in vivo*. The marginal gingiva/gingival crest (2), the lamina propria (3) and the periodontal membrane (4) are visible. B: higher magnification shows the alveolar bone (alv), the periodontal ligament (peri), the cement (c) and the dentine (d) of the apical region of the tooth. Magnification: 10x (A) and 20x (B).

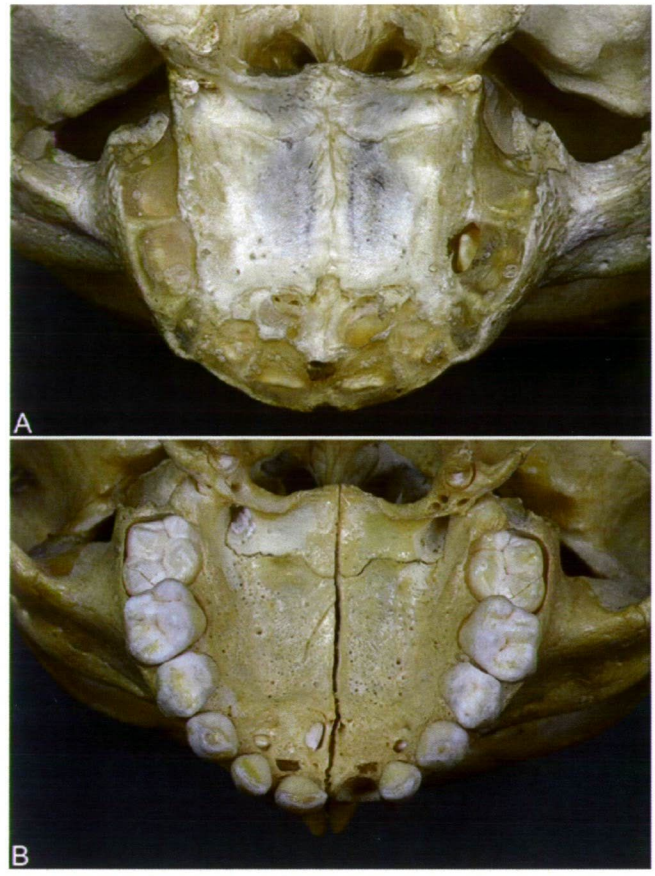

Figure 2. The upper dental arch in newborn (A) and 7 years old boy (B). The alveolar process of the maxilla is not developed in the newborn human; the deciduous teeth are located in the alveolar sockets covered by a dense connective tissue membrane. B: the first permanent molar is just before eruption. Deciduous teeth and alveolar processe are well developed. The palatine sutures are also visible.

the trigeminal nerve. The nerve endings are nociceptors and mechanoreceptors (Hattyasi 1982).

The aim of this work was to describe the anatomical and histological features of the human periodontium, using human skull and teeth samples and histological sections of extracted human teeth. The developmental aspects of the periodontium was investigated in rat pups, on the histological sections of the developing maxillae, mandibles, lower and upper teeth.

Material and Methods

Gross anatomy observations were carried out on human skulls and human permanent teeth: the skulls and teeth are properties of the anatomy specimen collection of the Department of Anatomy, Histology and Embryology (Faculty of Medicine, University of Szeged, Szeged, Hungary). The skulls and other bones were prepared by the technicians of the department during the years 1947-1966, according to the prevailing laws and ethical regulations of the Szeged Medical University (Mihály et al. 2014). The bones are stored in the museum of the department (Mihály et al. 2014). The bony structures of the dental alveoli (including the teeth) were photographed with MicroPublisher 5.0 RTV digital camera attached to a Nikon SMZ800 stereomicroscope (Nikon, Japan).

The collection of the histological sections of the extracted human teeth is the property of the Department of Anatomy, Histology and Embryology (Faculty of Medicine, University of Szeged, Szeged, Hungary). The extracted human teeth were obtained from the Dentistry Clinic of the Medical University in years 1982-1990. The ethical permission was

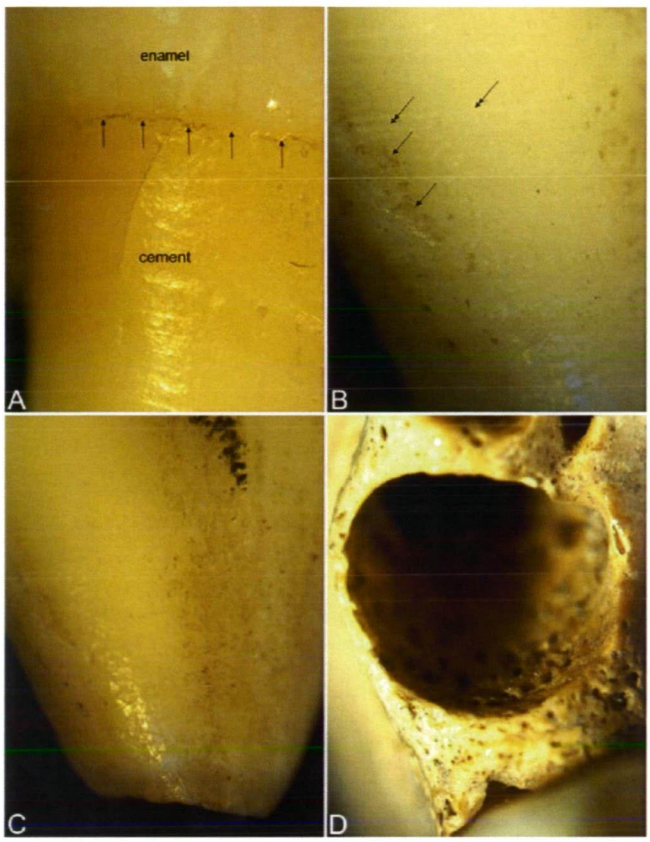

Figure 3. Permanent human tooth and alveolar socket in adult human mandible. A: the enamel and the cement are clearly separated by a serrate line (arrows) at the neck of the tooth. B: transverse ridges (double arrows), and shallow erosions (arrows) on the surface of the root cement of the adult tooth. C: the apical region of the cement is thick and shiny. D: the alveolar bone displays several minute canaliculi for vessels and nerves. Magnification: 3x.

obtained according to the prevailing laws in years 1982-1990. The extracted teeth were treated according to the following methods. The teeth were placed into buffered (pH 7.0) 10% (v/v) formalin solution: the apical foramina were widened in order to facilitate the diffusion of the fixative into the pulp chamber. Following the fixation, the teeth were washed in tap water and put into the decalcification solution, which contained 10% ethylenediamine tetraacetic acid (EDTA) in distilled water and/or 10% (v/v) formic acid supplemented with 10% (v/v) formalin in distilled water. Decalcification was made at room temperature for 5-15 days, which was followed by paraffin embedding (Kiernan 1999). Embedded tissues were sectioned (5-10 μm) and stained with hematoxylin and eosin (Borges Silva et al. 2011). Silver impregnation of the decalcificated teeth was performed according to Romanes (Romanes 1950; Hattyasi 1982). This silver staining method is suitable for the staining of axons, but not for nerve endings (Romanes 1950).

Developing teeth were studied in rat pups: 1, 3, 5, 9, 10 and 11 days old rats were used. The rats were deeply anesthetized with diethylether, decapitated and their heads were put into 4% phophate-buffered (pH 7.4) paraformaldehyde. The heads were fixed by immersion at 4 °C for 10 days. The paraformaldehyde solution has been changed three times during the 10 days. The mandibles and maxillae with soft tissues and teeth were separated from the skull and decalcificated. The decalcificating solution contained 1.4% (v/v) EDTA and 1% (v/v) dimethyl sulfoxide (DMSO) in distilled water (Sanderson et al. 1995). Decalcification was done for 5-10 days. The tissues were sectioned on a freezing microtome (25-30 μm) and the sections were used for immunohistochemistry. Other samples were embedded into paraffin; thin sections (5 μm) were cut and stained with hematoxylin-eosin and Mallory s trichrome stain for collagen fibers (Kiernan 1999). Immunohistochemistry sections were stained with rabbit anti-calcitonin-gene-related protein (CGRP) diluted to 1:10 000. The secondary antibody (goat anti-rabbit; 1:400 dilution) was biotinylated. The detection system was based on peroxidase (streptavidin-peroxidase; 1:2000 dilution). The peroxidase activity was localized with a diaminobenzidine-tetrahydrochloride (DAB-HCl) and hydrogen peroxide (H_2O_2) substrate solution containing nickel ammonium sulfate (Károly et al. 2015). Nerve fibers containing CGRP were appearing in black color. Controls of immunohistochemistry included incubations omitting the primary antibody. Detailed description of the CGRP immunostaining method is given in our previous article (Károly et al. 2015). Chemicals were purchased from Sigma-Aldrich (St. Louis, MO, USA).

Results

Alveolar processes of the maxilla and mandible in human

The alveolar process of the maxilla is not seen on newborn skulls – compared to the maxillae in 5-6 years old child. The alveoli are visible with the teeth inside. The alveoli are covered with a dense connective tissue membrane (Fig. 2). The bony surfaces of the mature alveoli present microscopic openings and canaliculi (cca. 0.1 mm wide) which are present inside, on the interalveolar septa and on the gingival surface of the alveolar bone (Fig. 3). Histology pictures display characteristic lamellar bone structure (Fig. 4).

The histology of the human and rodent periodontal ligament

The surface of the extracted teeth displays remnants of soft tissue: the periodontal ligament. This tissue is rich in

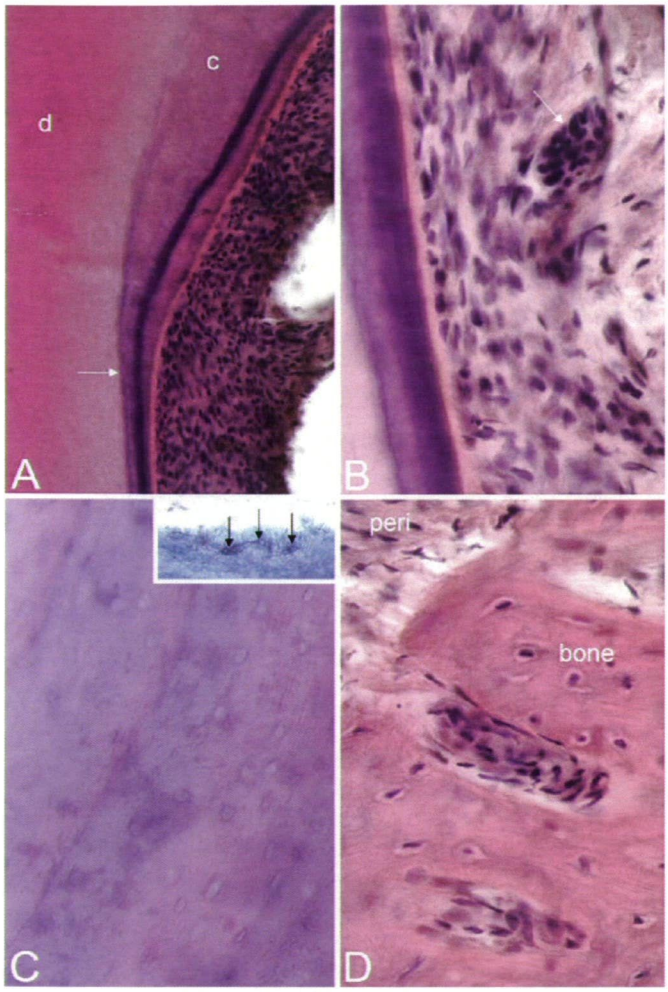

Figure 4. Histology of the human periodontium of extracted teeth (decalcification, hematoxylin-eosin staining). A: the border of the acellular and cellular cement is pointed by an arrow (c: cement; d: dentine; magnification: 10x). B: the periodontal membrane contains the epithelial rests of Malassez (arrow). C: the cellular cement displays layers with slightly different basophilia. Inset: cementocytes (arrows). Inset picture was taken from a Romanes-stained human tooth. D: the alveolar bone (bone) displays lamellar structure with osteocytes (peri: apposition of the periodontal membrane and the alveolar periosteum). Magnification on B, C, D: 20x.

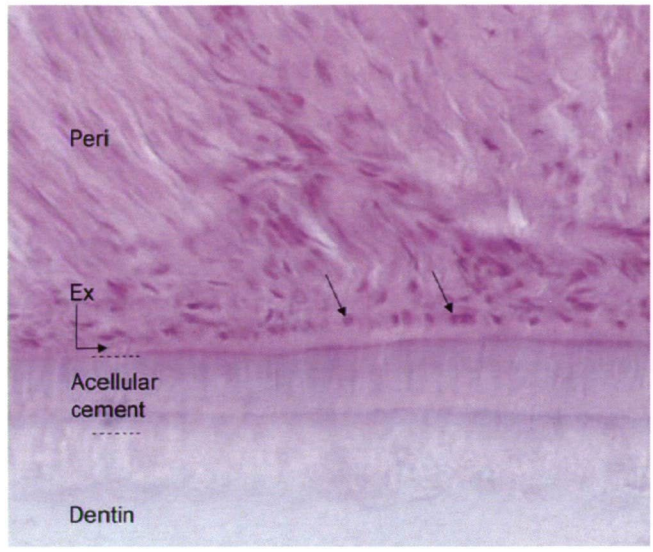

Figure 5. Higher magnification of the periodontal membrane (peri) and acellular cement (acellular cement). The fibers and cells of the periodontal membrane are visible. A single layer of cells (presumably cementoblats) are localed close to the surface of the cement (oblique arrows). The right-angled arrow points to a thin layer of eosinophilic collagen fibers attached to the cement (Ex). These are the Sharpey-fibers. The cement is covered by a thin basophilic layer and perpendicular to this, thin basophilic extensions showing the ordered internal structure of the matrix of the cement. Dentin: dentine layer. Hematoxylin-eosin staining, magnification: 40x.

cells resembling to spinocellular connective tissue. The hematoxylin-eosin staining did not reveal the exact nature of the cells, but some important features were observed. The cells of the connective tissue form a continuous layer on the surface of the cement: we suppose that most of these cells are cementoblasts (Fig. 5). The other cells could be fibroblasts/fibrocytes, eosinophils and macrophages although clear definition was not possible. The fibers of the connective tissue are arranged in parallel bundles, which are perpendicular or oblique to the surface of the cement (Fig. 5). We observed cell groups containing 20-30 cells located close to each other in the periodontal membrane: the cells resembled to epithelial cells and formed oval nests (Fig. 4). We identified them as the epithelial rests of Malassez (Tadokoro et al. 2008). Using the Romanes-technique we identified nerve fibers in the periodontal ligament: the Romanes-technique is not suitable for nerve endings, therefore only axon bundles and single axons were observed (Fig. 6). The nerves enter from the alveolar bone through the small bony canaliculi.

The structure of the human dental cement

The enamel-cement border is clear on the tooth: it is a serrate line on the neck of the tooth. The cement surface is shiny, yellowish with transverse lines visible under the stereomicroscope (Fig. 3). The root cement often displays shallow surface erosions (Fig. 3). Close to the root apex it becomes whitish, showing its thickening at the apex.

Histological investigation of the extracted human teeth revealed the clear border between the acellular- and cellular regions of the cement. Hematoxylin-eosin staining shows a thin, homogenous eosinophilic surface layer (2-4 μm), which contains the Sharpey-fibers (Fig. 4). In the acellular cement, a strongly basophilic layer follows, which is followed by a less basophilic layer: this layer displays the Sharpey-fibers running perpendicularly to the surface, and ending 30-50 μm

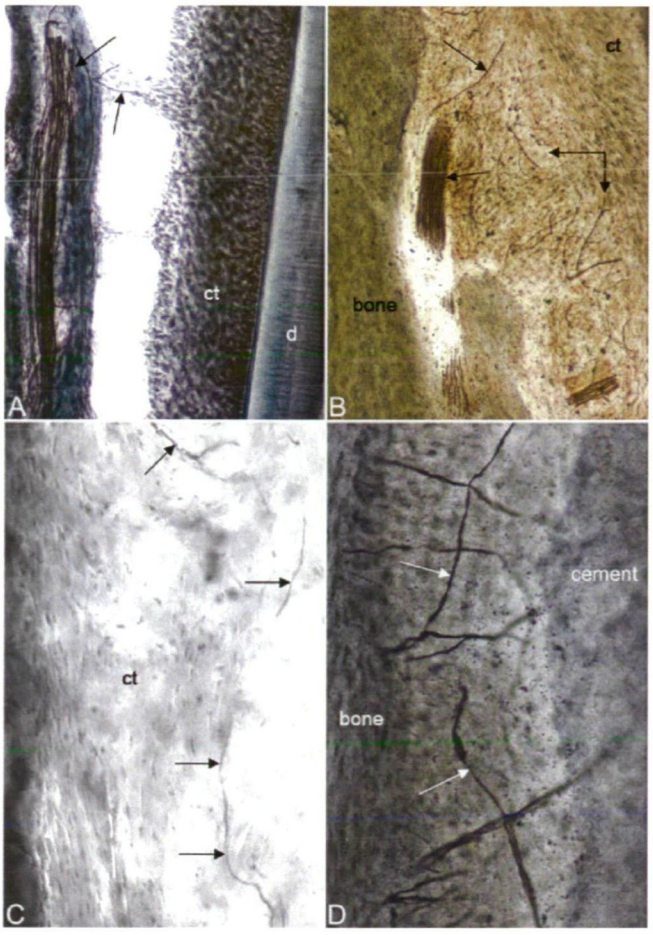

Figure 6. Innervation of the periodontium in human (C) and rat (A, B, D), Romanes staining. The axon bundles run in the bone (bone), and enter the periodontal membrane (ct) from there. The arrows point to single axons running in the connective tissue of the periodontal ligament (d: dentine). Magnification is 20x in A, B; 40x in C, D.

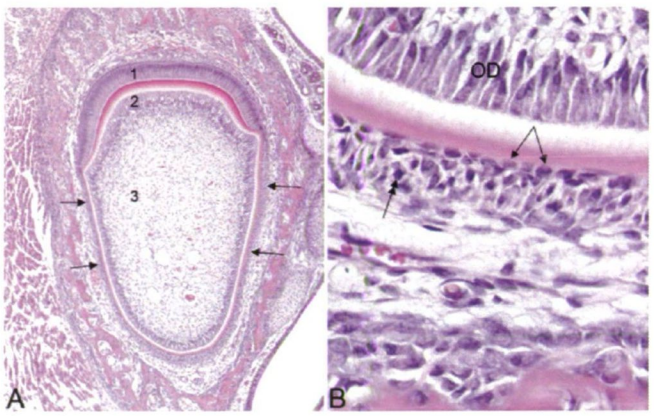

Figure 7. Developing tooth primordium in the maxilla of 2-day-old rat. Ameloblasts (1), odontoblasts (2) and the developing pulp (3) are seen on A. The arrows point to the sheath of Hertwig. Small amount of enamel and dentine are deposited. Magnification: 10x. B: higher magnification (40x) of the future root region. Odontoblasts (OD) and secreted dentine are visible. Outside of the dentine, a single layer of cementoblasts is visible (arrows). Outside of this cell layer, the Hertwig-sheath cells form an epithelium-like layer, with some mitotic figures (double arrow). Outside of the Hertwig-sheath richly vascularized periodontal connective tissue can be observed. Hematoxylin-eosin staining.

deep in the acellular cement (Fig. 4). In the cellular cement, the superficial basophilic layer becomes thinner, and the cementocytes appear under surface (Fig. 4). The cells possess short processes and are located in characteristic lacunae (Fig. 4). The cellular cement displays layers, which are visible because they differ from their basophilia. The thickness of the layers is between 20-50 μm (Fig. 4). The cellular cement contains elongated canaliculi rarely, resembling the Volkmann-canals in the bone: these may contain small blood vessels (not shown).

Periodontal structure in developing rat molars

Observations were made on the developing alveolar bone and periodontal membrane. The tooth primordium is embedded into the developing maxilla. In one-day-old rats, the alveolar bone is spongy, its surface is covered by osteoblasts and occasional oscteoclasts are observed, too (Fig. 7). Adamantoblasts and odontoblasts form a closed vesicle-like structure, inside which the future dental pulp tissue is located. The secreted dentine and enamel are first visible in 2 day-old-rats, and become thicker in later days (Fig. 7). The space between the tooth primordium and the alveolar bone is filled by a cell-rich connective tissue, containing blood vessels. The amount of collagen fibers was increasing with time during the 11 days long investigation. This was demonstrated with the Mallory-trichrome staining (not shown). The ameloblast layer covers the future crown; at the neck of the primordium it turns into a thinner, multi-layered epithelium-like structure, which covers the rest (the future root) of the primordium (Fig. 7). This structure was termed the epithelial root sheath of Hertwig (Hertwig 1847). The Hertwig-sheath was attached to the dentine, covering it completely (Fig. 7). The periodontal membrane is outside of it: whilst the Hertwig-sheath is a solid layer, the periodontal membrane is a loose connective tissue. The Hertwig-sheath does not contain blood vessels, whilst the periodontal ligament is richly vascularized (Fig. 7).

The CGRP-immunoreactive nerve fibers are present in the the periodontal membrane already in 1-day-old rats. The nerves enter from the alveolar bone and surround the entire tooth primordium (Fig. 8). The thinner fibers displayed fine varicosities. The density of the nerves increases during the development (days 1-11). We did not perform counting or densitometry of CGRP-containing axons in this study.

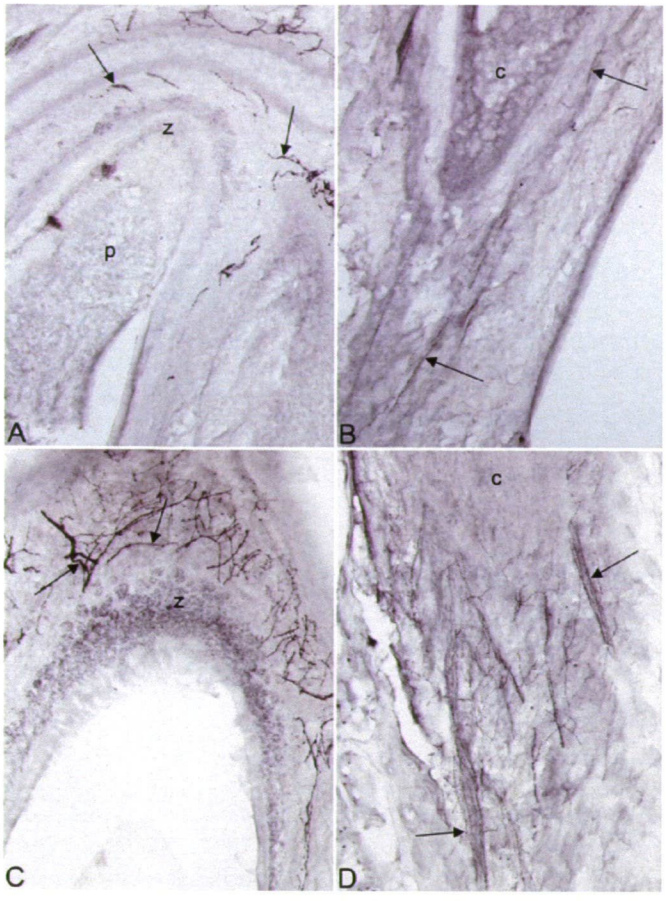

Figure 8. The CGRP-like immunoreactivity of the developing rat incisors. Arrows point to CGRP-stained axons. A, B: 1-day-old rat; C, D: 11-day-old rat (p: pulp; c: cement; z: enamel). Note the increase of immunoreactive axon number in 11-day-old animals. Magnification: 20x.

Discussion

Our results are in accordance with literature data of the periodontal apparatus (Liebgott 2001; Gera 2005). We discuss the most important issues, which were described in our experiments.

Basophilia of the cement

The acellular and the cellular cements contain layers which are seen with conventional stains (*e.g.*, hematoxylin-eosin stain). The thin basophilic layer on the surface of the acellular cement is due to the accumulation of glycosaminoglycans and proteoglycans (Kiernan 1999). These molecules are necessary for the fixation of the collagen fibers which come from the periodontal ligament and penetrate the cement as Sharpey-fibers (Yamamoto et al. 2010). The cellular cement also contains layers; these indicate the growth of the cement – the thin basophil staining between the layers may indicate the „glue" function of these matrix molecules (Yamamoto et al. 2010). These matrix components ensure the stability of the cement: the cement is fixed to the dentin and outside to the periodontal ligament, and therefore, it has a very important role in the fixation of the tooth.

The periodontal membrane

The periodontal membrane (or periodontal ligament) is a complicated connective tissue system, containing blood vessels, nerves, and connecting the alveolar bone to the radix of the tooth. The connective tissue contains organized and ordered collagen fiber bundles, which penetrate the bony tissues (cement and alveolar bone) and contribute to the fixation of the teeth (gomphosis). The periodontal membrane is rich in cells: we find fibroblasts/fibrocytes, cementoblasts, cementoclasts, osteoblasts, osteoclasts and a few immune cells. Literature data exist on the presence of stem cells in the periodontal ligament (Volponi et al 2010). Their functional role is a matter of recent investigations (Washio et al. 2010; Saito et al. 2015; Zhu and Liang 2015).

Probably related to undifferentiated cells, the human periodontal ligament contains the epithelial cell rests of Malassez (Becktor et al. 2007). We also observed these cells in the periodontal membrane of the extracted teeth. The cells are separated from the connective tissue by means of lamina basalis, and the cells are connected by intercellular junctions characteristic of the covering epithelia (Tadokoro et al. 2008). Experimental data prove that these cells secrete interleukins regulating the functional activity of periodontal cells (Cerri et al. 2009). Following injuries to the periodontal membrane, the cells secrete ameloblast-proteins, which indicates that these cells are less differentiated (Nishio et al. 2010). Other data indicated that these cells synthesize cytokeratins, neuropeptides and extracellular matrix proteins (Rincon et al. 2006). Maybe, the cell rests of Malassez play some role in the regeneration of the periodontal apparatus: they regulate the connective tissue matrix, cementoblast differentiation and mineralization (Rincon et al. 2006).

The nerves of the periodontal ligament are mainly sensory branches of the trigeminal nerve: these are mechanoreceptors (mainly Ruffini-endings) and nociceptors (Hattyasi 1982; Wakisaka et al. 2000). The CGRP is regularly used to stain these sensory nerves and nerve endings (Kosaras et al. 2009). Few postganglionic sympathetic axons are present, too (Hattyasi 1982). The nerve endings mediate brainstem reflexes, detecting the stretching of the tissue during mastication (Wakisaka et al. 2000; Umemura et al. 2010). The sympathetic axons probably mediate vasoregulation effects (Hattyasi 1982). The nociceptors participate in inflammation and pain sensation transmission (Wakisaka et al. 2000). The

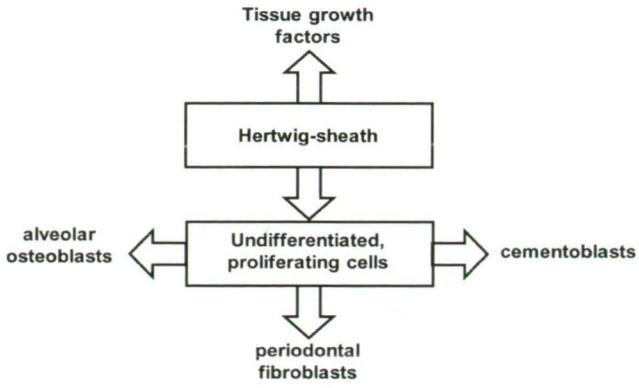

Figure 9. Summarizing diagram of the functional role of the Hertwig-sheath in the developing tooth.

CGRP immunohistochemistry proved the early appearance of the nociceptors: pointing to a growth regulatory (trophic) function of the thin axons during the development (Higuchi et al. 2008).

Developmental aspects of the parodontal apparatus: the epithelial sheath of Hertwig

The development of the parodontal apparatus is strongly related to the function: the mastication. In human, the alveolar processes (in maxilla) are not present at birth. As the teeth develop and erupt, the alveolar process grows, too. In rats, the eruption of the teeth happens during the first month: the incisors erupt first, then the molars in order of their position. The teeth develop in the bony socket of the alveolus and at the time of the eruption, they are mineralized. The periodontal apparatus develops earlier: the periodontal membrane is present already on the first day of life in rats, although the composition and the innervation are not fully developed. The innervation of the periodontal membrane is developing faster than the cement. In newborn rats, the cement is not developed, instead, the root is covered by a cell-rich sheath, which is known as the epithelial root sheath of Hertwig (Hertwig 1847). This sheath is the continuation of the ameloblast layer: the ameloblast stops at region of the tooth neck, where a stratified epithelial rooth sheath, the Hertwig-sheath follows. This sheath contains mitotic, proliferating cells, which cells probably contribute to the generation of the cementoblasts and the cement (Kumakami-Sakano et al. 2014). The Hertwig-sheath cells are probably differentiating from the neuromesenchyme of the tooth bud (Luan et al. 2009). On the other hand, this sheath also produces fibroblasts and osteoblasts, thereby contributing to the development of the alveolar bone and periodontal membrane (Kumakami-Sakano et al. 2014). We think that the Hertwig-sheath cells secrete growth factors which regulate the developmental processes of the periodontium, including the ingrowth of sensory axons (Kumakami-Sakano et al. 2014). It is tempting to speculate that the cell rests of Malassez are the remains of the epithelial sheath of Hertwig. The functional role of the Hertwig-sheath as a cell generator during tooth development is depicted on Figure 9.

Acknowledgements

The authors are grateful for the technical assistance of Szilvia Gyenes, Katalin Lakatos and Zoltán Imre, who are coworkers of the Department of Anatomy, Histology and Embryology, University of Szeged.

References

Becktor KB, Nolting D, Becktor JP, Kjaer I (2007) Immunohistochemical localization of epithelial rests of Malassez in human periodontal membrane. Eur J Orthodont 29:350-353.

Borges Silva GA, Moreira A, Bento Alves J (2011) Histological processing of teeth and periodontal tissues for light microscopy analysis. In Chiarini-Garcia H, Melo RCN, eds., Light Microscopy, Methods in Molecular Biology. Springer Science Business Media, 19-36.

Cerri PS, De Souza Goncalves J, Sasso-Cerri E (2009) Area of rests of Malassez in young and adult rat molars: evidences in the formation of large rests. Anat Rec 292:285-291.

Gera I (2005) Parodontológia. Semmelweiss Kiadó, Budapest [*in Hungarian*].

Harokopakis-Hajishengallis E (2007) Physiologic root resorption in primary teeth: molecular and histological events. J Oral Sci 49:1-12.

Hattyasi D (1982) Connecting transversal nerve fibres in the dentine. Z Mikrosk Anat Forsch 96: 679-688.

Hertwig O (1847) Über das Zahnsystem der Amphibien und seine Bedeutung für die Genese des Skeletts der Mundhöhle. Arch Mikrosk Anat Entw Mech 11:55-56 [*in German*].

Higuchi K, Santiwong P, Tamaki H, Terashima T, Nakayama H, Notani T, Iseki H, Baba O, Takano Y (2008) Development and terminal differentiation of pulp and periodontal nerve elements in subcutaneous transplants of molar tooth germs and incisors of the rat. Eur J Oral Sci 116:324-333.

Károly N, Dobó E, Mihály A (2015) Comparative immunhistochemical study of the effects of pilocarpine on the mossy cells, mossy fibers and inhibitory neurones in murine dental gyrus. Acta Neurobiol Exp 75:1-18.

Kiernan JA (1999) Histological and Histochemical Methods:

Theory and Practice. Butterworth, Oxford.
Kosaras B, Jakubowski M, Kainz V, Burstein R (2009) Sensory innervation of the calvarial bones in the mouse. J Comp Neurol 515:331-348.
Kumakami-Sakano M, Otsu K, Fujiwara N, Harada H (2014) Regulatory mechanisms of Hertwig's epithelial root sheath formation and anomaly correlated with root length. Exp Cell Res 325:78-82.
Liebgott B (2001) The anatomical basis of dentistry. Mosby (Elsevier), St. Louis, USA.
Luan X, Dangaria S, Ito Y, Walker C, Jin T, Schmidt M, Galang T, Druzinsky R, White K (2009) Neural crest lineage segregation: a blueprint for periodontal regeneration. J Dent Res 88:781-791.
Mihály A, Weiczner R, Süle Z, Czigner A (2014) The anatomy specimen collection of Albert Gellért: a unique paraffin wax method of body preservation. Austin J Anat 1(3):1013.
Nishio C, Wazen R, Kuroda S, Moffatt P, Nanci A (2010) Disruption of periodontal integrity induces expression of apin by epithelial cell rests of Malassez. J Periodontal Res 45:709-713.
Rincon JC, Young WB, Bartold PM (2006) The epithelial cell rests of Malassez – a role in periodontal regeneration? J Periodont Res 41:245-252.
Romanes GJ (1950) The staining of nerve fibers in paraffin sections with silver. J Anat (Lond) 84:104-115.
Saito MT, Silverio KG, Casati MZ, Sallum EA, Nociti Jr FH (2015) Tooth-derived stem cells: update and perspectives. World J Stem Cells 7:399-407.
Sanderson C, Radley K, Mayton L (1995) Ethylenediaminetetraacetic acid in ammonium hydroxide for reducing decalcification time. Biotech Histochem 70:12-18.
Tadokoro O, Radunovic V, Inoue K (2008) Epithelial cell rests of Malassez and OX6-immunopositive cells in the periodontal ligament of rat molars: a light and transmission electron microscope study. Anat Rec 291:242-253.
Umemura T, Yasuda K, Ishihama K, Yamada H, Okayama M, Hasumi-Nakayama Y, Furusawa K (2010) A comparison of the postnatal development of muscle-spindle and periodontal-ligament neuron sin the mesencephalic trigeminal nucleus of the rat. Neurosci Lett 473:155-157.
Volponi AA, Pang Y, Sharpe PT (2010) Stem cell-based biological tooth repair and regeneration. Trends Cell Biol 20: 715-722.
Wakisaka S, Atsumi Y, Youn SH, Maeda T (2000) Morphological and cytochemical characteristics of periodontal Ruffini ending under normal and regeneration process. Arch Histol Cytol 63:91-113.
Washio K, Iwata T, Mizutani M, Ando T, Yamato M, Okano T, Ishikawa I (2010) Assessment of cell sheets derived from human periodontal ligament cells: a pre-clinical study. Cell Tiss Res 341:397-404.
Yamamoto T, Li M, Liu Z, Guo Y, Hasegawa T, Masuki H, Suzuki R, Amizuka N (2010) Histological review of the human cellular cementum with special reference to an alternating lamellar pattern. Odontology 98:102-109.
Zhu W, Liang M (2015) Periodontal ligament stem cells: current status, concerns, and future prospects. Stem Cells Internat 2015: ID 972313.

Volume 59(Suppl.3):353-360, 2015
Acta Biologica Szegediensis
http://www2.sci.u-szeged.hu/ABS

ARTICLE

Advances of Squamata astroglia to other reptiles: numerous astrocytes and glial fibrillary acidic protein (GFAP)-free areas. A preliminary study

Dávid L. Lőrincz[1], Mihály Kálmán[2]*

[1]Faculty of Veterinary Science, Szent István University, Budapest, Hungary
[2]Department of Anatomy, Histology and Embryology, Semmelweis University, Budapest, Hungary

ABSTRACT Squamata are diapsid reptiles. Testudines were positioned formerly to the most ancient group, Anapsida, but recently they are also classified as diapsid reptiles, although their position within this group is uncertain. The investigated species of this study involved lizards (*Timon tanginatus,* Lacertidae; *Pogona vitticeps*, Agamidae; *Eublepharis macularis*, Gekkota; *Chameleo calypratus*, Chameleonidae), snakes (*Epicrates cenchria maurus*, Boidae; *Python regius*, Pythonidae; *Pantherophis guttata* and *P. obsoletus quadrivittatus*, Colubridae), and turtles (*Testudo hermanni*, Testudinidae; *Trachemys scripta* and *Mauremys sinensis*, Emydidae; *Pelomedusa subrufa*, Pleurodira). They were overanasthetised with Nembutal and transcardially perfused with 4% buffered paraformaldehyde. Coronal sections were processed according to the immunoperoxidase protocol. Monoclonal anti-GFAP and other glial markers were used. The main astroglia were the radial ependymoglia. There were two principal advances in Squamata. First, astrocytes were frequent in several areas, although, nowhere predominated. Furthermore, considerable GFAP-poor areas were found. They were extended in *Python*, and in *Pogona* and *Chamaeleo* GFAP was almost missing throughout the brain. The Squamata share more common astroglial features with birds than the turtles, although, represents a separate branch (Lepidosauria *versus* Archosauria). In mammals and birds the GFAP-free areas are usually advanced, expanded and plastic ones. Note that Squamata display quite complex behavioural phenomena related to other reptiles. **Acta Biol Szeged 59(Suppl.3):353-360 (2015)**

KEY WORDS
brain evolution
GFAP
lizards
snakes
turtles

Abbreviations

A: agama; ca: anterior commissure; C: chameleon; dp: dorsal pallia; DVR/dvr: dorsal ventricular ridge; G: gecko; hy: hypothalamus; L: lacertid lizard (*Timon)*; mp: medial pallia; to: optic tract; Sb: boa; Sp: python; Sc: colubrid snake (*Pantheropis*); sp: septum; st: striatum; Tg: greek tortoise; Tc: chinese turtle.

Introduction

The present study continues to our previous studies on the astroglia of vertebrates: Chondrichthyes (Kálmán and Gould 2001; Ari and Kálmán 2008), Actinopterygii (Kálmán 1998, Kálmán and Ari 2002), birds (Kálmán et al. 1993, 1998), turtles (Kálmán et al. 1994, 1997), and caiman (Kálmán and Pritz 2001).

Former studies found that there are similar features of astroglia of mammals and birds which have the most advanced vertebrate brains. One of them the predominancy of astrocytes the other is the appereance of large brain areas free of GFAP-immunopositivity or at least very poor in it but capable of GFAP expression following lesions (Kálmán 2002). Similar areas and/or predominancy of astrocytes were not observed in either turtles or crocodilians. In them, an almost evenly dense, thin, elongated ependymoglia actually, the 'tanycytes' of Horstmann (1954) are the predominant glia as well as in most of 'anamniotes' (Kálmán 2002; Appel 2013); although, astrocytes were found in several areas of the caiman brain. Present study investigates the phenomena of astroglial evolution in lizards and snakes.

Several species of Squamata (snakes and lizards) of different taxonomic positions (Table 1) were investigated. Considering that our former studies on turtle were based on Boehringer mouse monoclonal anti-GFAP antibody which was unavailable for this new analysis, we decided to inves-

Submitted June 15, 2015; Accepted July 30, 2015
*Corresponding author. E-mail: misimiska@gmail.com

Table 1. Species studied with their taxonomical data.

Classis	Ordo	Subordo	Familia	Species
Reptilia	Squamata	Scincomorpha	Lacertidae	Moroccan eyed lizard - *Timon tangitanus*
		Iguania	Agamidae	Bearded dragon - *Pogona vitticeps*
			Chamaeleonidae	Veiled chameleon - *Chamaeleo calyptratus*
		Gekkota	Eublepharidae	Leopard gecko - *Eublepharis macularius*
		Serpentes	Boidae	Columbian rainbow boa - *Epicrates cenchriamaura*
			Pythonidae	Ball python - *Python regius*
			Colubridae	Corn snake - *Pantherophis* (formerly: *Elaphe*) *guttatus*
				Yellow rat snake - *Pantherophis* (*Elaphe*) *obsoletus quadrivittatus*
	Testudines	Cryptodira	Testudinidae	Greek tortoise - *Testudo hermanni boettgeri*
			Emydidae	Yellow-bellied slider – *Trachemys* (formerly: *Pseudemys*) *scr. scripta* Red-eared slider - *Trachemys* (*Pseudemys*) *scripta elegans*
			Geoemydidae	Chinese stripe-necked turtle - *Mauremys* (formerly: *Ocadia*) *sinensis*
		Pleurodira	Pelomedusidae	African helmeted turtle - *Pelomedusa subrufa*

tigate more turtle species in parallel, including a representative of Pleurodira which group has not been studied earlier (Table 1).

Glial fibrillary acidic protein (GFAP), the characteristic cytoskeletal protein of astroglia (Bignami et al. 1980) of each vertebrate group has cross-reactivity to the anti-mammalian GFAP antibodies (Dahl and Bignami 1973; Dahl et al. 1985; Onteniente et al. 1983). However, according to several studies, not all astrocytes can be detected by the immunohistochemical reaction against GFAP (Connor and Berkowitz 1985; Linser 1985). Therefore, it is necessary to apply other astroglial markers, *i.e.* glutamine synthetase and S100 protein (Ludwin et al. 1976; Martinez-Hernandez et al. 1977). Our previous results (Kálmán et al. 1995) obtained on adult turtle brain suggested that vimentin-immunopositivity is also to be expected in adult reptile brains; therefore, these markers were also investigated. In this study, beside Novocastra reagent, four other anti-GFAP reagents were also tested.

Materials and Methods

Fixation and sectioning

Experimental animals (which were unable of breeding due to wounds or infertility) were obtained from breeders. They were sublethally overanasthetised with Nembutal and transcardially perfused with paraformaldehyde solution (4% in phosphate buffer-saline). Following two days postfixation, the brains were embedded into agarose and series of coronal sections (50-70 μm) were cut by Vibratome.

Immunohistochemical procedure

After a rinse in phosphate buffer the brains were embedded in agar, and then 50 μm thick serial sections were cut in the coronal plane by a Vibratome vibrating microtome. After rinsing overnight in phosphate buffer the floating sections were pre-treated with 3% H_2O_2 (for 5 min) to suppress the endogenous peroxidase activity and then incubated in 20% normal goat serum (at room temperature for 90 min) to block the non-specific antigen binding. These and all the following steps included a rinse with phosphate buffer between the change of reagents. Then primary immunoreagent (Table 2) was applied in phosphate buffer containing 0.5% Triton X-100, at 4 °C for 40 hours. As a secondary antibody, biotinylated anti-mouse or anti-rabbit immunoglobulin (Vector, Burlingam, CA, USA) was used. Then the sections were incubated with streptavidin-biotinylated horseradish peroxidase complex (Vector, Burlingam, CA, USA), diluted 1:100 in phosphate buffer and applied at room temperature for 90 min. The immunocomplex was visualized by diaminobenzidine (DAB) reaction, 0.05% 3-3'-DAB in 0.05 M Tris-HCl buffer (pH 7.4) containing 0.01% H_2O_2 at room temperature for 5 to 10 min (until brownish color appeared). No structure-bound color product was found when the anti-GFAP antibody was omitted from the procedure. Nissl counterstaining was applied on some sections. For positive controls rat brain sections were applied.

Results

General observations

This study does not demonstrate complete mappings on the different species studied. The common and the different features of the GFAP-immunopositive astroglial architecture are emphasized in parallel in the species, therefore, the results are arranged according to the brain areas, not the species.

The immunostaining revealed that the main astroglial type is the radial ependymoglia. Non-radial long fibers penetrated

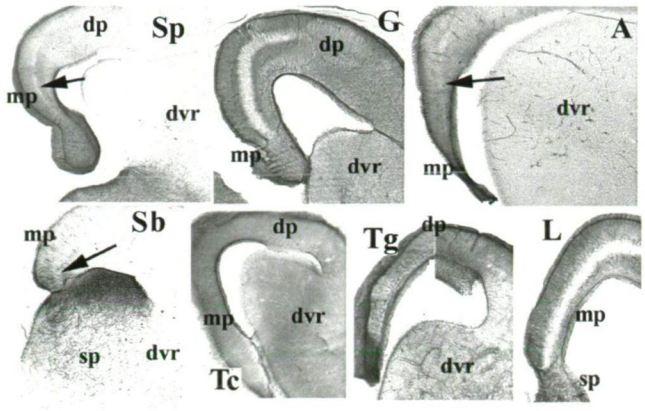

Figure 1. Cross-sections at the interventricular foramen. Three different distribution of GFAP are observed in the medial and dorsal pallium. In gecko and lacertid lizard these areas are full of GFAP-immunopositive radial, trans-pallial glial processes even a middle zone is conspicuously light. In snakes and agama this pattern is confined to the end of the medial pallium, the other areas are free of GFAP. In turtles these areas are evenly densely rich in GFAP.

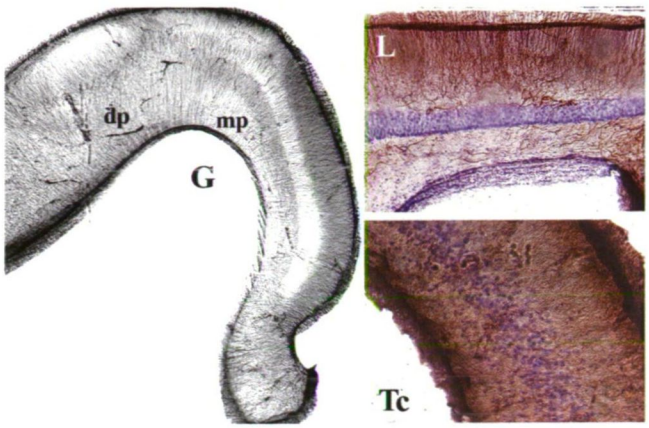

Figure 2. Enlarged parts of medial pallium. In gecko the radial arrangement is well visible. The glial processes traverse the GFAP-poor light zone but here the density of both their branching and staining is weaker. Counterstaining according to Nissl demonstrates (in lacertid lizard) that the 'light' area is occupied by neurons. Similar neuronal layer is found in turtles but does not alter the distribution of GFAP. In gecko there is another GFAP-free ellipsoid area in the dorsal pallium. Their septum is also poor in GFAP.

this system around the large vessels. In snakes and lizards astrocyte-like elements occurred in several areas, *e.g.*, in the pallium and the striatum, but nowhere predominated. GFAP-free areas were also found. Nothing similar was found in turtles. The Squamata may form three groups. In gecko and *Timon* GFAP immunopositivity was found throughout the brain, with some exceptions (see later). As an intermediate group GFAP-free areas were extended in snakes, in the dorsal pallium, in the septum, in the dorsal ventricular ridge and in the hypothalamus. The opposite end was represented by the chameleon and agama in which the GFAP was almost absent, only in a few areas GFAP immunopositive elements were found.

Telencephalon

Three different patterns of GFAP immunopositivity were observed in the medial and dorsal pallium: 1) In gecko and lacertid lizard (*Timon*) these areas were full of GFAP-immunopositive radial, trans-pallial glial processes but a middle zone was conspicuously light. 2) In snakes and agama this pattern was confined to the end of the medial pallium, the other areas were free of GFAP. 3) In turtles the pallium was evenly densely rich in GFAP. In gecko there was another GFAP-free ellipsoid area in the dorsal pallium (Fig. 1).

In higher magnification the radial arrangement of glial processes was well visible (Fig. 2). These processes traversed the GFAP-poor light zone but here the density of both their branching and staining was weaker. Counterstaining according to Nissl demonstrated that the 'light' area is occupied by neurons. Similar neuronal layer is found in turtles but does not alter the distribution of GFAP.

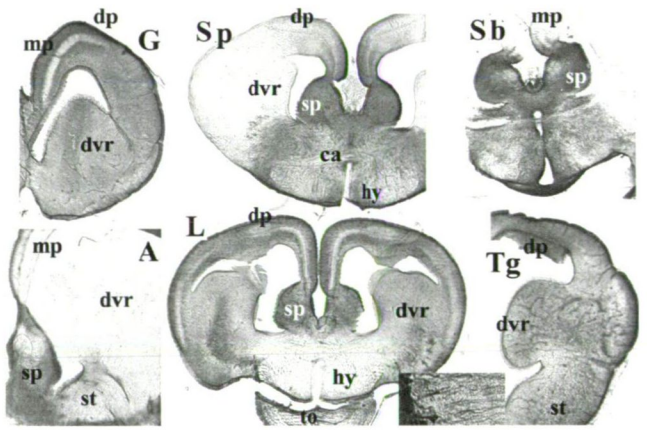

Figure 3. Cross-sections at the anterior commissure. Within a brain the adjacent areas may have strikingly different GFAP-staining in snakes and lizards. In agama, boa and python the DVR has hardly any GFAP immunopositivity, whereas the striatum is intensely stained (inset shows the radial glial pattern). Identical areas have different GFAP immunopositivity in different species: the staining patterns of DVR, striatum, and hypothalamus are just opposite in python and lacertid lizard. Similar differences can you see in the case of the septum (see also Fig. 4). The GFAP-immunopositivity of a part of brain may alter throughout the series of sections (see, *e.g.*, the agama septum, here and in Fig. 4).

The septum had an intense staining in most species (Fig. 3 and 4) but not in the agama and chameleon. In geckos the anterior septal nuclei formed a characteristic thickening. In it, mainly rostrally, the GFAP-immunopositivity was rather weak. The dorsal ventricular ridges (DVRs) also displayed

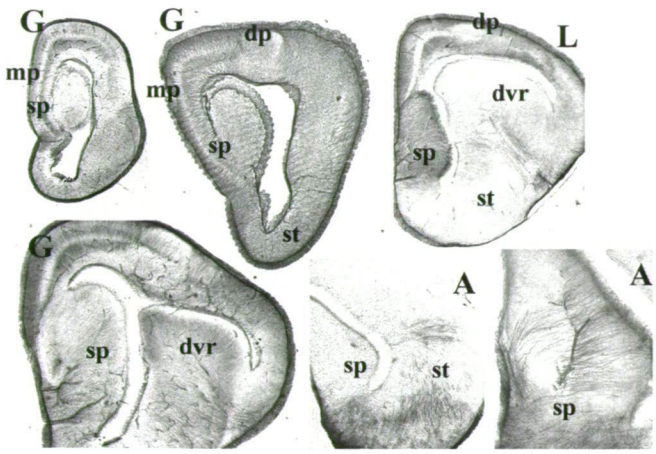

Figure 4. In front of the anterior commissure. The septum had an intense staining in most species (see also Fig. 3), but not in the agama. In geckos the anterior septal nuclei formed a characteristic thickening, in which, mainly rostrally, the GFAP immunopositivity was rather weak.

different density of GFAP-immunopositivity. Whereas lacertid lizard (*Timon*), gecko and turtles had densely stained DVR, in python, boa, agama and chameleon DVR was almost free of GFAP-immunopositivity (Fig. 3 and 4). We observed three main tendencies: 1) Within a brain the adjacent areas had strikingly different GFAP-staining in snakes and lizards. In agama, boa and python the DVR had hardly any GFAP immunopositivity, whereas the striatum was intensely stained. In turtles, however, both area had intense staining; 2) Identical areas had different GFAP immunopositivity in different species: the staining patterns of DVR, striatum, and hypothalamus are just opposite in python and lacertid lizard. Similar differences can you see in the case of the septum (Fig. 3 and 4); 3) The GFAP-immunopositivity altered throughout the series of sections, see *e.g.*, the agama septum (Fig. 3 and 4).

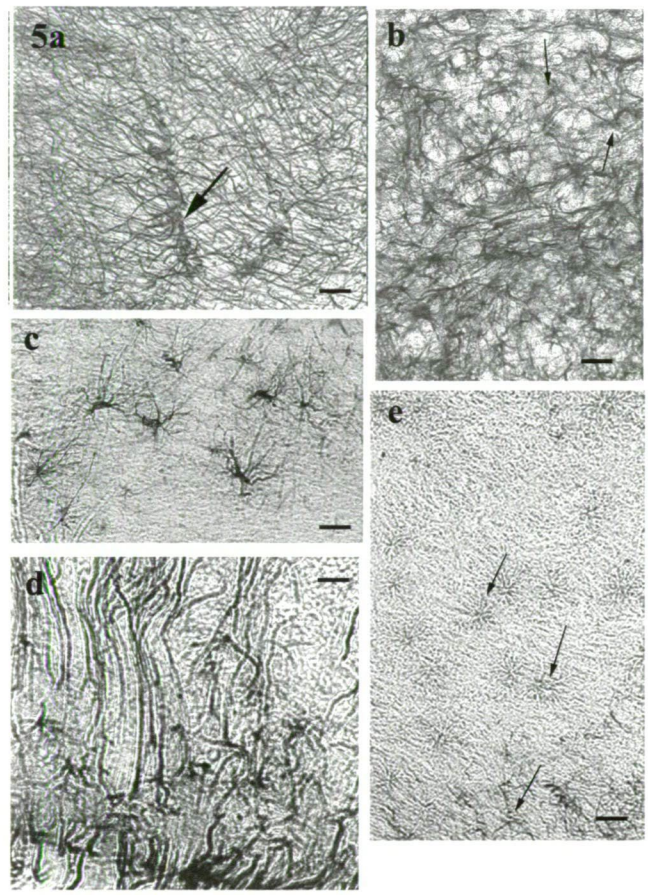

Figure 5. The fine pattern. a) The radial pattern was sometimes masked beyond recognition by other processes, mainly around the vessels (arrow) (colubrid snake, *Pantherophis*, DVR). Scale bar: 20 μm; b) Sometimes it was almost insolvable (arrows) whether astrocytes or superpositions of processes are in view (*Timon*). Scale bar: 10 μm; c) In some areas the presence of astrocytes is obvious (mesencephalon, chameleon). Scale bar: 10 μm; d) Long radial processes may also emerge from astrocytes, not only ependyma ('radial astrocytes', chameleon, mesencephalon). Scale bar: 10 μm; e) Faint contours (arrows) of unstained astrocytes (colubrid snake, *Pantherophis*, medulla)? Scale bar: 10 μm.

Sub-telencephalic brain parts

In lizards and snakes in the thalamus GFAP was rather confined to the borders of the nuclei, and the hypothalamus was rather negative whereas turtles had a rather even distribution except fot the prosencephalic fascicles.

In most of the species studied, the tectum was GFAP-immunopositive except for the Chamaeleon. The layered structure and, mainly medially, a radial glial pattern was recognizable, mainly in the gecko. Tegmentum was rather immunonegative in all the species examined.

In the medulla, the dorsoventral nuclei have usually an intense staining as vell as the median glial septum. The radial pattern is usually recognizable (agama, python and boa). The reticular formation has a reticular glial pattern rather extended in turtles and gecko but confined in the lacertid lizard *Timon*, agama, and snakes; except for colubrid ones (*Pantherophis*), where the pattern was not delineated by the immunostaining at all. The medial longitudinal fasciculus is recognizable, the white matter tracts are usually lighter than their environment. In the cerebellum Bergmann-fibers proved to be GFAP-immunopositive.

The fine pattern

In every species local modifications usually masked the basic system, the radial ependymoglia. This basic pattern, however, was sometimes masked beyond recognition by processes,

Table 2. The primary antibodies used in this study.

Against	Type	Supplier	Code	Dilution	Final concentration (µg/ml)
GFAP	Mouse*	Novocastra, Newcastle, UK	ga5	1:100	100
	Rabbit**	DAKO, Galstrup, Denmark	Z0334	1:100-500	6-28
	Mouse*	Biosciences, San Diego, CA, USA	GA5	1:100	5
	Rabbit**	Sigma, Saint Louis, MO, USA	G9269	1:100-500	***
	Rabbit**	Santa Cruz, San Diego, CA, USA	Sc-32956	1:100	2
Glutamine synthetase	Mouse*	Transduction Labs., Erembodegem, Belgium	610518	1:100	2.5
	Rabbit**	Novus Biologicals, Littleton, CO, USA	NB-110-41404	1:1000	***
S100	Rabbit**	Sigma, San Louis, MO, USA	s-2644	1:100	81
	Mouse*	Abcam, Cambridge, UK	B-32.1	1:100	***
Vimentin	Mouse*	Abcam, Cambridge, UK	Vim3B4	1:100	***
	Mouse*	Calbiochem, Darmstadt, Germany	IF01-100UG	1:1000	0.5
	Chicken**	Novus Biologicals, Littleton, CO, USA	NB300-223	1:1000	20

* monoclonal, ** polyclonal, *** original concentration is not given by the supplier

mainly around the vessels (Fig. 5a). In some areas it was almost insolvable whether astrocytes or superpositions of processes are in view (Fig. 5b). In some areas the presence of astrocytes was obvious (Fig. 5c). Long radial processes also emerged from astrocytes, not only ependyma ('radial astrocytes', Fig. 5d). In some GFAP-free areas faint contours suggested the presence of unstained astrocytes (Fig. 5e).

Effect of other markers

When in some areas GFAP immunopositivity was not detected with the Novocastra monoclonal mouse anti-GFAP antibody, other markers were also applied (Table 2). Though four other anti-GFAP reagents tested, only the other mouse-derived (Biosciences) reagent resulted in similar staining as the Novocastra product. Anti-glutamine synthetase and anti-S100 antibodies visualized only a small fragment of the glial processes, mainly radial ependymoglia in the tectum and around the dorsal and ventral sulci beside the DVR. These antibodies worked well in the controll sections cut from rat brains.

Antigenes did not reveal new localisations of GFAP; the immunopositivity was more conspicuous due to a weaker background staining. Those anti-vimentin antibodies which were raised against mammalian vimentin were ineffective. With anti-vimentin antibody raised against bird vimentin the preliminary results were encouraging.

Discussion

Comparison of present and former results

The main Squamata astroglial type is radial ependymoglia, with several local modifications. However, there are two principal differences from turtles. In different Squamata species considerable GFAP-poor or -free areas were found. Furthermore, true astrocytes were found in several areas, although, nowhere predominated (true astrocytes are stellate-shaped cells with equally-sized processes, independent from the ependyma).

True astrocytes have been demonstrated at least in some areas in lizards, Iguanidae (*Anolis carolinensis*, Dahl et al. 1985; *Anolis sagrei*, Lazzari and Franceschini 2005a; Lacertidae, *Gallotia galloti*, Monzon-Mayor et al. 1990a; Yanes et al. 1990; *Lacerta lepida*, recently *Timon lepidus*, Bodega et al. 1990; *Podarcis sicula*, Lazzari and Franceschini 2001), geckos (*Eublepharus macularius*, Lazzari and Franceschini 2005b; *Tarentola mauretanica*, Ahboucha et al. 2003). Only one data referred to snake (*Elaphe quadrivirgata*, recently *Pantherophis quadrivirgata*, Onteniente et al. 1983). No former study emphasized the occurrence of large GFAP-poor or GFAP-free areas.

In the turtle brains (including that of the Pleurodira *Pelomedusa*) the findings corresponded to that found formerly in *Trachemys* (formerly: *Pseudemys*) *scripta elegans* (Kálmán et al. 1994) and *Mauremys leprosa* (Kálmán et al. 1997): no GFAP-free areas and no astrocytes were found. Independent studies with GFAP-immunostaining have also not detected astrocytes (*Clemmys japonica*, Onteniente et al. 1983; *T. scripta elegans*, Dahl et al. 1985, Kriegstein et al. 1986; *Trionyx sinensis*: Lazzari and Franceschini 2006).

Comparison of Squamata to birds and mammals

Lizards and snakes (Squamata) share more common astroglial features with birds than the turtles and crocodilians (Kálmán and Pritz 2001). Some representatives (*e.g.*, agama, snakes) have so extended GFAP-free areas which match the avian ones. However, there are two meaningful differences in the homologuous areas: the molecular layer of cerebellum and the upper layers of tectum contain GFAP in lizards but not

in birds (Linser 1985; Roeling and Feirabend 1988; Kálmán et al. 1993). Those areas which are GFAP-free in mammals and birds are desribed usually as the advanced, expanded and plastic ones (Butler and Hodos 2005). Note that Squamata display quite complex behavioural phenomena related to other reptiles (Zug et al. 2001). Mammals and birds belong to different amniote clads: Synapsida and Diapsida, respectively. Their similar glial features most likely evolved independently, during parallel, separate evolutions (Kálmán 2002) because they have not found in turtle or caiman so far examined (Kálmán et al. 1994; Kálmán and Pritz 2001). On the other hand, Squamata represents a separate diapsid clad divergent from that the crocodiles and birds (Lepidosauria *versus* Archosauria). Whereas lizards of different taxonomic positions had rather different distribution of GFAP and glial architecture (Ahboucha et al. 2003), but no considerable differences were found in turtles, including the Pleurodira *Pelomedusa subrufa*.

Other glial markers

Vimentin immunopositivity was repeatedly documented in the brain of different lizards: Iguanidae (*Anolis sagrei*, Lazzari and Franceschini 2005a), Lacertidae (*Gallotia galloti*, Monzon-Mayor et al. 1990a; Yanes et al. 1990; *Podarcis sicula*, Lazzari and Franceschini 2001), and gecko (*Eublepharus macularius*, Lazzari and Franceschini 2005b). Our preliminary findings obtained on adult turtle brain (*T. scripta elegans*) by an antibody presented by P. Viklicky (Lukas et al. 1989) is supported by the observations of Lazzari and Franceschini (2006, *Trionyx sinensis*). The present results with anti-vimentin antibody raised against bird vimentin are promising. It is immportant to emphasize that usually different monoclonal anti-vimentin antibodies are applied in mammalian and bird brain (Bohn et al. 1992; Gereben et al. 1995). Further experimental evidence is required in this field.

In their experiments, Monzon-Mayor et al. (1990b, 1998) used anti-chicken glutamine syntethase to detect glial elements in *Gallotia galloti* (this was not available for our study). Scarce data were found with S100 (Romero-Aleman et al. 2003).

Importance of turtle phylogeny

Formerly turtles were classified as anapsids, therefore, the closest living relatives of the extinct stem-amniotes (Carroll 1988; Reiner 1990). This opinion has recently been challenged by several studies based on classic fossil data and DNA analyses which point to that turtles are diapsids, like the other extant reptiles and the birds, although their position within this group is uncertain (Zardoya and Meyer 1998; Shen et al. 2011; Carroll 2013). Critical analyzis of these contradictory opinions is beyond the scope of this study (for a detailed review, see Kálmán et al. 2013). In either case the turtle glial structure seems to be the simplest one among reptiles since no astrocytes intermingle with the ependymoglia, which have a rather even density. The turtles are the sole extant Amniota group without true astrocytes (*Sphenodon*, which is nearest to the stem of Lepidosauria, has not been investigated).

Surveying the divergent opinions there are two possibilities:

- The turtles emerged earlier than lepidosaurs and archosaurs separated from each other. In this case they may have preserved a glial system ancestral to that of the other extant reptiles.

- The turtles emerged following that lepidosaurs and archosaurs separated from each other. In this case absence of astrocytes in them may be a secondary phenomenon, not an ancestral characterisctics. We have to mention that according to some opinions the occurrance and frequency of astrocyte depends rather the brain structure than the phylogenetical position (Wicht et al. 1994).

Conclusion

The glial structure of Squamata seems to be most advanced among reptiles. So conspicuous differences within a taxonomic ordo have not found yet in other vertebrates. Further studies are requested, how the differencies of astroglia have formed in the different Squamata, and what is their functional (behavioural) importance.

References

Ahboucha S, Laalaqui A, Didier-Bazes M, Montange M, Cooper HM, Gamrani H (2003) Differential patterns of glial fibrillary acidic protein immunolabeling in the brain of adult lizards. J Comp Neurol 464:159-171.

Appel B (2013) Nonmammalian vertebrate glia. In Kettenmann H, Ransom BR, eds., Neuroglia, 3rd ed. Oxford University Press, New York, Oxford, 24-34.

Ari C, Kálmán M (2008) Evolutionary changes of astroglia in Elasmobranchii comparing to amniotes: a study based on three immunohistochemical markers (GFAP, S-100, and glutamine synthetase). Brain Behav Evol 71:305-324.

Bignami A, Dahl D, Rueger DC (1980) Glial fibrillary acidic protein (GFA) in normal neural cells and in pathological conditions. Adv Cell Neurobiol 1:285-310.

Bodega G, Suarez I, Rubio M, Fernandez B (1990) Distribution and characteristics of the different astroglial cell types in the adult lizard *(Lacerta lepida)* spinal cord. Anat Embryol (Berl) 181:567-575.

Bohn W, Wiegers W, Beuttenmuller M, Traub P (1992) Species-specific recognition patterns of monoclonal antibodies directed against vimentin. Exp Cell Res 201:1-7.

Butler AB, Hodos W (2005) Comparative Vertebrate Neuroanatomy, Evolution and Adaptation. 2nd ed. John Wiley and Sons Inc, New York, Chichester, Brisbane, Toronto, Singapore, 84-89.

Carroll RL (2013) Problems of the ancestry of turtles. In Brinkman PB, Halvoyd PA, Gardner JD, eds., Morphology and Evolution of Turtles. Vertebrate Paleobiology and Evolution. Springer, Dordrecht, 19-36.

Carroll RL (1988) Vertebrate Paleontology and Evolution. WH Freeman and Co, New York.

Connor JR, Berkowitz RM (1985) A demonstration of glial filament distribution in astrocytes isolated from rat cerebral cortex. Neuroscience 16:33-44.

Dahl D, Crosby CJ, Sethi A, Bignami A (1985) Glial fibrillary acidic (GFA) protein in vertebrates: immunofluorescence and immunoblotting study with monoclonal and polyclonal antibodies. J Comp Neurol 239:75-88.

Dahl D, Bignami A (1973) Immunohistochemical and immunofluorescence studies of the glial fibrillary acidic protein in vertebrates. Brain Res 61:279-283.

Gereben B, Gerics B, Gálfi P, Rudas P, Hajós F, Jancsik V (1995) Species-specifity of glial vimentin as revealed by immunocytochemical studies with the Vim 3B4 and V9 monoclonal antibodies. Neurobiology 3:150-164.

Horstmann E (1954) Die Faserglia des Selachegehirns. Z Zellforsch 39:588-617.

Kálmán M, Somiya H, Lazarevi L, Milosevi I, Ari C, Majorossy K (2013) Absence of *post-lesion* reactive gliosis in elasmobranchs and turtles and its bearing on the evolution of astroglia. J Exp Zool (Mol Dev Evol) 320:351-367.

Kálmán M (2002) GFAP expression withdraws - a trend of glial evolution? Brain Res Bull 57:509-511.

Kálmán M, Ari Cs (2002) Distribution of GFAP immunopositive structures in the rhombencephalon of the sterlet (*Acipenser ruthenus*): difference from Teleostei has evolutionary implication. J Exp Zool 293:395-406.

Kálmán M, Gould R (2001) GFAP-immunopositive structures in spiny catshark, *Squalus acanthias*, and little skate, *Raia erinacea*, brains: differences have evolutionary implications. Anat Embryol 204:59-80.

Kálmán M, Pritz MB (2001) Glial fibrillary acidic protein-immunopositive structures in the brain of a crocodilian, *Caiman crocodylus* and its bearing on the evolution of astroglia. J Comp Neurol 431:460-480.

Kálmán M (1998) Astroglial architecture of the carp (*Cyprinus carpio*) brain as revealed by immunohistochemical staining against glial fibrillary acidic protein (GFAP). Anat Embryol 198:409-433.

Kálmán M, Székely A, Csillag A (1998) Distribution of glial fibrillary acidic protein and vimentin immunopositive elements in the developing chicken brain from hatch to adulthood. Anat Embryol 198:213-235.

Kálmán M, Martin-Partido G, Hidalgo-Sanchez M, Majorossy K (1997) Distribution of glial fibrillary acidic protein-immunopositive structures in the developing brain of the turtle *Mauremys leprosa*. Anat Embryol 196:47-65.

Kálmán M, Kiss Á, Majorossy K (1995) Vimentin-immunopositive structures in the brain of the adult turtle *Pseudemys scripta elegans*. Ann Anat Suppl 177:195.

Kálmán M, Kiss Á, Majorossy K (1994) Distribution of glial fibrillary acidic protein-immunopositive structures in the brain of the red-eared freshwater turtle (*Pseudemys scripta elegans*). Anat Embryol 189:421-434.

Kálmán M, Székely A, Csillag A (1993) Distribution of glial fibrillary acidic protein-immunopositive structures in the brain of the domestic chicken *(Gallus domesticus)*. J Comp Neurol 330:221-237.

Kriegstein AR, Shen JM, Eshhar N (1986) Monoclonal antibodies to the turtle cortex reveal neuronal subsets, antigenic cross-reactivity with the mammalian neocortex, and forebrain structures sharing a pallial derivation. J Comp Neurol 254:330-340.

Lazzari M, Franceschini V (2006) Glial architecture in the central nervous system of the soft-shell turtle, *Trionyx sinensis,* revealed by intermediate filament immunohistochemistry. Anat Embryol 211:497-506.

Lazzari M, Franceschini V (2005a) Astroglial cells in the central nervous system of the adult brown anole lizard, *Anolis sagrei*, revealed by intermediate filament immunohistochemistry. J Morphol 265:325-334.

Lazzari M, Franceschini V (2005b) Intermediate filament immunohistochemistry of astroglial cells in the leopard gecko, *Eublepharis macularius*. Anat Embryol 210:275-286.

Lazzari M, Franceschini V (2001) Glial fibrillary acidic protein and vimentin of astroglial cells in the central nervous system of adult *Podarcis sicula* (Squamata, Lacertidae). J Anat 198:67-75.

Linser PJ (1985) Multiple marker analysis in the avian optic tectum reveals three classes of neuroglia and carbonic anhydrase-containing neurons. J Neurosci 5:2388-2396.

Ludwin SK, Kosek JC, Eng LF (1976) The topographical distribution of S-100 and GFAP proteins in the adult rat brain. An immunocytochemical study using horseradish peroxidase labeled antibodies. J Comp Neurol 165:197-208.

Lukas L, Draber P, Bucek J, Draberková E, Viklicky V, Straskova Z (1989) Expression of vimentin and glial fibrillary acidic protein in human developing spinal cord. J Histochem 21:693-702.

Martinez-Hernandez A, Bell KP, Norenberg MD (1977) Glutamine syntethase: glial localization in brain. Science 195:1356-1358.

Monzon-Mayor M, Yanes C, Tholey G, de Barry J, Gombos G (1990a) Glial fibrillary acidic protein and vimentin immunohistochemistry in the developing and adult midbrain of the lizard *Gallotia galloti*. J Comp Neurol 295:569-579.

Monzón-Mayor M, Yanes C, Tholey G, De Barry J, Gombos G (1990b) Immunohistochemical localization of glutamine synthetase in mesencephalon and telencephalon of the lizard *Gallotia galloti* during ontogeny. Glia 3:81-97.

Monzón-Mayor M, Yanes C, De Barry J, Capdevilla-Carbonell C, Renau-Piqueras J, Tholey G, Gombos G (1998) Heterogeneous immunoreactivity of glial cells in the mesencephalon of a lizard: A double labeling immunohistochemical study. J Morphol 235:109-119.

Onteniente B, Kimura H, Maeda T (1983) Comparative study of the glial fibrillary acidic protein in vertebrates by PAP immunohistochemistry. J Comp Neurol 215:427-436.

Reiner A (1990) A comparison of neurotransmitter-specific and neuropeptide-specific neuronal cell types present in the isocortex of mammals: implications for the evolution of isocortex. Brain Behav Evol 38:53-91.

Roeling TAP, Feirabend HKP (1988) Glial fiber pattern in the developing chicken cerebellum: vimentin and glial fibrillary acidic protein immunostaining. Glia 1:398-402.

Romero-Alemán MM, Monzón-Mayor M, Yanes C, Arbelo-Galván JF, Lang D, Renau-Piqueras J, Negrín-Martínez C (2003) S100 immunoreactive glial cells in the forebrain and midbrain of the lizard *Gallotia galloti* during ontogeny. J Neurobiol 57:54-66.

Shen XX, Liang D, Wen JN, Zhang P (2011) Multiple genome alignments facilitate development of NPCL markers: a case study of tetrapod phylogeny focusing on the position of turtles. Mol Biol Evol 28:3237-3252.

Wicht H, Derouiche A, Korf H-W (1994) An immunocytochemical investigation of glial morphology in the Pacific hagfish: radial and astrocyte-like glia have the same phylogenetic age. J Neurocytol 23:565-576.

Yanes C, Monzon-Mayor M, Ghandour MS, de Barry J, Gombos G (1990) Radial glia and astrocytes in the adult and developing telencephalon of the lizard *Gallotia galloti* as revealed by immunohistochemistry with anti-GFAP and anti-vimentin antibodies. J Comp Neurol 295:559-568.

Zardoya R, Meyer A (1998) Complete mitochondrial genome suggests diapsid affinities of turtles. Proc Natl Acad Sci USA 95:14226-14231.

Zug GR, Vitt LJ, Caldwell JP (2001) Herpertology. An Introductory Biology of Amphibians and Reptiles. 2nd ed. Academic Press, San Diego, San Francisco, New York, Burton, Sydney, Tokyo.

Volume 59(Suppl.3):361-369, 2015
Acta Biologica Szegediensis
http://www2.sci.u-szeged.hu/ABS

ARTICLE

Early phenomena following cryogenic lesions of rat brain – a preliminary study

László Tóth[1], Dávid Szöllősi[1], Katalin Kis-Petik[2], Erzsébet Oszwald[1], Mihály Kálmán[1]*

[1]Department of Anatomy, Histology and Embryology, Semmelweis University, Budapest, Hungary,
[2]Department of Biophysics and Radiation Biology, Semmelweis University, Budapest, Hungary

ABSTRACT The cerebrovascular laminin becomes detectable following lesions, whereas the lamina basalis-receptor β-dystroglycan disappears. These alterations may be indirect markers of a glio-vascular detachment which may result in the impairment of blood-brain-barrier. The present study estimates the correlations between the *post-lesion* exudation and the aforementioned phenomena. Lesions were performed in ketamine-xylazine anaesthesia with a copper rod cooled with dry ice. Immediately, or in 5 or 10 min brains were fixed in buffered 4% paraformaldehyde. Immunohistochemical reactions were performed in floating sections. Exudation was estimated with immunohistochemical detection of plasma-fibronectin and immunoglobulins. Glio-vascular connections were investigated with immunohistochemistry (GFAP, S100, glutamine synthetase), and electron microscopy. Laminin immunoreactivity appeared already at immediate fixation. Exudate was found only around the vessels. β-dystroglycan was still detectable. At five-ten minutes the territory of exudate became confluent and dystroglycan disappeared. Some but not all vessels were free of astrocytes. Electron microscopy demonstrated wide perivascular 'spaces'. '*In vivo*' monitoring was attempted with a multiphoton microscope in the Department of Biophysics of Semmelweis University. Astrocytes were labeled supravitally with sulforhodamine 101 so glio-vascular connections were visible. However, neither in the intact brain nor in 30-min *post-lesion* period astrocyte motility was observed.

Acta Biol Szeged 59(Suppl.3):361-369 (2015)

KEY WORDS

blood-brain barrier
β-dystroglycan
laminin
multiphoton microscope
post-lesion exudation

Introduction

The blood-brain barrier (BBB) becomes 'leaky' following lesions. The astrocytes, the glio-vascular connections have a basic importance in the formation and maintenance of the blood-brain barrier (Janzer and Raff 1987; Abbott 2002; Abbott et al. 2010). According to Jaeger and Blight (1997), the astrocytic end-feet 'decouple' (detach) from the vessels and a substantial expansion of perivascular spaces becomes evident. It may have role in the impairment of BBB.

Former studies revealed characteristic immunohistochemical alterations of cerebral vessels following various lesions (*e.g.*, stab wounds, cryogenic lesion, excitotoxic lesion, arterial occlusions). Cerebrovascular laminin which usually not detectable in the formaldehyde fixed intact brain tissue except some circumventricular organs becomes detectable in the area of lesion (Sosale et al. 1988; Shigematsu et al. 1989; Krum et al. 1991; Szabó and Kálmán 2004), whereas the immunoreactivity of the lamina basalis-receptor β-dystroglycan which delineates the vessels of intact brain (Uchino et al. 1995; Zaccaria et al. 2001) disappeares from the lesioned area (Szabó and Kálmán 2008; Kálmán et al. 2011; Wappler et al. 2011). These alterations are supposed to be indirect markers of glio-vascular detachment. The phenomena proved to be reversible.

Dystroglycan consists of two subunits: the α-dystroglycan binds laminin and other basal lamina components; the β-dystroglycan is a transmembrane protein that anchors α-dystroglycan to the cell membrane. The β-dystroglycan immunoreactivity delineates the brain vessels but the β-dystroglycan itself is localized in the perivascular glial end-feet (Tian et al. 1996). The β-dystroglycan and other proteins (dystrophin, syntrophin, etc.) form a complex, which is responsible for the proper distribution of ion channels and receptors including the water-pore channel protein aquaporin-4. (For recent reviews, see *e.g.*, Wolburg et al. 2009; Waite et al. 2012). The dystroglycan-laminin connection is necessary for the glio-vascular coupling which is in turn a condition of the formation and maintenance of blood-brain barrier by the endothelial cells (Janzer and Raff 1987; Abbott

Submitted June 1, 2015; Accepted July 20, 2015
*Corresponding author. E-mail: misimiska@gmail.com

2002; Abbott et al. 2010). Deletion of β-dystroglycan in mice results in discontinuity of the cerebrovascular basal laminae (Moore et al. 2002).

The aims of the present study were to investigate in rats following brain lesion: 1) the correlation between the exudation, the breakdown of the blood-brain barrier and the alteration of the vascular β-dystroglycan and laminin immunoreactivity; 2) whether the change of the vascular β-dystroglycan and laminin immunoreactivity is really a marker of a glio-vascular decoupling; 3) the sequence of these phenomena.

The area of *post-lesion* exudation can be estimated with various tracers. Intrinsic tracers can be immunoglobulins of the animal or the plasma fibronectin (Sundström et al. 1985; Nag et al. 2002) which leave the vessels following the breakdown of the blood-brain barrier, and can be detected by immunohistochemical reaction. The territories labeled by the abovementioned tracers are to be compared in double-labeling experiments to the territory where the cerebral vessels are immunoreactive to laminin but not to β-dystroglycan.

Perivascular glia can be detected by the immunohistochemical staining of GFAP (glial fibrillary acidic protein), the characteristic intermediate filament protein of mature astrocytes (Bignami et al. 1980). However, according to several studies, not all the astrocytes are detectable by this way. It is necessary, therefore, to examine other astroglial markers, *i.e.*, glutamine synthetase, and S100 protein (Ludwin et al. 1976; Martinez-Hernandez et al. 1977). Glio-vascular connections can be studied by confocal microscopy on specimens double-labelled for glial markers *plus* laminin, β-dystroglycan or endothelial marker (*e.g.*, RECA; Duijvestijn et al. 1992).

Electron microscopy and electron microscopic immunohistochemistry were also applied to investigate the correlation between the absence of β-dystroglycan and/or presence of laminin immunoreactivity and presence/absence of glio-vascular connections.

The lesions were cryogenic lesions. A previous study already described the alterations of laminin and β-dystroglycan immunopositivities following longer survival periods (Kálmán et al. 2011). In the present study the *post-lesion* time intervals were: immediate *post-lesion* fixation, or 5, 10, 30 min. There is, however, a time limit, within the immediate *post-lesion* events are impossible to follow confidently with classic, *post-mortem* methods. This early events are to be *in vivo* monitored. The multiphoton microscope allows examination of thick specimens, including living brain. The *in vivo* investigation, however, needs *in vivo* staining. A possibility is a supravital fluorescent labeling. The astrocytes can be labeled with sulforhodamine 101 (Nimmerjahn et al. 2004) whereas the exudation can be detected applying *e.g.*, fluoresceine isothiocyanate (FITC)-dextran. Before the lesion, the observation of the intact brain is also interesting. It can be visualized, whether the glio-vascular connections are stable or dynamic (attaching/detaching), whether the decoupling of the cell processes precedes or follows the breakdown of the blood-brain barrier.

Materials and Methods

Animals

Adult rats (Wistar) of either sex weighing 250 to 300 g were to be used, supplied with food and water *ad libitum,* and kept in artificial 12/12 h light-and-dark periods. All experimental procedures were performed in accordance with the guidelines of European Community Council Directive (86/609/EEC). For multiphoton experiments mice were used kept in similar circumstances since the holder of the instrument was not large enough for rats.

Cryogenic lesions

Cryogenic lesions were performed in deep ketamine-xylazine anaesthesia (20 and 80 mg/kg body weight, resp., intramuscularly). The skin was opened and a bone piece was removed by drilling, so a 'window' was formed on the skull. The lesion was performed on the dorsoparietal cortex by a copper rod adjusted to a stereotaxic instrument and cooled in carbondioxyde 'snow', contacted for 20 sec the brain surface covered only with leptomeninx. Preliminary experiments suggested that the optimal time is 20 sec. In this case the lesions were quite large and similarly sized. Then the bone piece was reposed and the skin sutured. Survival periods were 5, 10, 30 min or in some cases the brains were fixed immediately *post-lesion.*

Fixation and sectioning

Anaesthesia was similar as before. The animals were perfused through the aorta with 100 ml 0.9% sodium chloride followed by 300 ml 4% paraformaldehyde in 0.1 M phosphate buffer (pH 7.4). After perfusion brains were removed and post-fixed in the same fixative for 1-2 days at 4 °C. Then serial coronal sections of 50 μm were cut with Vibratome through the lesioned area, and washed in phosphate buffered-saline 0.1 M, pH 7.4 (PBS, Sigma) overnight. To check whether perfusion has an influence on the distribution of exudate, some experiments were repeated with immersive fixation but it did not affect the immunohistochemical reactions.

Immunohistochemistry

Floating sections were pretreated with normal goat serum diluted to 20% in PBS for 90 min to block the non-specific binding of antibodies. This and the following steps were fol-

lowed by an extensive wash in PBS (30 min, at room temperature). Primary antibodies were diluted to as described in Table 1, in PBS containing 0.5% Triton X-100 and 0.01% sodium azide. Sections were incubated for 40 h at 4 °C. Fluorescent secondary antibodies (Life Technologies, Eugene, OR, USA; fluorogens: Alexa 488 and 555) were used at room temperature for 3 h. The sections were finally washed in PBS at room temperature for 1 h, mounted onto glasses, cover-slipped in a mixture of glycerol and bi-distilled water (1:1), and sealed with lacquer. Control sections were done by substituting the primary antibody with normal serum. No structure-bound fluorescence was observed in these specimens.

Area of *post-lesion* exudation was estimated with immunohistochemical detection of plasma-fibronectin or immunoglobulins exudated. These labelings were combined with immunohistochemical reactions against laminin or β-dystroglycan.

In double-labeling experiments the corresponding primary antibodies were applied together, otherwise the protocol was similar as before.

Fluorescent microscopy and digital imaging

Slides were photographed by a DP50 digital camera mounted on an Olympus BX-51 microscope (both from Olympus Optical Co. Ltd, Tokyo, Japan), or, in the case of double labelings, by a Radiance-2100 (BioRad, Hercules, CA) confocal laser scanning microscope. Digital images were processed using Photoshop 9.2 software (Adobe Systems, Mountain View, CA) with minimal adjustments for brightness and contrast.

Preembedding electron microscopic immunohistochemistry

In this case 0.5% glutaraldehyde is added to the perfusive solution for a better fixation. The immunohistochemical reaction was performed on vibratome sections according to the avidin-biotinylated peroxidase (ABC) method against β-dystroglycan and laminin. In this case endogenous peroxidase was inactivated with 3% H_2O_2 in PBS, for 5 min, at room temperature, followed by an extensive washing in PBS at room temperature for 30 min. Incubations with normal goat serum and primary antibodies (see in Table 1) occurred as above, except for that Triton X-100 detergent was reduced to 0.1% to decrease the tissue destruction. Procedure continued by applying biotinylated antibodies, followed by the avidin-biotinylated peroxidase complex (both from Vector Laboratories, Burlingam, CA, USA). Both incubations lasted for 90 min at room temperature, and were followed by PBS at room temperature for 30 min. To visualize the immunohistochemical reaction product 0.05% 3,3'-diaminobenzidine-tetrahydrochloride (DAB) and 0.01% H_2O_2 in Tris-HCl buffer (0.05 M, pH 7.4, at room temperature) were used. The peroxidase-reaction was stopped at visual color control replacing the solution by changes of PBS.

Electron microscopic investigation

Following the immunoreactions tissue areas were selected under light microscope, and were cut from the vibratome sections. They were immersed for 30 min into 1% osmium tetroxide solution in phosphate buffer (0.1 M, pH 7.4), then washed in phosphate buffer and dehydrated through a graded series up to absolute ethanol. Following immersion in propylene oxyde (10 min), the tissue pieces were embedded flat into epoxy resin (Durcupan, Fluka). Semithin sections were cut with a Reichert Ultracut S ultramicrotome, the proper wereas were selected and the samples were adequately trimmed, then ultrathin sections were prepared with the same ultramicrotome. Finally, ultrathin sections were mounted on grids. The photomicrographs were taken by a JEOL 100B elecron microscope equipped with a Sys Morada digital camera.

Multiphoton microscopy

The multiphoton microscope is based on the phenomenon that the energy of two photons may randomly summed to achieve the absorption thus the required excitation wavelength is approximately twice of the wavelength required in the case of a one-photon absorption of the dye. That means, red-infrared range can excite molecules in UV-blue-green range. Deep tissues are accessible due to the less light scattering of the longer wavelength light applied. This method makes possible the microscopic investigation of the living, *in situ* brain in the depth of hundreds of micrometers. The instrument (Femtonics 2D-Inverted Multi-Photon Laser Scanning Microscope, INMIND 278850) was provided by the Institute of Biophysics and Radiation Biology of Semmelweis University.

In 2 h before the experiment supravital dyes (sulphorhodamine 101 and FITC-dextran, 70 kDa) were administered through the caudal vein. The skull and envelopes have been removed, and the intact brain was also studied. The lesion was performed as described above. Immediately after lesion the animals were positioned into the instrument.

Results

Area of exudation corresponded to the area of altered vascular laminin and β-dystroglycan immunoreactivity

The lesioned tissue was well recognizable in transparent illumination as a lens-like light area with darker border zone (Fig. 1a). Following a 30-min postoperative period this territory was completely penetrated by exudate (Fig. 1b). Anti-rat

Table 1. The primary antibodies applied in the study.

Against	Type	Supplier	Code	Dilution	Final concentration (μg/mL)
β-Dystroglycan	Mouse*	Novocastra, Newcastle upon Tyne, UK	ncl-b-dg	1:100	0.19
Fibronectin	Rabbit**	Sigma, San Louis, MO, USA	F 3648	1:200	***
GFAP	Mouse*	Novocastra, Newcastle, upon Tyne, UK	ga5	1:100	100
Glutamine synthetase	Mouse*	Transduction Labs., Erembodegem, Belgium	610518	1:100	2.5
Rat immuno-globulin	Goat**	Thermo Scientific, Rockford, IL, USA	31680	1:200	***
Laminin 1	Rabbit**	Sigma, San Louis, MO, USA	l 9393	1:100	5
RECA-1	Mouse*	ABCAM, Cambridge, CO, USA	ab9774	1:1000	100
S100	Rabbit**	Sigma, San Louis, MO, USA	s-2644	1:200	81

*monoclonal, **polyclonal, ***no data (the original concentration is not given by the supplier)

immunoglobulin and anti-fibronectin marked the same area. In the intact brain tissue some vessels are also marked with anti-rat immglobulin and anti-fibronectin immunostaining.

Vascular laminin immunoreactivity was detectable throughout in the area of lesion and the vascular β-dystroglycan immunoreactivity has disappeared (Fig. 1c and d). When laminin and β-dystroglycan immunostainings were combined vascular laminin immunopositivity was usually confined to the vessels not labeled for β-dystroglycan (not shown, see Kálmán et al. 2011). Sections that were double stained against laminin and rat immunoglobulin revealed that laminin marked the vessels in the territory penetrated by immunoglobulin (compare Fig. 1b and c). Similarly, double immunostaining for β-dystroglycan and fibronectin revealed that lack of β-dystroglycan immunopositivity corresponded to the area of exudation.

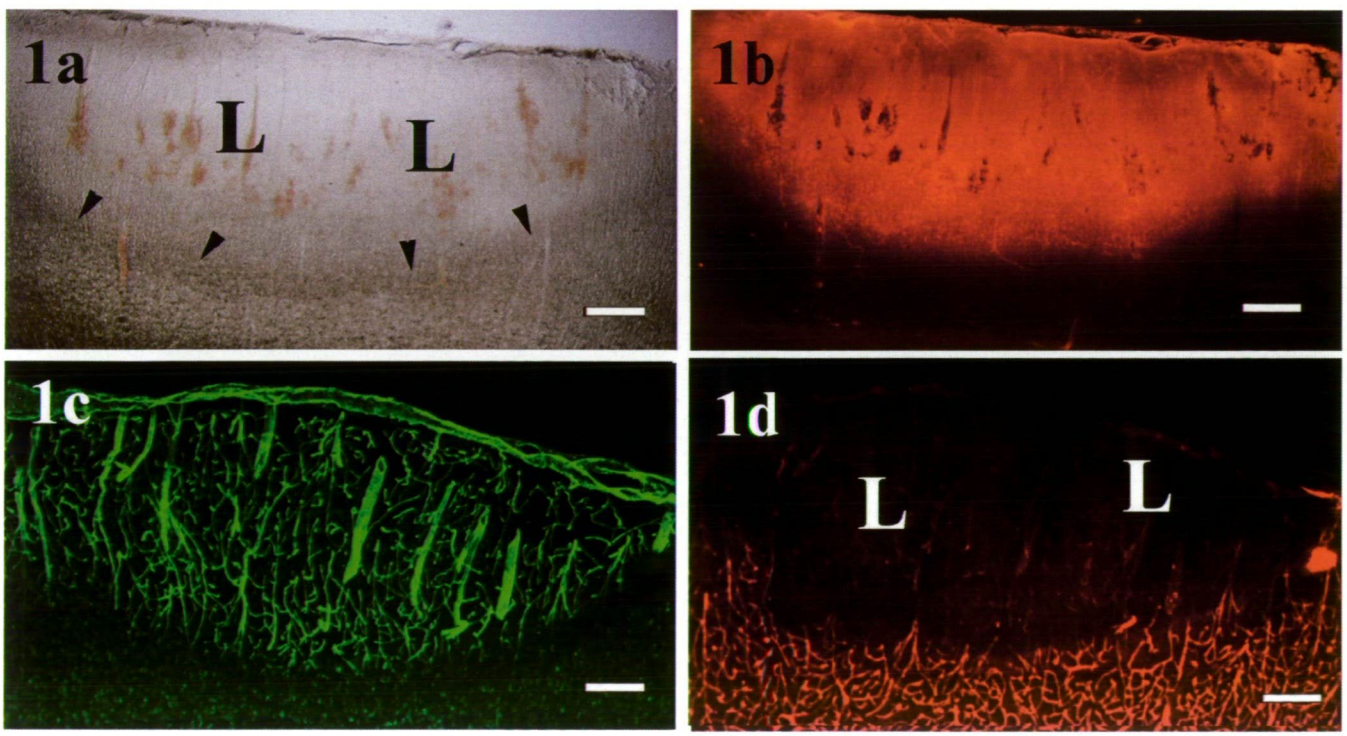

Figure 1. Cryogenic lesions in 30 min after operation. a) Transparent illumination. The area of lesion (L) is lighter, surrounded by a darker border zone (arrowsheads). b) Immunostaining for rat immunoglobulin demonstrates exudation in the whole area of lesion. c) Laminin immunostaining, a number of vessels (probably all of them) are immunopositive to laminin in the territory of lesion but not in the intact tissue. d) β-dystroglycan immunoreactivity is missing in the territory of lesion (L). Apart from this territory the vasculature is intensely labeled. Scale bars: 200 μm.

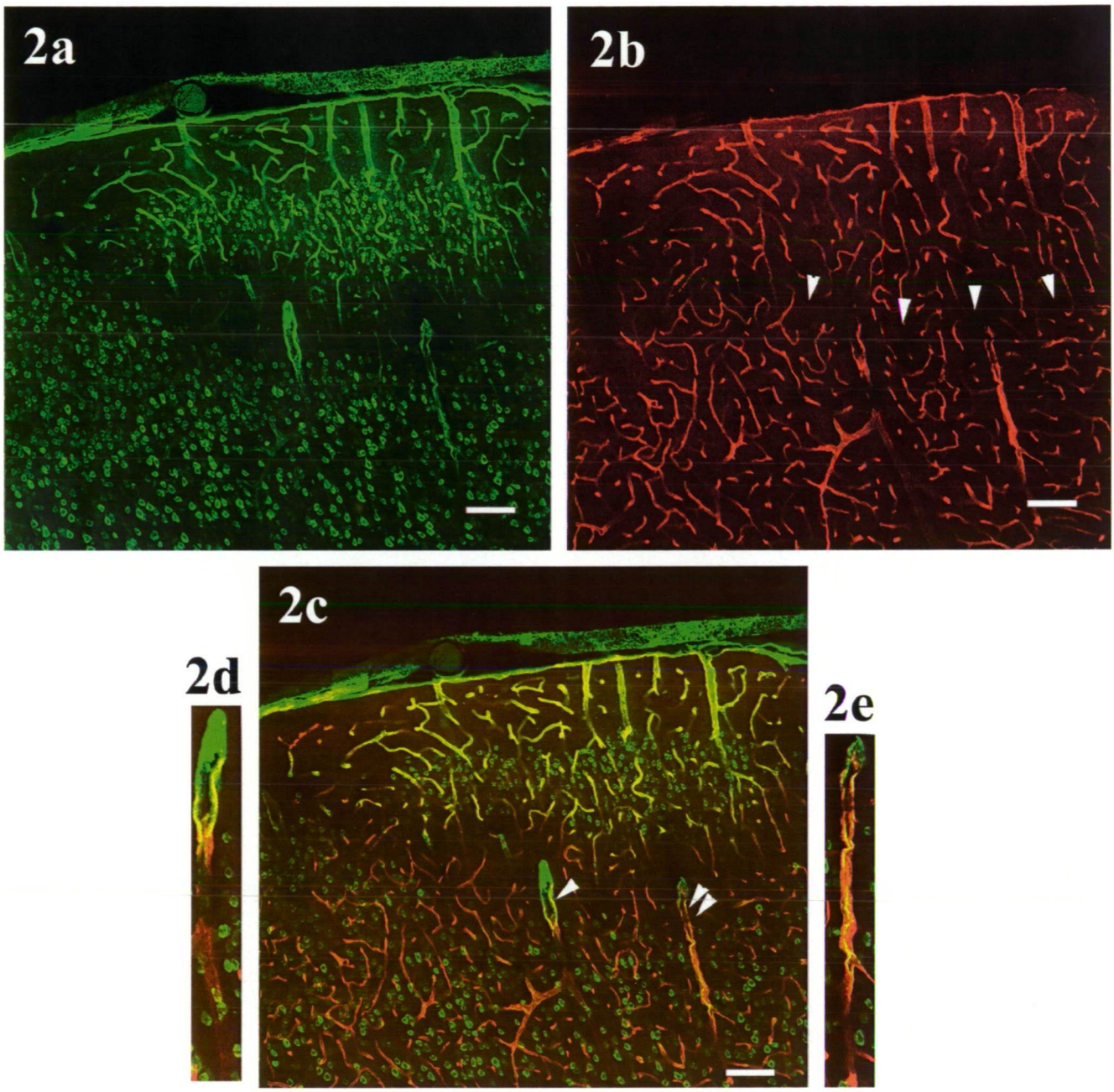

Figure 2. Double labeling for laminin and β-dystroglycan following immediate post-lesion fixation. a) Vascular laminin immunopositivity has appeared. The small green spots (arrowheads) are laminin-immunopositive neurons, it also occurs in the intact brain (see *e.g.*, Powell and Kleinmann 1997). b) The vessels are still immunopositive for β-dystroglycan. c) The merge picture demonstrates that the two immunopositivities are co-localised. d and e) High-power photomicrographs show that change of immunopositivity is gradual. Scale bars: 100 μm; for panels d and e: 50 μm.

Effects of immediate and short-timed fixations: laminin changes abrupt, exudation gradually, later dystroglycan

In the brains fixed immediately following the lesion the laminin immunopositivity already was found in the vessels througout the area of lesion. However, the β-dystroglycan immunopositivity had not disappeared. Even in five minutes several vessels were still immunopositive and even at ten minutes some immunopositive vessels were found. When

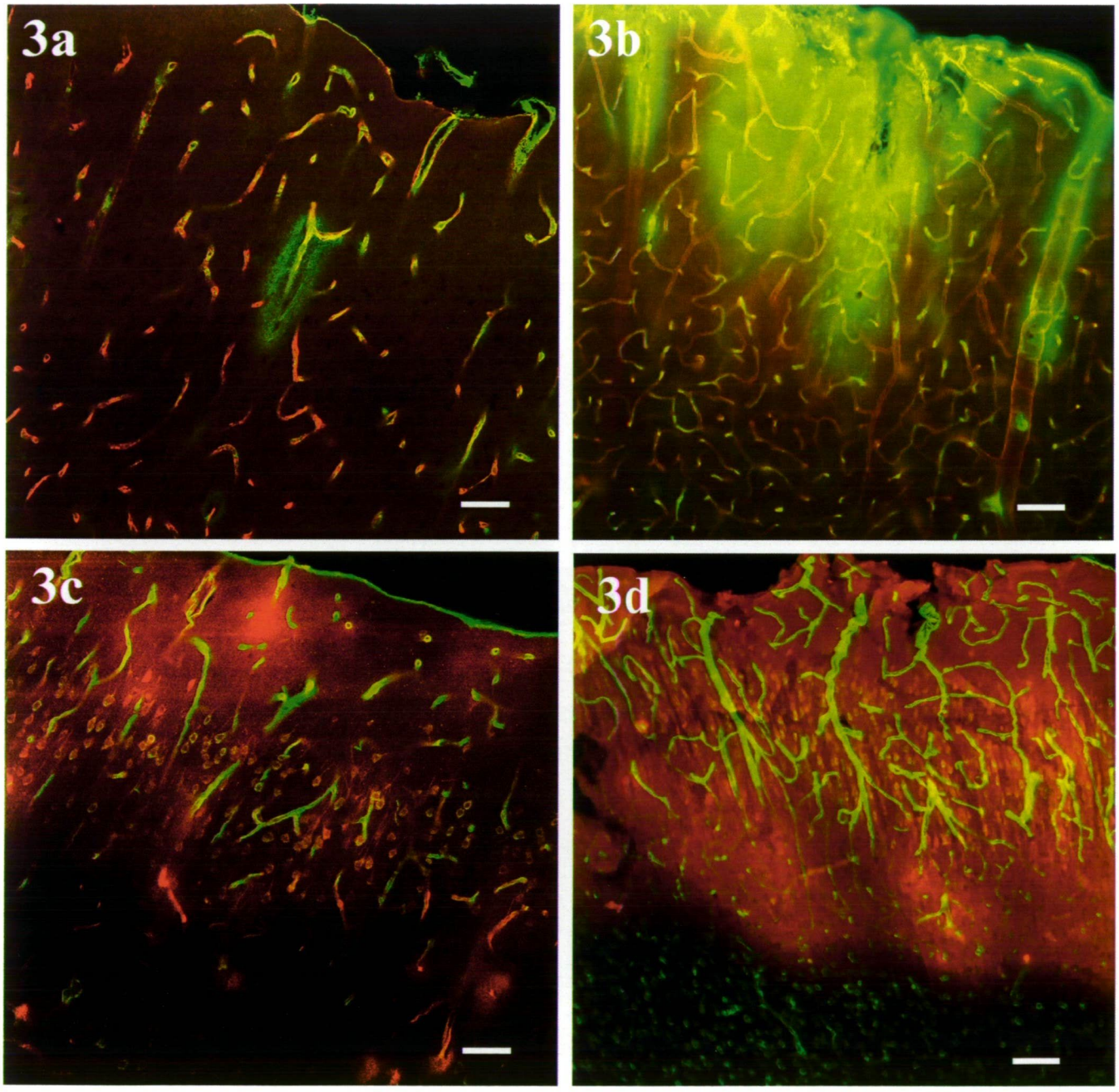

Figure 3. Double labeling for vessels and exudate. a) Immediate fixation. Vascular β-dystroglycan immunostaining (red) still exists but some vessels are surrounded with exudated fibronectin (green). b) In ten minutes the exudate-penetrated areas are almost confluent with each other. c) Immediate fixation, labeling of laminin (green) and rat immunoglobulin (red). The exudate is still confined to strips adjacent the vessels, even not each of them. d) In ten minutes the exudate has penetrated almost the whole area of lesion. Scale bars: 70 μm.

double labeling was applied for laminin and β-dystroglycan immunopositivity (Fig. 2), laminin-immunopositive vessels also proved to be immunopositive for β-dystroglycan. Confocal microscopy demonstrated that the former one appeared at first only discontinuously (Fig. 2c-e).

In these brains the exudate was still confined to stripes adjacent to vessels (Fig. 3a and c), even not each of them. In brains fixed by ten minutes the exudate penetrated continuously almost the whole area of lesion (Fig. 3b and d). Despite the exudation, β-dystroglycan immunopositivity was still detectable in the vessels surrounded with exudate (Fig. 3a and b).

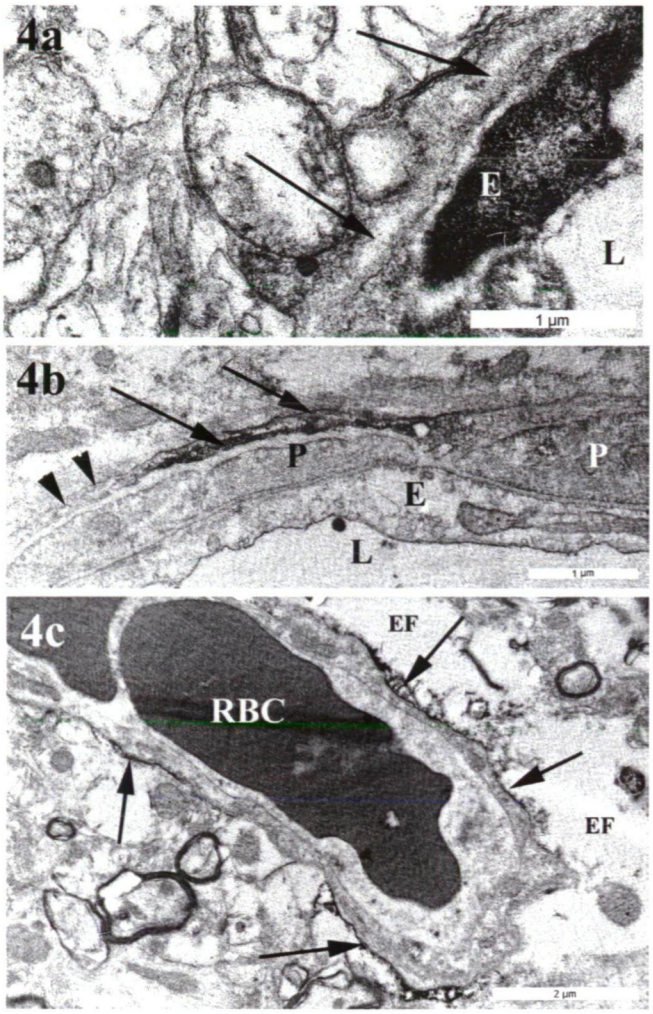

Figure 4. Electron microscopic investigation following immediate post-lesion fixation. a) Gap (arrows) between the glial and endothelial basal laminae in the lesioned area. b) Laminin immunopositivity (arrows) between the separate glial and endothelial basal laminae. Arrowheads point to tight cell contact without immunohistochemical reaction product. c) β-dystroglycan immunopositivity (arrows) around a capillary. Swollen astrocyte endfeet (EF) may imitate 'perivascular gaps'. E – endothelial cell, L – capillary lumen, P – pericyte, RBC – red blood cell.

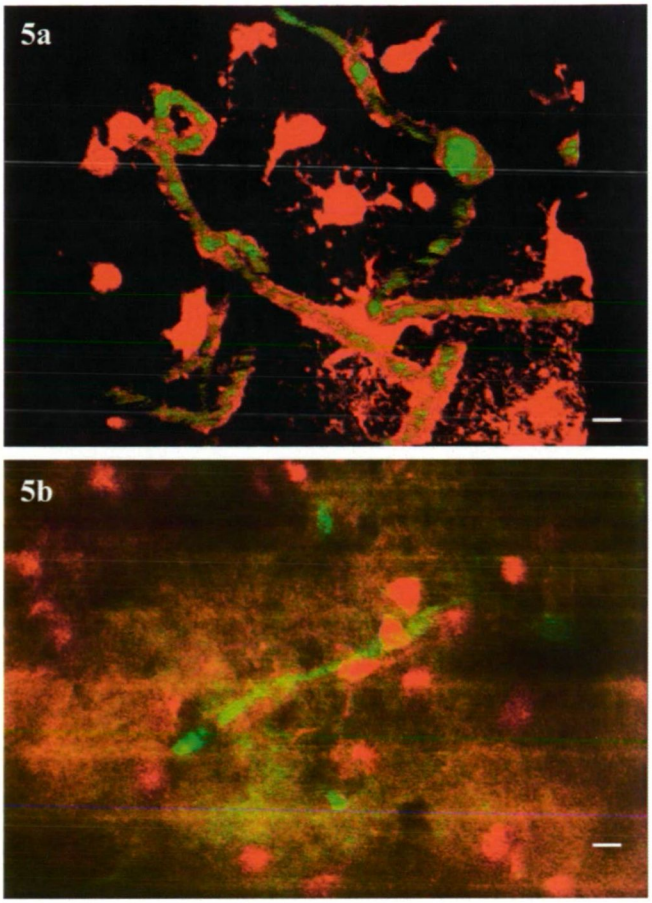

Figure 5. Multiphoton microscopic investigation. a) Intact brain, note the glio-vascular connections. b) Immediately following cryogenic lesion. Exudate almost covers the vessel and the astrocytes. Glia-covered vascular surface is smaller but connections still exist. Astrocytes are labeled with sulphorhodamine 101, vessels with FITC-dextran (Mw 70 kD). Scale bars: 10 µm.

When glial markers were applied, connections were detected on the vessels visualized with RECA or labeled for laminin or β-dystroglycan, although the visualized glial processes did not completely surrounded the vessels (not shown). Astrocytes had not got yet the classical shape of the reactive glia which appears only in a few days *post-lesion* (see, *e.g.*, Kálmán et al. 2011).

Electron microscopic observations

Two different alterations were found around the vessels in the area of the lesion: the glial and endothelial basal laminae were going to separate and the perivascular glial endfeet were swallen so they seemed to be 'perivascular gaps' (Fig. 4a-c). The electron microscopic observations supported the data on the localisations of laminin and β-dystroglycan. Laminin immunoreactivity appeared between the separate glial and endothelial basal laminae (Fig. 4b) whereas β-dystroglycan immunoreactivity was found within the endfeet (Fig. 4c). Such wide, true perivascular spaces, however, which were shown by Jaeger and Blight (1997) we never seen.

Multiphoton microscopy

In the intact brain the FITC-isothiocyanate delineated the vessels, and sulforhodamine 101 visualized astrocyte processes so glio-vascular connections were visible (Fig. 5a).

In the intact brain the glio-vascular connections proved to be stable, no spontaneous detaching/attaching of the processes was observed. Following lesion the bloodstream stopped, hemostasis formed, the vessels became 'leaky' and the tracers penetrated the surrounding area. The glio-vascular connections were not clearly detectable. At the margin of the area of lesion bloodstream and glio-vascular connections were still observed. No motion of astroglial processes were found during 30-min *post-lesion* periods, which overlap the delay resulted by the fixation in the *post-mortem* investigations was observed.

Discussion

Correlations between the phenomena investigated

The results presented here are in accordance with previous data on the immunoreactivities observed in the intact brain, as well as on the post-lesion alterations of laminin and β-dystroglycan (Kálmán et al. 2011). New result is that the territory, where laminin gained immunopositivity and β-dystroglycan lost it corresponded to the area of exudation marked by either fibronectin or rat immunoglobulin immunostaining. Cryogenic lesion caused an immediate leakage of plasma proteins. These alterations become near complete by 10 min. The laminin immunoreactivity appeared before the leakage of the blood-brain barrier which, however, preceded the disappearance of β-dystroglycan immunoreactivity. These phenomena, both β-dystroglycan immunonegativity and laminin immunopositivity, can be regarded as indirect signs of glio-vascular decoupling.

The mechanisms supposed

To explain these phenomena we accept the opinions of Krum et al. (1991) and Milner et al. (2008). In the brain there are two basal laminae around the vessels, an astroglial one and an endothelial one which fuse into a common glio-vascular basal lamina, except in the circumventricular organs and in the Virchow-Robin spaces where laminin immunoreactivity remains detectable. It is supposed therefore that the fusion of the basal laminae has a "hiding" effect on laminin epitopes (Krum et al. 1991) making them unavailable for immunoreagents. The phenomenon that the vascular and glial laminins are detected following lesions may be attributed to a *post-lesion* separation of glial and vascular basal laminae (Krum et al. 1991; Sixt et al. 2001; Hallmann et al. 2005): the laminin epitopes become temporarily 'uncovered'.

Post-lesion disappearance of the β-dystroglycan immunoreactivity is attributed to the cleavage of β-dystroglycan by matrix metalloproteinases (MMP 2 and 9), as Milner et al. (2008) suggested it, demonstrating a decrease of β-dystroglycan level with Western-blot studies. MMP (collagenase) activity also promotes the immunohistochemical detectability of cerebrovascular laminin (Mauro et al. 1984).

Electron microscopic and multiphoton microscopic investigations, however, do not support an abrupt withdrawal of the perivascular glial end-feet in such a manner as figures of Jaeger and Blight (1997) demonstrated it following longer *post-lesion* periods.

References

Abbott NJ (2002) Astrocyte-endothelial interactions and blood-brain barrier permeability. J Anat 200:629-638.

Abbott NJ, Patabendige AAK, Dolman DEM, Yusof SR, Begley DJ (2010) Structure and function of the blood-brain barrier. Neurobiol Dis 37:13-25.

Bignami A, Dahl D, Rueger DC (1980) Glial fibrillary acidic protein (GFAP) in normal cells and in pathological conditions. Adv Cell Neurobiol 1:285-310.

Duijvestijn AM, van Goor H, Klatter F, Majoor GD, van Bussel E, van Breda Vriesman PJ (1992) Antibodies defining rat endothelial cells: RECA-1, a pan-endothelial cell-specific monoclonal antibody. Lab Invest 66:459-466.

Hallmann R, Horn N, Selg M, Wendler O, Pausch F, Sorokin LM (2005) Expression and function of laminins in the embryonic and mature vasculature. Physiol Rev 85:979-1000.

Jaeger CB, Blight AR (1997) Spinal cord compression injury in guinea pigs: structural changes of endothelium and its perivascular cell associations after blood-brain barrier breakdown and repair. Exper Neur 144:381-399.

Janzer RC, Raff MC (1987) Astrocytes induce blood-brain barrier properties in endothelial cells. Nature 325:253-257.

Kálmán M, Mahalek J, Adorján A, Adorján I, Pocsai K, Bagyura Z, Sadeghjan S (2011) Alterations in the perivascular dystrophin-dystroglycan complex following brain lesions. An immunohistochemical study in rats. Histo Histopathol 26:1435-1452.

Krum JM, More NS, Rosenstein JM (1991) Brain angiogenesis: variations in vascular basement membrane glycoprotein immunoreactivity. Exp Neurol 111:151-165.

Ludwin SK, Kosek JC, Eng LF (1976) The topographical distribution of S-100 and GFA proteins in the adult rat brain. An immunocytochemical study using horseradish peroxidase labeled antibodies. J Comp Neurol 165:197-208.

Martinez-Hernandez A, Bell KP, Norenberg MD (1977) Glutamine syntethase: glial localization in brain. Science 195:1356-1358.

Mauro A, Bertolotto A, Germano I, Giaccone G, Giordana MT, Migheli A, Schiffer D (1984) Collagenase in the immunohistochemical demonstration of laminin, fibronectin and factor VIII/Rag. Histochem 80:157-163.

Moore SA, Saito F, Chen J, Michele DE, Henry MD, Messing A, Cohn RD, Ross-Barta SE, Westra S, Williamson RA, Hoshi T, Campbell KP (2002) Deletion of brain dystroglycan recapitulates aspects of congenital muscular dystrophy. Nature 418:422-425.

Milner R, Hung S, Wang X, Spatz M (2008) The rapid decrease in astrocyte-associated dystroglycan expression by focal cerebral ischemia is protease-dependent. J Cereb Blood Flow Metabol 28:812-823.

Nag S, Eskandarian MR, Davis R, Eubanks JH (2002) Differential expression of vascular endothelial growth factor-A (VEGF-A) and VEGF-B after brain injury. J Neuropathol Exp Neurol 61:778-788.

Nimmerjahn A, Kirchhoff F, Kerr JN, Helmchen F (2004) Sulforhodamine 101 as a specific marker of astroglia in the neocortex in vivo. Nat Methods 1:31-37.

Powell S, Kleinman HK (1997) Neuronal laminins and their cellular receptors. Int Biochem Cell Biol 29:401-414.

Shigematsu K, Kamo H, Akiguchi J, Kimura J, Kameyama M, Kimura H (1989) Neovascularization in kainic acid-induced lesions of rat striatum. An immunocytochemical study with laminin. Brain Res 501:215-222.

Sixt M, Engelhardt B, Pausch F, Hallman R, Wendler O, Sorokin LM (2001) Endothelial cell laminin isoforms, laminin 8 and 10, play decisive roles in T cell recruiment across the blood-brain barrier in experimental autoimmun encephalomyelitis. J Cell Biol 153:933-945.

Sosale A, Robson JA, Stelzner DJ (1988) Laminin distribution during corticospinal tract development and after spinal cord injury. Exp Neurol 102:14-22.

Sundström R, Müntzing K, Kalimo H, Sourander P (1985) Changes on the integrity of the blood-brain barrier in suckling rats with low dose lead encephalopathy. Acta Neuropathologica 68:1-9.

Szabó A, Kálmán M (2008) Post traumatic lesion absence of β-dystroglycan immunopositivity in brain vessels coincides with the glial reaction and the immunoreactivity of vascular laminin. Curr Neurovasc Res 5:206-213.

Szabó A, Kálmán M (2004) Disappearance of the post-lesional laminin immunopositivity of brain vessels is parallel with the formation of gliovascular junctions and common basal lamina. A double-labeling immunohistochemical study. Neuropath Appl Neurobiol 30:169-170.

Tian M, Jacobson C, Gee SH, Campbell KP, Carbonetto S, Jucker M (1996) Dystroglycan in the cerebellum is a laminin α2-chain binding protein at the glial-vascular interface and is expressed in Purkinje cells. Eur J Neurosci 8:2739-2747.

Uchino M, Hara A, Mizuno Y, Fujiki M, Nakamura T, Tokunaga M, Hirano T, Yamashita T, Uyama E, Ando Y, Mita S, Ando M (1995) Distribution of dystrophin and dystrophin-associated protein 43DAG (beta-dystroglycan) in the central nervous system of normal controls and patients with Duchenne muscular dystrophy. Intern Med 35:189-194.

Waite A, Brown S, Blake DJ (2012) The dystrophin-glycoprotein complex in brain development and disease. Trends Neurosci 35:487-496.

Wappler AE, Adorján I, Gál A, Galgóczy P, Bindics K, Nagy Z (2011) Dynamics of dystroglycan-complex proteins and laminin immunoreactivities and expression due to angiogenesis in the rat brain following permanent bilateral carotid occlusion. Microvasc Res 81:153-159.

Wolburg H, Noell S, Mack A, Wolburg-Buchholz K, Fallier-Becker P (2009) Brain endothelial cells and the gliovascular complex. Cell Tissue Res 335:75-96.

Zaccaria ML, Di Tommaso F, Brancaccio A, Paggi P, Petrucci TC (2001) Dystroglycan distribution in adult mouse brain: a light and electron microscopic study. Neuroscience 104:311-324.

Volume 59(Suppl. 3):370-419, 2015
Acta Biologica Szegediensis
http://www2.sci.u-szeged.hu/ABS

ABSTRACTS
of the
19th Congress of the Hungarian Anatomical Society

June 11–13, 2015

University of Szeged

Szeged, Hungary

The hypothalamic regulation of growth

Bertalan Dudás

Neuroendocrine Organization Laboratory, Lake Erie College of Osteopathic Medicine (LECOM), Erie, Pennsylvania, USA

The hypothalamo-hypophyseal axis plays a pivotal role in the regulation of growth. Growth hormone (GH) is released by the somatotropes from the anterior lobe of the hypophysis and either exerts direct effect on target cells or stimulates the production of insulin-like growth factor (IGF)-I to induce metabolic changes leading to growth.

The release of GH is under the stimulatory effect of the hypothalamic growth hormone-releasing hormone (GHRH) that is antagonized by somatostatin synthesized in the anterior periventricular zone. Both substances reach the anterior lobe through the hypophyseal portal capillaries in the median eminence. In addition, somatostatin appears to directly inhibit the release of GHRH.

The secretion of GHRH and somatostatin is regulated by neurotransmitters, neuropeptides, and hormones. Neurotransmitter systems can control GHRH and somatostatin release by either endocrine/paracrine route, via autocrine regulation based on colocalization of multiple chemical messengers or via direct synaptic contacts. Indeed, in our recent studies we have revealed intimate associations between several neurotransmitter systems and GHRH/somatostatinergic neurons in the human hypothalamus using light microscopic double-label immunohistochemistry. These associations may be functional synapses and may represent the regulatory effect of several neurotransmitters/neuromodulators on growth.

Plasticity of C-fibre spinal afferent neurons

Gábor Jancsó, Péter Sántha

Department of Physiology, University of Szeged, Szeged, Hungary

Lesions of peripheral nerves induce multifold changes in the distribution, connections, chemistry and function of C-fibre primary afferent neurons which transmit pain. Investigations into the mechanisms of lesion-induced neuroplastic alterations suggested a vigorous sprouting into the most superficial layers of the spinal dorsal horn of myelinated A-fibre primary afferents which bind and transport the B subunit of choleratoxin (CTB). Studies in our laboratory have revealed that this phenomenon may largely be explained by a phenotypic change of injured C-fibre afferents expressing increased levels of GM1 ganglioside rather than a sprouting response of A-fibre afferents. Studies on cultured dorsal root ganglion neurons have revealed that GM1 ganglioside plays an important role in both the nociceptive and nocifensor functions of C-fibre primary sensory neurons. Importantly, inhibition of ganglioside synthesis resulted not only in a decreased activation of the major nociceptive ion channel, the transient receptor potential vanilloid type 1 receptor (TRPV1), but also in a decreased expression of the TRPV1 protein. In contrast, the proportions of neurons which show CGRP and/or substance P immunoreactivity or bind the Bandeira simplicifolia isolectin B4 were similar to the control. The capsaicin- but not the high potassium-induced release of calcitonin gene-related peptide (CGRP) was inhibited in DRG cultures pretreated with an inhibitor of ganglioside synthesis. Collectively, these findings suggest that neural gangliosides and/or the enzymes of ganglioside metabolism may be novel targets for the modulation of nociceptor function and pain.

Supported by OTKA K-101873.

Novel approaches to promote neuroprotection and long-distance axon regeneration by enhanced FGFR1 signaling

Lars Klimaschewski, Letizia Marvaldi, Sitthisak Thongrong, Barbara Hausott

Division of Neuroanatomy, Department of Anatomy and Histology, Innsbruck Medical University, Innsbruck, Austria

Nerve injuries cause motor and sensory deficits with often serious clinical consequences such as prolonged paralysis, anaesthesia and neuropathic pain. Improvement of long-distance axon growth is required for faster regeneration of axons to the skin and into target muscles which atrophy in the absence of reinnervation. Primary sensory neurons derived from adult dorsal root ganglia are particularly suitable to study regeneration-associated neuronal plasticity. Their axons rapidly regenerate after lesion because of the permissive environment provided by Schwann cells, cytokines and neurotrophic factors.

FGF-2 is up-regulated in response to nerve injury and has been shown to promote neuronal survival and neurite outgrowth via activation of FGFR1. Our laboratory focusses on the signaling pathways activated by FGFR1 to exert neurotrophic effects and to influence different modes of axon regeneration, such as elongation and branching. FGFR1 overexpression and inhibition of receptor degradation stimulate the neuronal ERK pathway and promote elongative axon growth of adult sensory neurons. Degradation of FGFR1 is reduced by the lysosomal inhibitor leupeptin which leads to enhanced receptor recycling.

Sprouty proteins act as negative feedback inhibitors of the ERK pathway. Down-regulation of Sprouty2 via transfection of shRNA promotes elongative axon growth by peripheral and central neurons. In response to Sprouty2 knockdown, enhanced RTK-induced activation of ERK and Ras is observed, but phosphorylation of Akt and p38 remains unaffected. Adult neurons dissociated from Spry2 knock-out mice reveal enhanced axon outgrowth on laminin exhibiting prominent elongation in neuronal cultures obtained from Spry2+/- mice while Spry2-/- neurons extend more axon branches. Following sciatic nerve crush, significantly more myelinated axons regenerate in heterozygous Spry2+/- mice which is accompanied by faster recovery of sensomotor performance and higher number of motor endplates in distal muscles. Axonal growth-associated-protein (GAP43) mRNA and protein levels are elevated in the distal sciatic nerve of Spry2+/- mice after crush as compared to wildtype littermates.

Furthermore, applying double heterozygous Spry2/4 knockout mice, we analyzed the effects of Spry2/4 deficiency in the brain following local kainic acid (KA) injection into the dorsal hippocampus. Neuronal cell death in Spry2/4+/- mice is significantly reduced in CA1 and CA3c principal neuron layers and in interneurons of CA1 or hilus of the contralateral hippocampus. GFAP labeling reveals significant increases in intensity and number of reactive astrocytes in the contralateral cortex and ipsilateral molecular layer of knock-out mice that exhibit a significant reduction in granule cell dispersion as well.

Taken together, our data demonstrate neuroprotective effects of Spry2/4 reduction in an epilepsy model of KA induced neuronal cell death and corroborate the functional significance of the neuronal Ras/Raf/ERK pathway as well as downstream GAP43 induction for neuroprotection and axon regeneration following nerve injury suggesting a novel role for Spry2 as potential target downstream of FGFR1 (funded by the Austrian Science Fund).

Molecular composition of extracellular matrix in the vestibular nuclei of the rat

Éva Rácz, Botond Gaál, Szilvia Kecskés, Klára Matesz

Department of Anatomy, Histology and Embryology, Faculty of Medicine, University of Debrecen, Debrecen, Hungary

Previous studies have demonstrated that the molecular and structural composition of the extracellular matrix (ECM) shows regional differences in the central nervous system. By using histochemical and immunohistochemical methods, we provide a detailed map of the distribution of ECM molecules in the vestibular nuclear complex (VNC) of the rat. We have observed common characteristics of the ECM staining pattern in the VNC and a number of differences among the individual vestibular nuclei and their subdivisions. The perineuronal net (PNN), which is the pericellular condensation of ECM, showed the most intense staining for hyaluronan, aggrecan, brevican and tenascin-R in the superior, lateral and medial vestibular nuclei, whereas the HAPLN1 link protein and the neurocan exhibited moderate staining intensity. The rostral part of the descending vestibular nucleus (DVN) presented a similar staining pattern in the PNN, with the exception of brevican, which was negative. The caudal part of the DVN had the weakest staining for all ECM molecules in the PNN. Throughout the VNC, versican staining in the PNN, when present, was distinctive due to its punctuate appearance. The neuropil also exhibited heterogeneity among the individual vestibular nuclei in ECM staining pattern and intensity. We find that the heterogeneous distribution of ECM molecules is associated in many cases with the variable cytoarchitecture and hodological organization of the vestibular nuclei, and propose that differences in the ECM composition may be related to specific neuronal functions associated with gaze and posture control and vestibular compensation.

Molecular organization of the endocannabinoid system in the spinal dorsal horn of rodents

Zoltán Hegyi[1], Klaudia Dócs[1], Tamás Oláh[2], Attila Kiss[3], Sándor Gonda[4], Áron Kőszeghy[2], Krisztina Holló[1], Tamás Patonay[3], László Csernoch[2], Miklós Antal[1,5]

[1] Department of Anatomy, Histology and Embryology; University of Debrecen; Debrecen, Hungary
[2] Department of Physiology; University of Debrecen; Debrecen, Hungary
[3] Department of Organic Chemistry; University of Debrecen; Debrecen, Hungary
[4] Department of Botany; University of Debrecen; Debrecen, Hungary
[5] MTA-DE Neuroscience Research Group, Debrecen, Hungary

Although cannabinoids are widely known as powerful regulators of nociceptive information processing, the molecular organization of the endocannabinoid system is poorly defined in the spinal dorsal horn, representing the primary relay station of pain processing pathways. Thus, we investigated the distribution and function of cannabinoid-1 receptor (CB1-R), as well as diacylglycerol lipase alpha (DGL-alpha) and monoacylglycerol lipase (MGL), synthesizing and degrading enzymes of the endocannabinoid ligand 2-AG, in the rodent spinal dorsal horn, using immunocytochemical and calcium imaging methods.

DGL-alpha was primarily associated with dendrites, in close vicinity to synapses, as well as with astrocytic profiles, suggesting that 2-AG can be released by postsynaptic dendrites and astroglial cells. The released 2-AG may activate CB1-Rs, which were found on axonal varicosities of a number of primary afferents and spinal interneurons, as well as on astrocytes. Here we show also, that activation of CB1-R evokes calcium transients in astrocytes, in spinal cord slices as well as in primary astrocyte cultures, which results in Ca-dependent endocannabinoid release. Importantly, the distribution of MGL suggests that 2-AG can be broken down only in some of the axon terminals and glial cells, indicating that 2-AG may act in both phasic and tonic manners.

Our results suggest that the activity-dependent release of 2-AG and consecutive activation of CB1-R may put an unexpectedly diverse signaling mechanism into action. In addition to presynaptic inhibition of various axon terminals, it can also turn on a bidirectional neuron-astrocyte-neuron communication pathway, which may further modulate pain processing in the spinal dorsal horn.

This work was supported by the Hungarian Academy of Sciences (MTA-TKI 242) and the Hungarian Brain Research Program (KTIA_NAP_13-1-2013-0001).

Interleukins in spinal pain processing

K. Holló[1], L. Ducza[1], K. Hegedűs[1], E. Bakk[1], A. Gajtkó[1], K. Dócs[1], Z. Hegyi[1], M. Antal[1,2]

[1]Department of Anatomy, Histology and Embryology, University of Debrecen, Debrecen, Hungary
[2]MTA-DE Neuroscience Research Group, Debrecen, Hungary

Although the contribution of interleukin signaling to the development of chronic pain is generally accepted, our present knowledge about the cellular expression of interleukin receptors and their ligands in the spinal dorsal horn is insufficient. There is general agreement in the literature that due to the activation of nociceptive primary afferents (among other substances) pro-inflammatory cytokines are released from glial cells which will act on their neural receptors, resulting in the modulation of neuronal excitability.

Based on gene expressional data (TLDA method) our work focused on the study of the pro-inflammatory cytokine, interleukin-1beta and the ligand-binding unit of its receptor (IL-1R1) in the spinal dorsal horn in the Complete Freund Adjuvant (CFA)-induced inflammatory pain model. In agreement with the TLDA results, Western blot analysis showed a gradual increase of IL1-R1 protein during the course of the model. Immunohistochemical investigations revealed that in the superficial spinal dorsal horn in addition to neurons IL1-R1 is abundantly expressed by astrocytes and only sparsely by microglial cells in animals suffering from CFA-evoked inflammatory pain, while IL-1beta is primarily synthetised by astrocytes. Factors that stimulate the synthesis and release of IL-1beta were further studied in primary astrocyte cultures.

Our data indicate that spinal astrocytes but not microglial cells play dominant role in interleukin-mediated signaling mechanisms which strongly contribute to the development of central sensitization of spinal pain processing neural circuits in CFA-evoked chronic inflammatory pain. This work was supported by the Hungarian Academy of Sciences (MTA-TKI242) and Hungarian Brain Research Program (KTIA_NAP_13-2013-0001).

Radial and non-radial migratory forms of spinal dorsal horn neurons during embryogenesis

Zoltán Mészár[1], Rita Varga[1], Anita Balázs[1], Fujio Murakami[2], Miklós Antal[1,3]

[1]Department of Anatomy, Histology and Embryology, MDHSC, University of Debrecen, Debrecen, Hungary
[2]Laboratory of Neuroscience, Graduate School of Frontier Biosciences, Osaka University, Osaka, Japan
[3]MTA-DE Neuroscience Research Group, Debrecen, Hungary

Superficial spinal dorsal horn neurons differentiate from late-born progenitor cells and assemble into circuits fundamental for nociception. During their early development they may follow unique migratory pathways since they have to migrate through or around the earlier born neurons populating the deep dorsal horn. To examine this process, we labelled neurons in the cervical spinal cords of mice embryos by in utero electroporation of GFP and BrdU incorporation assays. We found that most of the neurons migrating into the superficial spinal dorsal horn born in a remarkably narrow time interval at around 12.5 gestation day (E12.5) in the ventricular zone of the mouse cervical spinal cord. We also demonstrated that the first neurons arrive to the superficial layers of the dorsal gray matter at around E14. Investigating the immunoreactivity of electroporated neurons for Pax2 and Brn3a, it was revealed that GFP labelled neurons display immunostaining for Pax2 and Brn3a in a non-overlapping manner indicating that the differentiation of superficial spinal dorsal hon neurons into inhibitory (dILA, Pax2 positive) and excitatory (dILB, Brn3a positive) neurons had been completed by E14 – E15. Time-lapse microscopy on electroporated spinal cord explants revealed that the migration of the investigated neurons can be divided into two phases. First they migrate radially, bur after reaching the superficial dorsal horn they change their migratory pathway and move parallel to the pial surface into medio-lateral direction until they find their final destination.

This research was supported by TÁMOP 4.2.4.A/2-11-1-2012-0001 „National Excellence Program". The project was subsidized by the European Union and co-financed by the European Social Fund. Further support was provided by the Hungarian Scientific Research Fund (OTKA PD 108467), the Hungarian Brain Research Program (KTIA_NAP_13-1-2013-0001) and the Hungarian Academy of Sciences (MTA-TKI 242; MTA-JSPS bilateral mobility grant).

The effect and mechanism of action of clonal stem cell lines on the regenerative capacity of the injured spinal cord

Antal Nógrádi, Krisztián Pajer, Tamás Bellák

Department of Anatomy, Histology and Embryology, Faculty of Medicine, University of Szeged, Szeged, Hungary

Spinal cord injury has a devastating effect on the patients, leaving the body without motor and sensory functions distal to the the injury. Transplantation of stem cells provides a successful experimental therapeutic strategy to treat spinal cord injuries.

Clonal stem cells are reliably reproducible cells with constant features. Their possible mechanism of action is based upon their neuroprotective role (preventing the formation of secondary injury), promoting regeneration of injured axons by downregulating the development of the non-permissive glial environment and replacement of lost glial cells and neurons. Indeed, grafting various types of clonal stem cells into the injured cord results in functional improvement and improved morphological characteristics. Our data suggest that undifferentiated clonal stem cells secrete a variety of cytokines and some of the neural growth factors for a limited time after transplantation into the injured cord. On the other hand, some cells of graft origin appear to have been integrated into the injured cord, especially those that have differentiated towards a oligodendrocyte phenotype. The administration of function-blocking antibodies via osmotic pumps along with grafted stem cells nearly completely abolished the effect of stem cell grafting, suggesting a minor, but not negligible role for the stem cell-derived glial and neuronal cells in the cellular replacement process. These data suggest that clonal stem cells exert their effects via multiple mechanisms of action, resulting in considerably improved outcome after a severe experimental spinal cord injury.

Survival and regeneration of adult motoneurons induced by grafted neuroectodermal stem cells following ventral root avulsion injury: The effect of various administration routes

Krisztián Pajer, Zoltán Fekécs, Dénes Török, Tamás Bellák, Antal Nógrádi

Department of Anatomy, Histology and Embryology, Faculty of Medicine, University of Szeged, Szeged, Hungary

Spinal cord motoneurons are severely injured and destined to die due to a ventral root avulsion injury. Stem cell transplantation is a possible strategy to induce the survival and regeneration of the injured motoneurons.

In our experimental model the left lumbar 4 (L4) ventral root of the spinal cord was avulsed in Sprague-Dawley rats, increasing number of NE-GFP-4C neuroectodermal stem cells were grafted into the L4 segment of the spinal cord or injected into the blood-stream and the avulsed ventral root was reimplanted. In control animals only the L4 ventral root was avulsed and reimplanted without stem cell transplantation. After 3 months survival the L4 spinal nerve was labelled with Fast Blue and the transplanted cells were detected by immunhistochemical markers.

The grafted cells settled mainly in the dorsal horn, in the intermedier gray matter and differentiated into neurons or astrocytes. On the other hand, both stem cell-derived astrocytes and neurons were found on the pial surface of the cord, although they appeared to be less differentiated. The stem cells induced a dose-dependent survival and regeneration of the host motoneurons in both transplantation paradigms, but the motoneuron-rescuing effect was considerably lower in the case of intravenous application. Moreover, these motoneurons not only survived but were able to extend their axons into the vacated ventral root and reinnervate the peripheral targets.

Our results provided evidence that both the intravenous or intraspinal application of stem cells are able to promote the survival and regeneration of the host motoneurons.

Spinal microgliosis induced by peripheral nerve lesions: the role of A- and C-fiber primary afferent neurons

Péter Sántha[1], Orsolya Oszlács[1], Ivett Szeredi[1], Hajnalka Hegedűs[2], Gábor Jancsó[1]

[1] Department of Physiology, Faculty of Medicine, University of Szeged, Szeged, Hungary
[2] Department of Anatomy, Histology and Embryology, Faculty of Medicine, University of Szeged, Szeged, Hungary

Lesions of peripheral nerves induce striking microgliosis in the spinal cord. The mechanisms and, in particular, the types of primary afferents crucial for the development of this microglial reaction are unclear. Therefore, in the present study, by making use of the selective C-fibre chemodenervation technique utilizing capsaicin, we examined the contributions of C- and A-fibre primary afferents to the spinal microglial response in the rat.

The sciatic nerve of adult male Wistar rats was either transected or treated perineurally with capsaicin (1%) under anesthesia. Two weeks later, the animals were sacrificed and sections of the lumbar spinal cord were processed for the demonstration of microglia and C-fiber primary afferents by applying OX42-immunohistochemistry and Bandeiraea simplicifolia isolectin (IB4) histochemistry, respectively. The microglia reaction was quantitatively evaluated in thin optical sections obtained with a laser-scanning confocal microscope using an image analysis software.

Peripheral nerve transection resulted in robust microgliosis in the segmentally and somatotopically appropriate regions of the spinal cord. The density of microglial elements increased significantly by 237±36% and 525±78% in laminae I-II and III-X, respectively, as compared to the contralateral control side. In contrast, perineural treatment with capsaicin resulted only in small increases of microglial density by 58±22% and 59±17% in laminae I-II and III-X, respectively.

These findings indicate that transganglionic changes of injured A-fibre afferents predominate in the initiation of the spinal microglia reaction following peripheral nerve injury. The results also suggest that spinal microgliosis may be a good biomarker for neuropathic pain but not peripheral nerve lesions.

Supported in part by János Bolyai Research Felowship of H.A.S.

Prolactin responsive neurons in the maternal rat brain

Melinda Cservenák[1,2], Éva R. Szabó[1,2], Árpád Dobolyi[1,2]

[1]Laboratory of Neuromorphology, Department of Anatomy, Histology and Embryology, Semmelweis University, Budapest, Hungary
[2]Laboratory of Molecular and Systems Neurobiology, Institute of Biology, Hungarian Academy of Sciences and Eötvös Loránd University, Budapest, Hungary

We confirmed previous studies that 2 hours suckling resulted in a widespread induction of pSTAT5 in some forebrain regions such as the arcuate nucleus, the para- and periventricular nuclei, the medial preoptic area, the bed nucleus of the stria terminalis, and the medial amygdala. We also demonstrated by double labeling that pSTAT5 appears in oxytocin neurons in the lateral subcommissural nucleus of the preoptic area. Following direct intracerebroventricular injection of prolactin, pSTAT5 appeared in all the nuclei as following suckling suggesting that prolactin mediated the effect of suckling.

To investigate the time course of prolactin response, pups were allowed to suckle for 30 min, 2 h and 6 h, respectively. At 30 min, only neurons in the arcuate and periventricular nuclei showed significant pSTAT5 labeling. At 6 h, all the nuclei we observed in earlier time points, as well as the posterior intralaminar complex of the thalamus (PIL) contained prolactin-activated cells. Most of the responsive cells in the PIL were identified as TIP39 neurons. In contrast, other TIP39 neurons in the brain did not contain pSTAT5 labeling.

In conclusion, we demonstrated that prolactin affects neurons in a complex spatial and temporal pattern, which overlaps to some degree with the Fos activation pattern following suckling. However, peculiar differences were found including TIP39-containing relay neurons in the PIL, which showed Fos activation immediately after suckling but pSTAT appeared in them with a time delay.

The work was supported by HAS Postdoctoral Research Fellowship Program for MCS, OTKA K100319 and KTIA_NAP_B_13-2-2014-0004 Program.

Protective effects of pituitary adenylate cyclase activating polypeptide (PACAP) in mouse hind-limb ischaemia

Balázs Dániel Fülöp[1], András Császár[1], Dóra Reglődi[1], Zsuzsanna Helyes[2], Balázs Gaszner[1], Andrea Tamás[1]

[1]Department of Anatomy, Medical School, University of Pécs, Pécs, Hungary
[2]Department of Pharmacology and Pharmacotherapy, Medical School, Szentágothai Research Center, University of Pécs, Pécs, Hungary

PACAP is expressed by the central nervous system and peripheral organs. It has neurotrophic, neuroprotective and general cytoprotective effects. It regulates vascular functions: endothelial cells express PACAP and its receptors, and PACAP increases the level of cAMP in smooth muscle cells, resulting in vasodilatation. PACAP protects endothelial cells in vitro against ischaemia and has proangiogenic effects.

In our research we investigated the protective effects of endogenous PACAP in a mouse hind-limb ischaemic model. We ligated the right femoral artery of 5-month-old male wild-type (WT, n=5) and PACAP-deficient (KO, n=5) mice. Blood perfusion in the upper layers of the sole of hind limbs was measured with PERIMED PSI before the ligature, 1 hour and 7 days thereafter. After transcardial perfusion cross sections were cut from the soleus muscle and immunofluorescence staining followed with the endothelium specific anti-lectin antibody.

After the ligature, the proportion of the perfusion of right and left leg showed a significantly greater decrease in KO mice compared to the WT mice. The cross sections of the soleus muscle showed significantly lower capillary density in KO mice compared to WT ones.

We proved that KO mice show a greater decrease of perfusion in acute ischemia, and in ischaemic muscle tissue they have decreased capillary density compared to WT mice. We confirmed, that endogenous PACAP can play an important role in the protection against ischaemia and in subsequent angiogenesis, but for discovering the exact mechanisms further experiments are needed.

Support: MTA-PTE „Lendület" Program, Arimura Foundation, OTKA K104984, PD109644, KTIA_NAP_13-1-2013-0001.

Spine pruning in the frontal cortex leads to abnormal synaptic contacts in a mouse model of schizophrenia

Il Hwan Kim[1], Mark A. Rossi[1], Dipendra K. Aryal[1], Bence Rácz[3], Namsoo Kim[1], Akiyoshi Uezu[1], Fan Wang[1], William C. Wetsel[1], Richard J. Weinberg[2], Henry Yin[1], Scott H. Soderling[1]

[1]Duke University Medical School, Durham, North Carolina, USA
[2]University of North Carolina, Chapel Hill, North Carolina, USA
[3]Department of Anatomy and Histology, Faculty of Veterinary Science, Szent István University, Budapest, Hungary

Psychiatric and neurodevelopmental disorders may arise from anomalies in long-range neuronal connectivity downstream of pathologies in dendritic spines. However, the mechanisms that may link spine pathology to circuit abnormalities relevant to atypical behavior remain unknown. Using a mouse model to conditionally disrupt a critical regulator of the dendritic spine cytoskeleton, the actin-related protein 2/3 complex (Arp2/3), we examined the ultrastructural morphology of frontal cortical pyramidal neuron synapses of these Arp2/3 mutant mice. Our data demonstrate that the main effect of Arp2/3 loss in cortical neuropil is on excitatory synaptic contacts, which leads to a reduction in the number of normal axospinous synapses. Although axonal contacts remain, they either shift directly onto dendritic shafts or form multi-axonal synaptic contacts on the remaining spines. Our findings reveal a mechanism that unexpectedly reveals the inter-relationship of progressive spine pruning, elevated frontal cortical excitation of pyramidal neurons, which may lead to striatal hyperdopaminergia in a cortical-to-midbrain circuit abnormality.

Transcriptomic and proteomic analysis of a human chondrogenic progenitor cell line

Csaba Matta[1,2], Susan Liddell[3], Julia R. Smith[4], Marcos Castellanos Uribe[5], Sean May[5], Nicolai Miosge[6], Ali Mobasheri[1]

[1]Department of Preclinical Sciences, School of Veterinary Medicine, University of Surrey, Guildford, United Kingdom
[2]Department of Anatomy, Histology and Embryology, Faculty of Medicine, University of Debrecen, Debrecen, Hungary
[3]Proteomics Laboratory, School of Biosciences, University of Nottingham, United Kingdom
[4]Bruker UK Limited, Coventry, United Kingdom
[5]The Nottingham Arabidopsis Stock Centre (NASC), School of Biosciences, University of Nottingham, United Kingdom
[6]Georg August University, Goettingen, Germany

Osteoarthritis (OA) is one of the ten most disabling musculoskeletal conditions in developed countries. As there is currently no effective treatment for OA, there is a pressing need for the development of novel therapeutic strategies to preserve articular cartilage. In order to develop such methods a better understanding of normal and OA chondrocyte physiology is necessary. As cells in OA cartilage reside in a significantly altered, inflammatory extracellular matrix, it is logical to assume that these cells may be characterised by a transformed "membranome" – an assembly of plasma membrane ion channels and transporters. This work focuses on the analysis of mRNA and protein expression of plasma membrane proteins in a human chondrogenic cell population from OA knee cartilage with the help of transcriptomics and proteomics. Samples with enriched cell surface proteins were prepared using EZ-Link Sulfo-NHS-SS-Biotin and analysed using the short GeLC-MS/MS method on a Bruker Impact HD instrument. Approximately 25% of the proteins identified were plasma membrane proteins, which support the efficacy of the biotinylation method. In total, different 78 plasma membrane proteins were identified, some of which play important roles in chondrocyte cell biology, such as integrins, CD44, or PMCA4. To further enhance the efficacy of membrane protein enrichment, we are considering combining the biotinylation method with a Triton X-114 phase separation protocol. Correlating ion channel expression with altered function during the development of OA will provide a better understanding of pathophysiological mechanisms controlling disease progression and will contribute to the understanding of cartilage degeneration.

LPS can modify the mineralization of tooth germ

Tamas Papp[1], Krisztina Hollo[1], Eva Meszar-Katona[1], Zoltan Nagy[1], Angela Polyak[1], Szabolcs Felszeghy[1,2]

[1]Department of Anatomy, Histology and Embryology; Faculty of Medicine, University of Debrecen, Debrecen, Hungary,
[2]Department of Oral Anatomy; Faculty of Dentistry, University of Debrecen, Debrecen, Hungary

Several TLR receptor recognized on odontoblasts, however data is scanty about the its developmental effects during tooth development. TLR4 is well known to inhibit mineralization of dentin and cause inflammation by mature odontoblasts and dental pulp cells. However, unlike these pathological functions of TLR4, little is known about the developmental aspect of TLR4 during odontogenesis.

The goal of this work is to investigate the possible presence and role of Toll-like receptor 4 during the development of mouse tooth germ. TLR4 expression was detected by Western blot in developing lower mouse incisors during the bell stage. To learn more about the effects of TLR4, a specific agonist (LPS) was applied to the medium of *in vitro* cultures, followed by Western blot, histochemical staining, *in situ* hybridization and ELISA. Increased accumulation of biotin-labeled LPS was detected in the enamel organ and in preodontoblasts. LPS treatment induced the activation of the NF- B signaling pathway through the degradation of inhibitor molecule (I B). However, no morphological alterations were detected in cultured tissue after LPS addition at the applied dosage. Activation of TLR4 decreased the mineralization of enamel and dentin matrix, as we demonstrated by alizarin-red staining and as decreased levels of collagen type X. mRNA expression of ameloblastin was elevated after LPS administration.

These results indicate that TLR4 may decrease the mineralization of enamel and dentin of the developing tooth and it may trigger the maturation of ameloblasts.

Volume and distribution of the cerebrospinal fluid in dogs

László Reinitz[1], Gábor Bajzik[2], Rita Garamvölgyi[2], Bianka Benedek[1], Örs Petneházy[2], András Lassó[3], Zsolt Abonyi-Tóth[4], Borbála Lőrincz[2], Péter Sótonyi[1]

[1]Department of Anatomy and Histology, Faculty of Veterinary Science, Szent István University, Hungary
[2]Institute of Diagnostic Imaging and Radiation Oncology, University of Kaposvár, Kaposvár, Hungary
[3]School of Computing, Queen's University, Kingston, Canada
[4]Department of Biomathematics and Informatics, Faculty of Veterinary Science, Szent István University, Hungary

The cerebrospinal fluid (CSF) has a central role in multiple symptoms and clinical procedures like myelography or hydrocephalus. Despite that, very little information is available about its volume in dogs. All major dosage systems are based on the assumption that the volume is directly proportional to the bodyweight of the animal, although multiple research data proved that false.

In this study we aimed to measure the volume of the entire CSF using an MRI based in vivo measurement method in 12 healthy, male mongrel dogs, between 2-5 years of age. We developed a SPACE sequence and validated it with two different methods. We measured not only the overall CSF volume, but the volume of every compartment (extra cranial subarachnoid (SA) space, intracranial SA space, ventricles) individually.

Our results show that the correlation between the subjects CSF volume and bodyweight is linear but not directly proportional, while the proportional distribution of the CSF between the compartments is highly constant and independent from the physical measurements (bodyweight, shoulder-height, total spinal length). Based on our data, the first, approximate base values for the canine CSF volume and distribution can be defined which will be very useful in the diagnosis of hydrocephalus or syringomyelia.

Despite the small number of subjects, our findings should be taken into consideration when working with the canine SA space, and any dosage system that uses the traditional approach for the injection of material into the SA space should be reconsidered.

Interstrain differences in ionotropic glutamate receptor subunits enhanced by pilocarpine treatment in mice

Ibolya Török, Endre Dobó, Norbert Károly, Beáta Krisztin-Péva, András Mihály

Department of Anatomy, Histology and Embryology, University of Szeged, Szeged, Hungary

Rodent strains used in epilepsy research have various neurological characteristics. These differences were suggested to be attributed to the diverse densities of the ionotropic glutamate receptor (iGluR) subunits. However, previous studies failed to find interstrain differences in the hippocampal receptor levels.

We supposed that a detailed layer-to-layer analysis of the iGluR subunits in the hippocampus might reveal strain-dependent differences in their base lines and long-term reactions induced by pilocarpine (PILO) between two mouse strains without documented common ancestors.

Levels of iGluR subunits in Balb/c and NMRI mice were compared that underwent PILO-induced severe seizures in the hippocampal layers using semiquantitative immunohistochemistry after two–month post-treatment period. The alterations in the neuronal circuitry were validated by neuropeptide Y (NPY) and neuronal nuclear antigen (NeuN) immunostainings.

Immunohistochemistry showed interstrain laminar differences in some subunits of both the control and PILO-treated animals. The seizure-induced irreversible neuronal changes were accompanied by reduced GluA1 and GluA2 levels. Their alterations were inversely correlated in the individual NMRI mice by Pearson's method. Increase in NPY immunoreactivity showed positive correlation with GluA1, and negative correlation with GluA2.

Basal levels of iGluRs differ in mouse strains, which may account for the interstrain differences in their reactions to the convulsant. Also, strain-dependent changes were found in the iGluR subunit densities of some hippocampal layers after PILO treatment. The ratio of the GluA1 and GluA2 levels might be dynamically fine-tuned by certain delicate intracellular machinery.

Examination of bioactive factors in human milk

Réka Vass[1], Ágnes Kemény[2], Dora Reglodi[2], Janos Garai[3], Zsuzsanna Helyes[2], Ibolya Tarcai[4], Andrea Tamas[1]

[1]Departments of Anatomy, MTA-PTE „Lendület" PACAP Research Team, Pécs, Hungary
[2] Pharmacology and Pharmacotherapy, János Szentágothai Research Center, Pécs, Hungary
[3]Pathophysiology and Gerontology, University of Pécs, Pécs, Hungary,
[4]Unified Health Institutions, Pécs, Hungary

Breast milk contains several bioactive compounds that play important roles in the development of the nervous system and in gaining immuncompetence. Recently, we have shown that PACAP, a multifunctional neuropeptide, is present in high level in breast milk and we have described changes of PACAP levels during lactation. In the present experiment we aimed to examine the changes of MIF, a proinflammatory cytokine, and other bioactive factors (Fractalkine, MIP-1, Eotaxin, MDC, RANTES, EGF,MCP-1, GRO, Flt-3L, CD40) both in the water and lipid phase of milk samples during the first 6 months of lactation. We also analyzed the difference between the milk samples of male and female newborns.

We collected 5 ml milk every month during the first 6 months of nursing. First we separated the milk samples to lipid and water phase by centrifugation. We used ultrasonication to factor the lipid phase to additional lipid and water fraction. We measured the MIF concentration with ELISA, the other bioactive factors with Luminex and the PACAP level with radioimmunoassay examination.

We detected the presence of examined factors in the lipid phase of milk for the first time. We measured higher concentrations in the water fraction than in the lipid fraction. With Luminex technique we also detected significant differences in the concentration of different bioactive factors in 3 different milk fraction during the first 6 month of lactation. Our preliminary examinations did not find significant differences between milk samples of male and female newborns. Our future aim is to establish the exact influence of the above-mentioned factors in the process of lactation.

Support: MTA-PTE "Lendület" Prog., OTKA K10498, Arimura Foundation.

New innovative surgical solutions of congenital laryngeal malformations in newborns

Ádám Bach[1], Balázs Sztanó[1], Zoltán Tóbiás[1], Ilona Szegesdi[2], Péter Gál[3], László Rovó[1]

[1]Department of Otorhinolaryngology and Head- Neck Surgery, University of Szeged, Szeged, Hungary
[2]Department of Anaesthesiology and Intensive Therapy, University of Szeged, Szeged, Hungary
[3]Department of Pediatrics and Pediatric Health Center, University of Szeged, Szeged, Hungary

Congenital malformations of the larynx are relatively rare but may be life-threatening. The most common causes include laryngomalacia, vocal cord paralysis, and subglottic stenosis. Even nowadays, tracheotomy is the most often performed surgical intervention due to respiratory failure. The conventional glottis widening procedures can't be applied on account of the narrow anatomical situation. New minimally invasive surgical procedures were introduced in our clinic to perform airway reconstruction surgeries at the earliest possible age.

The authors present the three most common congenital anomalies of the larynx and describe their surgical treatment. Unilateral endoscopic arytenoid abduction lateropexy, laser aryepiglottoplasty and cricotracheal resecion were performed in a case of laryngomalacia, bilateral vocal cord paraysis and subglottic stenosis. The infants were 8, 4, and 9 days-old, respectively.

Tracheostomy could be avoided in all cases. The infants were extubated successfully after a short postoperative intubation period. No further surgical interventions were required.

Tha cases show that the minimally invasive surgical procedures might be performed even in early childhood. The „quality of life destroying" tracheostomy and its consequential complications could be avoided. Continuous cooperation among the surgical team, the anaesthesiologist and the paediatric intensive care unit may improve the postoperative results.

Pathological aspects of congenital heart defects detected prae and postnatally

Patrícia Forrás, László Kaiser

Department of Pathology, Faculty of Medicine, University of Szeged, Szeged, Hungary

In the past, most of the congenital heart defects belonged to congenital malformations with a dismal prognosis. Due to the improvement of prenatal detection and postnatal therapeutic options, the prognosis dramatically improved.

In our work, we examined the distribution of congenital heart defects between 2004 and 2013 in the Department of Pathology, University of Szeged. We compared our findings with a previous survey conducted between 1996 and 1999 in the same Department, and with international publications. 78 postnatal and 13 prenatal cases were analysed.

In the postnatal heart defects the left to right (LTR) shunt represented 35%, the right to left (RTL) shunt 37%. In 27 % of the cases the dominant finding was obstruction. 1% of the cases belonged to the other category. Out of the 78 postnatal cases, there were 46 males, 32 females. The average survival period was 163 days, the oldest patient was 9.5 years old. In the prenatally detected cases 37% was characterised by obstruction, 26-26%- were the RTL and LTR heart defects. There was operation in 63% of the cases. Associated malformations were seen in 11 cases, including 8 Down syndrome. In 10 cases, prenatal termination of pregnancy was carried out due to the detected malformation, three cases were discovered in spontaneous abortions. Gestational age of the foetuses was 20-23 weeks.

The prenatal detection of congenital heart defects might reach 80-90 % detection rate in specialised centres. Our data indicates that we do not reach this rate, that requires further improvements of prenatal care, also widening and organising the prenatal monitoring system of pregnant women.

Transapical endoscopic investigation model of the tricuspid valve

Mátyás Ilyés[1], Gábor Baksa[1], Gergely Rácz[2], Károly Havlik[1], Tamás Ruttkay[3]

[1]Department of Anatomy, Histology and Embryology, Semmelweis University, Budapest, Hungary
[2]1st Department of Pathology and Experimental Cancer Research, Semmelweis University, Budapest, Hungary
[3]Sana Cardiac Surgery Stuttgart, Stuttgart, Germany

An increasing number of tricuspid valve repairs requires new demonstrational viewpoints of both valvular and subvalvular complex for the better understanding of the correlation between anatomical and functional aspects, and for achieving better patient outcomes. The aim of our study was to reveal the functional anatomy of the tricuspid valve under simulated physiological circumstances on human heart model.

Investigations were carried out in eight *ex situ* human hearts, excluded organs with previous cardiac surgery and/or visible valvular disease. One centimetre wide apical incision was made next to the interventricular groove and the pulmonary trunk was ligated while leaving both caval veins open. In order to document the role of the subvalvular structures, 0 and 70 degrees rigid endoscopes were introduced through the apical incision into the right ventricle under continuous irrigation with saline.

Closure of the valve was properly demonstrated in all cases according to the coaptation areas. The ventricular surfaces of the valve leaflets with their three zones, the five types of adherent chords and the papillary muscle system could be precisely determined. We constructed a 'double triangle' concept, which clearly explains the relative placement of the tricuspid and pulmonary valvular complexes for the better identification of potential vulnerable points during standard surgical stitches.

Our tricuspid valve visualization model provides additional insight into the functional anatomy of the subvalvular complex, supporting the development of safer surgical procedures.

A rare Mullerian-duct anomaly - a missing kidney illuminated the case

Daniel Kardos[1,2], Andras Farkas[1], Dora Reglodi[2], Judit Horvath[2]

[1]Department of Paediatrics, University of Pécs, Pécs, Hungary
[2]Department of Anatomy, University of Pécs, Pécs, Hungary

Mullerian-duct anomalies affect 2-4% of the female population. The spectrum varies from uterus septa to total agenesia. Anomalies of the urinary tract can associate with these malformations, due to their common origin from the intermediate mesoderm. We present a rare case of Mullerian-duct anomaly.

A 16-year-old adolescent girl was admitted at our clinic with progressing abdominal pain. She had experienced periodic abdominal discomfort for several months. Her period started at age 13 (regular hypomenorrhoea). On physical examination a solid abdominal mass was detected in the lower abdomen that extended to the umbilical line. The vulval vestibule was anatomically normal. The ultrasound scan revealed a cyst-like structure arising from the lesser pelvis. On the right side no kidney was found. These findings led us suspect a Mullerian-duct anomaly with double uterus and vagina, with the atresia of the distal end of the right hemivagina. The MRI scan confirmed our hypothesis. The obstructed system was punctured, the retained menstrual blood was aspirated, then the hemivaginas were united by removing the septum partially. During the postoperative period no complications were detected.

Uterus didelphys, obstructed hemivagina and ipsilateral renal agenesis were diagnosed, which is also known as Herlyn-Werner-Wunderlich syndrome. Besides the patient's history and the physical examination, the "incidentally" found renal agenesis helped the diagnosis.

Without embryological background the proper diagnosis and treatment of this malformation would have been impossible. This case is a perfect example to show the importance of embryology in the every day's clinical practice.

Congenital external auditory canal atresia and methods of rehabilititation

Ádám Perényi, Attila Nagy, József Géza Kiss, László Rovó

[1]Department of Oto- Rhino- Laryngology and Head- Neck Surgery, University of Szeged, Szeged, Hungary

Congenital external auditory canal atresia is a disorder with a prevalence of one in 10,000 - 20,000 live births and is bilateral in one third of patients. Because of the different developmental origin of the inner ear and the external and middle ear, the cochlea and sensorial elements are usually unremarkable. With a conductive hearing loss of 60 dB, even unilateral atresia restricts hearing related social skills. The degree of middle ear deformity may make reconstruction surgery impossible or hazardous, thus bone-conduction hearing aids have become the first-line therapy.

Children with unilateral cartilaginous and bony external auditory canal atresia were enrolled. High-resolution computed tomography with three dimensional reconstructions were made to precisely determine the position of the structures of the middle ear and to assist preoperative planning. Reconstruction surgery from retroauricular approach comprised maximal enlargement of the tympanic and mastoid cavities. The cavities were then closed with an adapted conchal cartilage.

Hearing improvement reached the level above the social threshold. The reconstructed auditory canal remained stable and widely patent and facial nerve function was unremarkable during the follow-up period of 1 year.

The authors highlight that surgical reconstruction of the external auditory canal is possible in selected cases. The procedure is safe and effective with a reasonably short surgical time, if it is supported by deep anatomical knowledge, careful preoperative imaging and intraoperative facial nerve monitoring. Stable audiological benefits improve patients' satisfaction and quality of life. If reconstruction surgery is not possible, bone-conduction hearing aids are beneficial.

Extremly large giant coronary aneurysm associated with inferior ST elevation myocardial infarction in adult patient

Tamás Szűcsborus[1], Éva Jebelovszki[2], Ferenc Nagy[1], Róbert Sepp[1], Imre Ungi[1], Tamás Forster[2]

[1]Department of Invasive Cardilogy, Second Department of Internal Medicine and Cardiology Center, Faculty of Medicine, University of Szeged, Szeged, Hungary
[2]Second Department of Internal Medicine and Cardiology Center, Faculty of Medicine, University of Szeged, Szeged, Hungary

A 66 year-old-man was admitted to our department with inferior ST segment elevation myocardial infaction. Coronary angiography revealed thrombotic occluded right coronary artery (RCA). Primary percutaneous coronary intervention of RCA was performed with a thrombus aspiration and bare-metal stent implantion.

Echocardiography (TTE) found an echolucent mass measuring 35 *mm* × *24 mm* in diameter in the pericardial space at the right heart border, however the relationship of the mass to the RCA was not well documented. Computer tomography (CT) demonstrated the mass to be a giant coronary aneurysm (GCA) measuring *38,7 x 32,3 mm* in diameter with a partially trombotic lumen. True lumen of the right GCA was *8 mm* in diameter. CT also found another, smaller totaly thrombotic anuerysm measuring *10 x 13,5 mm* in diameter of the left anterior descending artery.

According to „heart team" decision the patient was treated conservatively by means of oral anticoagulation (OAC) with close medical followup. After three months OAC therapy thrombus burden was only slightly smaller inside the aneurysm. At two years follow up CT showed progressive dilation of the GCA *(52 x 43 mm* in diameter) with lumen widening as well (*10 mm*). Due to progression of the disease heart surgery and aneurysmectomy is under consideration at this time.

Giant coronary artery aneurysm is a very rare disease, but with potentialy fatal complications. GCA may cause coronary artery rupture, thromboembolism and myocardial infarction leading to death. Due to the lack of clinical evidence concerning treatment case by case decision making is advised with close medical follow up.

Investigation of the small arterial vessels of the metacarpophalangeal joints using cryomacrotomisation

Gábor Baksa[1], Kálmán Czeibert[2], András Grimm[1], Péter Szabó[3], János Gyebnár[4], Handschuh Stephan[5], Örs Petneházy[6], Péter Bálint[7]

[1]Department of Anatomy, Histology and Embryology, Semmelweis University, Budapest, Hungary
[2]Department of Anatomy and Histology, Faculty of Veterinary Science, Budapest, Hungary
[3]360gigapixel.com Science Laboratory, Budapest, Hungary
[4]Department of Radiology and Oncotherapy, Semmelweis University, Budapest, Hungary
[5]Veterinärmedizinische Universität, VetCore Facility for Research, Wien
[6]College of Natural Science and Mathematics, University of Alaska, Fairbanks
[7]3rd Department of Rheumatology, National Institute of Rheumatology and Physiotherapy, Budapest, Hungary

Modern ultrasonography allows detailed imaging of small hand joint vessels from their origin up to entering the bones. This investigation modality is becoming mandatory in the follow-up of patients with chronic articular inflammation e.g. rheumatoid arthritis.

The aim of our study was to find a proper method to investigate the arterial supply of the 2nd - 5th metacarpophalangeal joints (MCP) of the hand, which should give the basics of data acquisition about these vessels in a future larger population in order to differentiate between normal and pathologic states.

The left hand of a 38-year-old woman were harvested above the wrist. The vessels were injected through the radial and ulnar arteries with red coloured resin. After polymerisation the hand was embedded into gelatine and stored at -80 °C. Cryosectioning of this block was then carried out in the frontal plane with a CNC machine calibrated to 0,1mm thickness. Each layer surface was then digitally photographed. 3D reconstructions were made.

From the resulting 516 layers 156 contained the investigated joints. The joint capsules were visible everywhere, but some on the dorsal sides and the muscle tendons showed unclear boundaries due to tearing of their fibrous tissue. The course of the arteries was detectable between their origin and bony entering, but in some cases their kinking led to discontinuities.

CNC milling combined with vessel injection is a proper method for investigation of metacarpophalangeal blood supply, but improving of surface clarity, reduction of layer thickness are necessary.

Experiences in 3D modeling and printing of a French bulldog skull's composite anatomical structures

Kálmán Czeibert[1], Gábor Baksa[2], István Kozma[3], András Grimm[2], Imre Fekete[3], Stephan Handschuh[4], György Falk[5], Örs Petneházy[6]

[1]Department of Anatomy and Histology, Faculty of Veterinary Science, Budapest, Hungary
[2]Department of Anatomy, Histology and Embryology, Semmelweis University, Budapest, Hungary
[3]Department of Materials Science and Technology, Széchenyi István University, Győr, Hungary
[4]Veterinärmedizinische Universität, VetCore Facility for Research, Wien, Austria
[5]Varinex IT Zrt., Budapest, Hungary
[6]College of Natural Science and Mathematics, University of Alaska, Fairbanks, USA

During academic and postgraduate training demands are getting higher on behalf of students to use new technological achievements (eg. ebook readers, tablet and cellphone related 3D-applications etc.) which give them a unique, interactive way of learning and understanding. We alloyed conventional preparation techniques with digitalization to make a useful 3D-model from a dog.

A French bulldog's cadaver was used to the study. Tubes have been inserted into left subclavian and brachiocephalic arteries and external jugular veins, and after flushing the vessels red methacrylate resin has been injected selectively into the cranio-cervical arterial system. 24 hours later when hardening completed the head has been removed together with neck at the level of the second thoracic vertebra and we placed it into a mixed detergent solution at 64 °C for 3 weeks. Careful bathing in 3% hydrogen-peroxid cleaned further the surface and minor channels from sediments. The bone-vessel composite corrosion cast was scanned with CT, then using different surface and volume reconstruction softwares DICOM images were segmented to distinguish arteries from bones based upon signal-intensity. STL-(Stereolithography) models were exported from both sequences and were eventually printed in 3D to have a concrete, palpable object in corresponding colors.

Using 3D pdf-s and 3D-printing allows us to make unlimited copies from a good resolution model, gives the possibility to modify, label or animate objects thus all the required details can be observed and learned, and helps graduate studies and clinical activities as well.

From cryosectioning to 3D-modeling: complex visualization of a feline head with milling, diagnostic imaging (CT, MRI) and volume rendering methods

Kálmán Czeibert[1], Gábor Baksa[2], Péter Szabó[3], András Grimm[2], Lajos Patonay[2], Szilvia Nagy[4], Péter Bogner[4], Stephan Handschuh[5], Bence Rácz[1], Örs Petneházy[6]

[1]Department of Anatomy and Histology, Faculty of Veterinary Science, Budapest, Hungary
[2]Department of Anatomy, Histology and Embryology, Semmelweis University, Budapest, Hungary
[3]360gigapixel.com Science Laboratory, Budapest, Hungary
[4]Diagnostic Center, Pécs, Hungary
[5]Veterinärmedizinische Universität, VetCore Facility for Research, Wien, Austria
[6]College of Natural Science and Mathematics, University of Alaska, Fairbanks, USA

Diagnostic imaging techniques are widely used in clinical medicine, especially to confirm pathological processes which cannot be detected with other (*e.g.*, ultrasound, x-ray) methods. Main limiting factor is usually resolution and tissue differentiation. In our study we wanted to provide comparable grey-scale and full color images from same locations to help better orientation and diagnostic work.

The study was performed on an adult cat cadaver. Arterial system was injected with red polyurethane resin through both common carotid arteries to improve contrast ratio during later segmentation process, then the head has been fixed into a special methacrylate box designed for this study which prevented displacement during examinations. Isovolumetric CT and MR imaging was performed involving complete skull till the third cervical vertebra. After imaging the whole body was freezed to -28 °C. Head was removed together with the box after concretion to embed layer by layer into a gelatin-water compound and freezed to -80 °C. The block under continuous cooling has been sectioned by 0.4 mm layer-thickness with a CNC milling machine, and each layer were photographed with high-resolution DSLR camera. Finally all the images from the three different modalities were merged into one stack allowing exact comparison of same structures, selective area display, segmentation and 3D reconstruction.

We provide an appropriate method for cryomacrotomisation, which enables precise and efficient work, image capturing and post-processing thereby we could created from these recordings the studied cat's head complex 3D model, including surface, bones, vessels.

Clinical anatomy of Eustachian tube from the aspect of ventilation disorders

András Grimm[1,2], Gábor Baksa[1], Kálmán Czeibert[3], Péter Szabó[4], Stephan Handschuh[5], Örs Petneházy[6], László Tamás[2]

[1]Department of Anatomy, Histology and Embryology, Semmelweis University, Budapest, Hungary
[2]Department of Otorhinolaryngology, Head and Neck Surgery, Semmelweis University, Budapest, Hungary
[3]Department of Anatomy and Histology, Faculty of Veterinary Science, Budapest, Hungary
[4]360gigapixel.com Science Laboratory, Budapest
[5]Veterinärmedizinische Universität, VetCore Facility for Research, Wien, Austria
[6]College of Natural Science and Mathematics, University of Alaska, Fairbanks, USA

Chronic middle ear ventilation disorders are usually caused by inadequate aeration of the Eustachian tube. Many cases with failed aeration converge on minor anatomic variations resulting in tube dysfunction, responsible for the disease.

The aim of our work was to demonstrate these structures.

We used 10 bilateral skull base blocks of formalin-fixed cadavers.

In five of them we performed layer-by-layer anatomical preparation. The same region of four specimens were sliced into 3 mm thick sections. The remaining specimens were histologically prepared for light microscopy investigation.

After injecting both external carotid arteries of a fresh cadaver with resin, we performed milling with a CNC machine, calibrated to 0,1 mm thickness. Layers were then photographed. A 3D model was created based on these photographic images.

We identified the Rüdinger's safety canal and the auxiliary gap -two structures of different role- on each fixed specimen. The inner diameter of the tube varied between 1.6-5.5 mm. The minimum was measured at the isthmus with a mean distance of 26 mm from the pharyngeal ostium. Next to the muscles we identified the Zuckerkandl ligament. On cross-sectional specimens Kirchner's diverticulum – of therapeutic importance -, the Weber-Liel fascia and Ostmann's fat pad - both significantly affecting the tubal function - were also demonstrated. The thickness of the latter varied between 4-18 mm.

The exact knowledge of these anatomical structures is mandatory for making causative therapy and restoring ventilation. These structures can be precisely demonstrated using different anatomical investigation methods.

3D modeling of a horse stifle joint based on fusioned CT and MR images

Örs Petneházy[1], Gábor Bajzik[1], Péter Zádori[1], Zsolt Vajda[1], Rita Garamvölgyi[1], Kálmán Czeibert[2], Imre Repa[1]

[1]Health Center, Institute of Diagnostic Imaging and Radiation Oncology, University of Kaposvár, Hungary
[2]Department of Anatomy and Histology, Faculty of Veterinary Science, Budapest, Hungary

Computed tomography (CT) gives superior spatial resolution possibility for image postprocessing and 3D reconstruction. Magnetic resonance imaging (MRI) makes possible the high resolution visualization of soft tissues of a certain anatomical region. With the combination of the two technique high detailed 3D images can be reconstructed for both, research and teaching.

An isolated horse stifle joint was placed in a special designed container which allowed us to scan the details in the same position during the CT and MR imaging. Isovolumetric CT (0.3 mm slice thickness) and MR (0.6 mm slice thickness) imaging was performed from the middle of the femur to the end of the extensory recess of the long digital extensor muscle. The DICOM images were imported to the 3DSlicer software. Fiducial markers were placed on the clearly remarkable anatomical points on the CT and MR images respectively and transformed and fusioned in a common series. The bones were reconstructed automatically on the CT sequences of the series, the joint cavities and soft tissue structures manually based on the MR sequences. The reconstructed models were saved in .stl format and finished in Autodesk software.

Image fusion gives the possibility for high accuracy 3D reconstruction on series of different modalities. The reconstructed models can be used for 3D printing, animation, virtual surgical planning, virtual arthroscopy and can serve as a base for 3D PDF files which can be used in teaching and education.

Clinicopathological correlation in spontaneous and medically induced abortions

Tamás Tóth, Kitti Brinyiczki, Attila Csikós, László Kaiser

Department of Pathology, Faculty of Medicine, University of Szeged, Szeged, Hungary

The aim of perinatal pathological examinations is evaluation of clinical findings and to offer data for subsequent clinical investigations. They also offer a potential for improvement of prenatal care.

In our retrospective study, we examined a four-year period of abortions in the University of Szeged, between 2009 and 2014. 185 (85 medically induced and 100 spontaneous) abortions were examined following Wigglesworth recommendations.

We studied the occurrence of spontaneous abortions and medically induced abortions, the occurrence of malformations, clinicopathological correlations, foetal and maternal age distribution. We compared our findings with data, available in international publications, with a previous work conducted between 2006 and 2008 at the University of Szeged, and with a similar work from Pécs (1992-1998).

The distribution of malformations in the 85 induced abortions was the following: 15.3% central nervous system (n=13), 10.6% congenital heart diseases (n=9), 7.1% urogenital (n=6), 2.4% gastrointestinal (n=2), 10.6% skeletal (n=9), 38.8% chromosomal defect (n=33). In 3.5% of the cases no morphological anomaly was detected (n=3). There were no isolated pulmonary malformations. 100 spontaneous abortions were examined, in 38% we could not determine the cause of abortion (n=38). There was a high proportion (39%) of chorioamnionitis (n=39), which could be associated with the termination.

Perinatal pathology is an important part of an interdisciplinary collaboration that gives feedback to the clinicians. With its help we can monitor not only the distribution, but the shifts in distribution of malformations.

Body-builder in the service of anatomy teaching

Jozsef Farkas, Zsolt Major, Dora Reglodi

Department of Anatomy, University of Pécs, Pécs, Hungary

The musculoskeletal anatomy is a large portion of the anatomy curriculum. Students are introduced to the anatomical science through the skeletal and muscular structures of the human body. It is crucial for the students to be able to understand the origin, insertion and course of muscles and ligaments. The dissection classes have always been vital in the hands of anatomists for teaching musculoskeletal anatomy. However, it is important for medical students to find the link between theory, cadavers and living patients. For the instructors it has been a great challenge to help students achieve this. Earlier we invited body builders several times to our classes to demonstrate surface anatomy; however, due to the increasing number of students recently we have been unable to provide this experience to all of our students. Based on this practice, we asked a multiple world champion body builder to help us develop new and innovative learning tool for our musculoskeletal module. We took photos of his muscle groups and labeled the images. As a pilot study we introduced these images to some of our students as study aids. Moreover we created practice tests based on the images. Our students received the new tool with great enthusiasm. According to them it not only helped them to understand the material better, but the new, visible connection between theory and the real life motivated them greatly.

Support: TÁMOP-4.1.1.C-13/1/KONV-2014-0001.

Introducing cutting edge technology to the anatomy curriculum at the University of Pécs

Jozsef Farkas[1, 2], Dora Reglodi[1], Gyorgy Nagy[2] and Sandor Vigh[2]

[1]Department of Anatomy, Medical School, University of Pécs, Pécs, Hungary
[2]Department of Anatomy, Ross University School of Medicine, Portsmouth, Dominica

Modern technology is a part of our life. Today, medical doctors utilize cutting edge technology in all fields for the benefit of their patients. It is essential for medical students to learn to live and work with modern technology as early as possible in their carrier.

Turning towards the latest technology in education is a clear tendency now. Newly founded and dynamically developing universities, such as Ross University, School of Medicine, are in the vanguard of utilizing technology in education. This process is significantly slower and more difficult in old medical schools where there are strong traditions of teaching. The University of Pécs (UP), Hungary is one of Europe's oldest universities (founded in 1367 A.D.). In the Medical School at UP the leadership realized the necessity of introducing modern technology to the curriculum, while keeping and respecting the old traditions. The anatomy curriculum provides an excellent opportunity for this. In the anatomy department students meet their first „patient". In the dissection rooms they meet the human body in the traditional way while dissecting cadavers, but at the same time an excellent opportunity is presented to introduce the latest technological innovations utilized both in medical education and clinical practice. With the support of the UP, School of Medicine, the Department of Anatomy started a robust modernization to help the future doctors to meet the challenges of the 21st century.

Clinical Anatomy course at the Department of Anatomy of University of Pécs

Balázs Dániel Fülöp, Dániel Kardos, Tibor Hollósy, Andrea Tamás, Dóra Reglődi

Department of Anatomy, Medical School, University of Pécs, Pécs, Hungary

There are significant differences in the medical curriculum among universities. In some countries (e.g. USA) the students receive less theoretical training and handle patients from the first year of medical school. Although we stand on the necessity of anatomy teaching on cadavers we think that a more clinical approach could be beneficial for medical students.

Therefore, we created an optional course for second year students studying currently splanchnology: Clinical Anatomy. The course was accessible for 20 students parallel with the regular splanchnology semester, following its thematic. Mostly clinicians held the 45-minute lectures in their own clinical fields. The students had the opportunity of practical training: they could try nose endoscope and ultrasound devices, and practice physical examination.

At the end of the course the students evaluated the course based on different questions in a scale from 1 to 10. Based on the students' reviews the course was beneficial for studying regular anatomy (8.55), showed the connection between anatomy and clinical work (9.73) and gave an insight to the clinical work (9.26). We evaluated whether these students have better results at splanchnology exams than students who didn't attend the course, but at this low number of participants we couldn't show significant difference between the two groups.

The course showed that students are concerned in getting more clinical lectures at the beginning of their studies. In the future we plan to start the course also for English program students and establish a Clinical Neuroanatomy course.

Supported by: TÁMOP-4.1.1.C-13/1/KONV-2014-0001.

Borderline Anatomy - A new course in the curriculum of Pécs University

D. Reglődi, B. Fülöp, J. Farkas, K. Szigeti, A. Lubics, A. Tamás, T. Hollósy

Department of Anatomy, Medical School, University of Pécs, Pécs, Hungary

A new optional course was introduced in the medical curriculum on the diverse aspects of anatomy. The topics include interesting anatomy-related topics with many different fields of anatomy. Although this knowledge is not required for the medical curriculum, it might help the student to learn anatomy with more interest and enthusiasm. The course also gives an insight into different kinds of Anatomy curriculum, like what kind of Anatomy does a massage therapist or a veterinary need in comparison to medical students and also shows some other Anatomy teahing systems from different universities worldwide. Expert lecturers were also invited for Dinosaur anatomy and for Anatomy teaching in Art Schools.

Main topics:

Anatomy and Art (Leonardo's Anatomy to modern artists, parallelism between anatomy stuctures and art, creating art from structures; Rembrandt's painting: Dr Tulp's Anatomy);

Dinosaurus Anatomy and Veterinary Anatomy;

Anatomy museums and bone collections;

Anatomy of Tortures and Body Modicifactions;

Anatomy of anthropology (from mummies to skull identifications);

Massage and body building anatomy;

Anatomy Teaching at other Universities;

Eponymes - who is behind the anatomical names?

Students were offered to collect an anatomy-related topic themselves and submit a powerpoint presentation instead of writing a test. In the first semester of the course, 62 students took it and 53 from them submitted a ppt work and only 9 students took the multiple choice test. The experience of the first course show that the acceptance of the course was very good, students enjoyed these broad and interesting „borderline" aspects of anatomy and most students enjoyed preparing for a presentation themselves.

Support: TÁMOP-4.1.1.C-13/1/KONV-2014-0001.

E-learning in anatomy: Online quizzes and dissection lab

Csaba Szigeti, András Mihály

Department of Anatomy, Histology and Embryology, Faculty of Medicine, University of Szeged, Szeged, Hungary

While traditional cadaver-based, instructor-led dissection was proven as the gold standard for teaching anatomy, over the last few decades computer-enhanced learning (e-learning) has evolved rapidly. There is no doubt that e-learning cannot replace the traditional educational methods, but is able to supplement it if designed and used properly. E-learning promotes students' cognitive effectiveness, motivation, and flexibility of learning style. It improves interactivity which places the student into a learner-centered model with stronger learning stimulus. E-learning contents must be developed, managed, delivered and standardized with learning-management system (LMS), which are predesigned software environments offering among others automatic tracking of student activity.

We utilized online interactive quizzes to increase the time spent studying anatomy of voluntary groups of first- and second-year medical students. The learners were responsible for completing the tests according to their own schedule. The tests were delivered through Coo-Space (University's own online platform) and the professional iSpring LMS (iSpring Solutions, Inc., www.ispringsolutions.com). Besides collecting information about the learning styles, the activity and the progress of students, we used questionnaires to measure the subjective opinions concerning the integration of this e-learning technology into the dissection lab practice.

Tempora mutantur... et nos? Teaching anatomy in Hungary and in Germany

Department of Forensic Medicine, Faculty of Medicine, University of Szeged, Szeged, Hungary

Roland Weiczner

Anatomy, the traditional four-semester complex subject is under the "threat" of reduction due to *external factors*; therefore it is considered as an "innocent victim" of curricular reforms by many fellow colleagues. There is, however, a paradoxical *intrinsic need* for the reorganisation, in the light of the new challenges.

To accommodate anatomy better to the changing environment, five questions should be addressed by comparing the German system with the Hungarian model. (1) *What* kind of knowledge should the medical students receive from studying anatomy? Could we agree in a national requirement system, applied by all Departments of Anatomy in Hungary? (2) *Who* should teach anatomy? What could be done for the quality development of teaching faculty? What is the role of student demonstrators, residents, physicians or non-medical scientists in the teaching duties? (3) *Whom* do we teach anatomy? What are the needs of the digital generations, should anatomy recur after the basic and preclinical modules or even after the Hippocratic Oath? (4) *How* should we teach anatomy? The shift from frontal, passive forms of teaching to the interactive, life-oriented modalities seems to be inevitable. (5) *Why* should anatomy be taught? Are the clinicians the "clients", is the anatomy the "supplier"? Do we emphasise enough the skills concerning applied anatomy, such as identifying superficial landmarks of the body, projections of internal organs, understanding sectional anatomy and the clinically relevant relations between structure and function in our current curricula? Or have we got lost in teaching unnecessary data subjected to be forgotten immediately?

Intralingual reflex arc in the rat tongue – a light- and electronmicroscopical study

Károly Altdorfer, Erzsébet Fehér

Department of Anatomy, Histology and Embryology, Semmelweis University, Budapest, Hungary

The most rostral parts of the enteric nervous system are the oral cavity and the pharynx. Our previous investigations demonstrated that a large number of ganglia were located in the tounge. The nerve cell bodies were immunoreactive (IR) for substance P (SP), vasoactive intestinal polypeptide (VIP), neuropeptide Y (NPY). In a few cases somatostatine positive neurons were also observed. A large number of calcitonin gene-related peptide (CGRP) and galanin IR nerve fibres were also oberserved in the tongue, especially in the gustatory epithelium and/or in the connective tissue around them.

In our present study a large number of IR nerve fibres were observed in the epithelium, in the tunica propria around the blood vessels. The other part of them were observed in the ganglia very close situation to the perikarya and to their processes. A large number of VIP and NPY IR nerve processes were also found in the glands and around the blood vessels. Immunocytochemical analysis demonstrated that some IR nerve fibers had axo-somatic and axo-dendritic synapses in the ganglia. In a few cases VIP immunopositive nerve fibres made synapses with the other VIP IR nerve elements.

Therefore, an intralingual reflex arc can exist in these ganglia based on light- and electronmicroscopical analysis, where the SP sensory nerve fibres might be the afferent part of it and can influence the activity of the glands and the blood flow. These intralingual ganglion cells might integrate the afferent informations and/or further send certain informations to the central nervous system.

Development of GABA-erg neurons in the mouse superficial spinal dorsal horn

Anita Balazs[1], Zoltan Meszar[1], Zoltan Hegyi[1], Klaudia Docs[1], Miklos Antal[1,2]

[1] Department of Anatomy, Histology and Embriology, Faculty of Medicine, University of Debrecen, Debrecen, Hungary
[2] MTA-DE Neuroscience Resaurch Group, Debrecen, Hungary

γ-Aminobutyric acid (GABA) is considered to be the main inhibitory neurotransmitter in the central nervous system, which is synthetized by two isoforms of glutamic acid decarboxylase (GAD65 and GAD67) enzyme. In the spinal cord GABA-erg neurons are abundant in the superficial spinal dorsal horn where they substantially contribute to spinal pain processing.

In the present study we investigated the development of the GABA-erg neurons in the cervical spinal cord of wild type and GAD65-GFP as well as GAD67-GFP „knock in" transgenic mice.

NeuN immunhistochemistry revealed, that neurons of the superficial spinal dorsal horn born before E14,5 than migrate to their final destination. Immunostaining for Pax2, an early transcription factor characteristic for GABA-erg neurons, first appeared at E11,5 and showed substantial colocalisation with both GAD65 and GAD67. Furhermore, we observed that the total number of GABA-erg neurons in the superficial spinal dorsal horn increased between E14,5 and E16,5, reached peak at E16,5-E17,5, and decreased after that.

Our results indicate that GABA-erg neurons of the superficial spinal dorsal horn born at E11-E13, migrate to their final destination between E14-E18 than their numbers decline during the late prenatal and early postnatal days.

The work was supported by the Hungarian Academy of Sciences (MTA-TKI 242) and the Hungarian Brain Research Program (KTIA_NAP_13_1_2013_0001).

Effects of D-aspartate and its interaction with L-glutamate on single neurons in striatal slice preparation from chicken brain

Dávid Balázs, András Csillag, Gábor Gerber

Department of Anatomy, Histology and Embryology, Semmelweis University, Budapest, Hungary

Evidence suggest that D-aspartate (D-Asp) is involved in the early development of the brain and modulates adult neural plasticity probably through regulation of neurogenesis. However, the mechanisms and molecular nature of this regulation remain to be clarified. Here we provide data on the postsynaptic effects of D-Asp alongside with L-glutamate (L-Glu) in striatal slices from chicken (1- to 10-day-old) using visually guided patch-clamp technique. Bath application D-Asp and L-Glu produced similar dose-dependent inward currents and an increase in spontaneous synaptic activity in all of the recorded striatal neurons. In the presence of TTX both the NMDA receptor antagonist D-AP5 and the AMPA/kainate receptor antagonist CNQX reduced and the co-application of these two antagonists almost abolished the postsynaptic effects of D-Asp and L-Glu in a reversible manner. In the two studied age-groups (2-3 days and 4-10 days) both D-Asp and L-Glu evoked inward currents were larger in the younger than in the older age-group. Testing the interaction of D-Asp and L-Glu in these striatal neurons we found that co-application of 1 mM D-Asp and 1mM L-Glu produced larger inward currents (165,7%) than 2 mM D-Asp (100%) or 2 mM L-Glu (82,3%) alone. This effect are similar but somewhat smaller than the potentiation observed by the co-application the L-Asp and L-Glu (261,3%). (The data are normalized amplitude % of D-Asp) However, inhibition of all glutamate transporters with TBOA eliminated this potentiating effect in both cases.

Supported by OTKA 109077.

Endoderm derived sonic hedgehog regulate the extracellular matrix patterning during enteric nervous system development

Csilla Barad[1], Nándor Nagy[1,2]

[1]Department of Human Morphology and Developmental Biology, Semmelweis University, Budapest, Hungary
[2]Departments of Pediatric Surgery, MGH, Harvard Medical School, Boston, MA, United States

The enteric nervous system (ENS) is a large neural network in the wall of the intestine which is colonized by a small number of enteric neural crest cells (ENCCs). These multipotent stem cells originate from vagal level of neural tube and migrate rostrocaudally along the entire length of the gastrointestinal tract to differentiate as neurons and glial cells that form the ganglionated ENS. Incomplete migration of ENCCs leads to Hirschsprung disease, a congenital disorder characterized by the absence of enteric ganglia along variable lengths of the distal intestine. Inductive interactions between gut epithelium and mesenchyme have been suggested to regulate the migration and differentiation of ENCCs. However, little is known about the function of epithelial derived factors, such as Sonic hedgehog (Shh), how they influence the intestinal extracellular matrix expression during ENS development.

Hindgut from 6 day old chicken embryo was cultured in the presence of Shh protein or after injection of Shh overexpressing replication competent retrovirus (RCAS)-virus. In presence of Shh the hindgut is aganglionic, while in the presence of Shh inhibitor (cyclopamine) large and ectopic ganglia developed. Shh treatment strongly induced the expression of chondroitin sulphate proteoglycans (CSPGs) such as versican and collagen type IX, whereas cyclopamine reduced the expression pattern of these inhibitory matrix molecules. These results indicate that versican and collagen IX is a candidate for mediating the effects of Shh on ENCC migration. Shh also inhibited the proliferation and promoted the differentiation of ENCCs. Abnormalities of NCC migration and extracellular pattern formation are characteristic of two human intestinal disorders, Hirschsprung disease and intestinal neuronal dysplasia. Our results support an essential role for epithelial-mesenchymal interactions in these aspects of ENS development.

Modelling Alzheimer's Disease with three-dimensional engineered neural tissue

Tamás Bellák[1,2], Anna Ochalek[3], Abinaya Chandrasekaran[2], Viktor Szegedi[2], Hasan Avci[2], Karolina Szczesna[2], Eszter Varga[2], Csilla Nemes[2], Antal Nógrádi[1], Julianna Kobolák[2], András Dinnyés[2,3,4]

[1]Department of Anatomy, Histology and Embryology, University of Szeged, Szeged, Hungary
[2]BioTalentum Ltd., Gödöllő, Hungary
[3]Molecular Animal Biotechnology Laboratory, Szent István University, Gödöllő, Hungary
[4]Departments of Equine Sciences and Farm Animal Health, Faculty of Veterinary Medicine, Utrecht University, The Netherlands

Differentiation of patient-derived induced pluripotent stem cells (iPSCs) into a three dimensional engineered neural tissue (3D-ENT) provides advantages to study the pathophysiology of neurodegenerative disorders including major pathologies such as Alzheimer's disease. Three-dimensional ENTs also allow preclinical analyses of selected neural drug candidates and could be a promising tool for neurotoxicology.

In this study mononuclear blood cells were isolated from genetically and clinically well-characterized patients with Alzheimer's Disease phenotype and from healthy individuals, reprogrammed into iPSCs and differentiated into neurons using an air-liquid interface based, scaffold-free system which allowed generation of a compact 3D neural tissue without added growth factors.

After 6 or 8 weeks of differentiation the 3D-ENTs were characterized with electrophysiology (multi-electrode array, MEA), calcium imaging technique and immunocytochemical methods.

MEA recordings and calcium imaging revealed that ENT neurons exhibited spontaneous firing activity and the evidence of functional synapses. Immunocytochemistry analyses confirmed these results with the presence of various neuronal (beta-III tubulin, NF200kD, MAP2), glial (GFAP, OSP) and synaptic markers (Synaptophysin, VGLUT1/2, VGAT, VAChT). The ENT structures were fairly homogeneous and the majority of cells differentiated into neurons, but we have found areas with strong nestin positivity, which indicates less differentiated cell types, as well as a sign of active proliferation.

In conclusion, these findings suggest that 3D-ENT neurons might be suitable for drug development and studying the pathophysiology of different neurodegenerative disorders, such as Alzheimer's disease, frontotemporal dementia (FTD) or spinocerebellar ataxia (SCA).

This work was supported by grants from EU FP7 projects (STEMMAD, PIAPP-GA-2012-324451; EpiHealth, HEALTH-2012-F2-278418; EpiHealthNet, PITN-GA-2012-317146; D-BOARD, FP7-HEALTH-2012-INNOVATION-1-305815).

Inner ear malformations – anatomical pitfalls in cochlear implant surgery

Gréta Csorba, Ferenc Tóth, Ádám Perényi, József Géza Kiss, László Rovó

Department of Oto- Rhino- Laryngology and Head- Neck Surgery Szeged, Szeged, Hungary

Several inner ear abnormalities result in severe sensorineural hearing impairment therefore require surgical procedure to improve hearing. Cochlear implantation is the most beneficial treatment option for these patients. The inner part of the cochlear implant contains of an electrode array which is surgically placed into the scala tympani and stimulates the spiral ganglion cells. Recent technological advancements in the design of implant electrode array enable to aid the electrode insertion in these cases. These special anatomical situations due to the high risk for complications have a great influence on the postoperative rehabilitation, the hearing and speech development. Prior to the surgery, determined preoperative investigations, including a high resolution computed tomography, are needed in order to measure the cochlear morphology.

The authors demonstrate two cases of inner ear malformations and the outcome results of each cases following the ear surgery. Both patients underwent cochlear implantation. One patient was diagnosed with a variant of Mondini dysplasia, and the other one had multiple middle and inner ear malformation.

Comparative analysis of the results presenting the postoperative hearing development was performed. The possible peri- and postoperative complications were also considered and compared to the benefits of the implantation.

The authors support the idea to perform cochlear implantation in patients with certain inner ear abnormalities. However, careful preoperative investigation, consideration of the cost-benefit ratio and the surgeon's experience are significant factors concerning the postoperative outcome.

Loss of mossy cells in the murine pilocarpine model of epilepsy: cause or effect?

Endre Dobó, Norbert Károly, Ibolya Török, Beáta Krisztin-Péva, András Mihály

Department of Anatomy, Histology and Embryology, University of Szeged, Szeged, Hungary

Pilocarpine (PILO) treatment induces variable pathological changes in the hippocampus, including loss of mossy cells (MCs) and mossy fibre (MF) sprouting, which are often associated with spontaneous recurrent seizures (SRS). Most theories on the epileptogenesis suggest that loss of MCs is of crucial importance in this process.

Our aim was to test whether the loss of MCs is coupled to the characteristic neuropathological landmarks of epileptogenesis after PILO treatment in one rat strain and three mouse strains without documented common ancestors.

Animals which exhibited intense PILO-induced convulsions for at least 30 min were used. After a 2-month survival period, the incidence of epileptic seizures was checked individually by Timm's method for zinc-containing sprouted ectopic MF and by immunohistochemical detection of increased quantity of neuropeptide-Y for hippocampal marker of SRS. The MCs were visualised by immunohistochemistry for calretinin, calcitonin gene-related peptide (CGRP) and GluA2/3 receptor subunit.

The CGRP immunoreactivity was severely reduced in rats exhibiting simultaneous increases in zinc content and neuropeptide-Y immunoreactivity in the supragranular layer and stratum lucidum. However, the calretinin immunoreactivity remained unchanged in the main terminal field of the MCs in each verified individual of all three mouse strains. Extrahippocampal source of calretinin immunoreactivity was excluded by its persistence after transfornical section. The numbers of GluA2/3 immunoreactive hilar cells were reduced to a strain-dependent way.

Our findings suggest that the MCs may survive PILO treatment in mice, but not in rats. Therefore, the loss of MCs may be rather concomitant than cause of the epileptogenesis.

Presence and role of primary cilia on chondrifying high density cell cultures (HDCs)

Nóra Dobrosi, Máté Engler, Csilla Szűcs, Tibor Hajdú, Tamás Juhász, Róza Zákány

Department of Anatomy, Faculty of Medicine, University of Szeged, Szeged, Hungary

The prime candidate for chondrocyte mechanosensation is the primary cilium, an organelle present on eukaryotic cell types, including chondrocytes. This immotile solitary cytoplasmic protrusion possess various type of mechanosensitive Ca^{2+}-permeable ion channels and a special intraflagellar transport (IFT) mechanism which plays a crucial role in ciliary signalling. Defects in the structure of the cilium or in the transport and/or function of ciliary signal proteins are associated with a series of pathologies, including certain developmental disorders of the skeletal system. High density cell culture system (HDC) established from chondrogenic mesenchymal cells isolated from limb buds of 4-day-old chicken embryos was used to investigate the presence and the role of this organelle. First, we have identified the expression of IFT88 (a special protein in the intraflagellar transport) and acetilated tubulin (a special microtubular protein in the primary cilium), which are typical of all phases in cell cycle. The expression of Kif3a and Kif3b (two subunits of the heterotrimeric motor protein, kinesin-2) were also confirmed in HDCs. Our aims are to study the effects of chloral hydrate on cartilage differentiation, because it is known that can inhibit the function of primary cilia. According to our preliminary results primary cilia play important role in the chondrogenesis.

Expression and cellular localization of P2X4 and P2X7 purinergic receptors in the superficial spinal dorsal horn of rats suffering from chronic inflammatory pain

László Ducza[1], Krisztina Holló[1], Erzsébet Bakk[1], Krisztina Hegedűs[1], Klaudia Dócs[1], Zoltán Hegyi[1], Miklós Antal[1,2]

[1]Department of Anatomy, Histology and Embriology, University of Debrecen, Debrecen, Hungary
[2]MTA-DE Neuroscience Research Group, Debrecen, Hungary

In chronic pain conditions in addition to glutamate, nociceptive primary afferents release also ATP in the spinal dorsal horn. Acting on purinergic receptors ATP can evoke the release of interleukin-1βeta (IL-1β) from glial cells that contributes to the development of central sensitization in pain processing spinal neuronal circuits. Although the contribution of interleukins to the development of chronic inflammatory pain is widely accepted, our present knowledge concerning the role of purinergic receptors in spinal pain processing mechanisms is insufficient. Thus, in the present experiment we investigated the expression of P2X4 and P2X7 receptors in the superficial spinal dorsal horn in adult male rats suffering in chronic inflammatory pain evoked by unilateral plantar injection of complete Freund adjuvant (CFA). Immunohistochemical staining showed that purinergic receptors are widely expressed by glial cells in the superficial spinal dorsal horn in chronic pain conditions. We also showed that the immunostainings for both receptors are enhanced in CFA evoked inflammatory pain. Elevation of purinergic receptor expression was also confirmed by Western blot analysis. Our data indicate that P2X4 and P2X7 receptors may play a role in spinal pain processing mechanisms.

This work was supported by the Hungarian Academy of Sciences (MTA-TKI 242) and the Hungarian Brain Research Program (KTI_NAP_13-1-2013-001).

Long time epigenetical consequences of intrauterine undernourishment

Máté Durst, Katalin Könczöl, Rita Matuska, Zsuzsanna E. Tóth

Department of Anatomy, Histology and Embryology, Semmelweis University, Budapest, Hungary

Intrauterine undernourished (IU) rats undergo altered fetal programming of the brain leading to epigenetical changes that predispose animals for obesity in adulthood. Reward is an essential component of food intake regulation and the accumbens nucleus (Acc) is a key centre in this respect. We examined hedonic food intake of IU adult offsprings, determined neuronal activity (Fos) evoked by consumption of highly palatable food, as well preproenkephalin, D1 and D2 dopamine receptor mRNA expressions in the Acc. IU rats were born smaller, but they have reached the body weight of controls by the time of the experiments. IU rats consumed significantly more palatable food than controls. The reward value of taste was reflected well as a correlation between the consumed quantity and the number of Fos+ cells in the medial shell region of Acc in both groups and in the core region in IU rats, however the number of Fos+ cells was similar in the groups. There was a decrease in D1 receptor mRNA expression in the Acc shell and a tendency for decrease in the core region of IU animals, while D2 receptor mRNA showed a tendency for increase, but only in the core region. Preproenkephalin mRNA showed also a tendency for decrease in the Acc core, but not in the shell. Data show that hedonic component of food reward plays a dominant role in consumption of IU animals. There is a reduced sensitivity of the reward center, probably related to the altered dopaminergic and opioid signaling in the Acc.

PACAP protects human retinal pigment epithelial cells against oxidative stress

E.Fabian[1], K.Kovacs[3], G.Horvath[1],L. Szereday[2], A.Tamas[1], D.Reglodi[1]

[1]Departments of 1 Anatomy, Medical School, University of Pécs, Pécs, Hungary
[2]Medical Microbiology and Immunology, Medical School, University of Pécs, Pécs, Hungary
[3]Biochemistry and Medical Chemistry, Medical School, University of Pécs, Pécs,Hungary

Angiogenesis plays a critical role in many retinal diseases, such as diabetic retinopathy and macular degeneration. Under these conditions the integrity of the pigment epithelial cells is disrupted, thus photoreceptor survival and normal vision is impossible. The retinal pigment epithelial cells are very important elements of the blood-retina barrier, and they are known to express different angiogenic factors, such as VEGF (vascular endothelial growht factor), so these cells are most likely key factors in the process of neovascularisation. PACAP is known to exert retinoprotective effects, against several types of retinal injuries in vivo, including optic nerve transection, retinal ischemia, excitotoxic injuries, UV-A-induced lesion and diabetic retinopathy. We have shown that PACAP activates antiapoptotic pathways and inhibits proapoptotic signaling in retinal lesions in vivo. Recently we proved that PACAP is also protective in oxidative stress-induced injury in human pigment epithelial cells (ARPE), but not in retinoblastoma cell line (Y79). According to these findings this could be a cell specific protection of the PACAP. In this study we also examined the possible antiangiogenic effect of PACAP on ARPE cells exposed to oxidative stress. Cells were treated with H_2O_2 and the expression of angiogenic markers was investigated by specific arrays, and flow cytometry. Our results showed that H_2O_2 administration increased different proangiogenic factors like VEGF, angiogenin, endothelin and TIMP-1 while PACAP treatment could decrease most of them.

This study was supported by OTKA K104984, Arimura Foundation, MTA-PTE "Lendulet" Program, NIH/NIGMS 2 SO6 GM08016-39, Hungarian Brain Research Program - Grant No. KTIA_13_NAP-A-III/5.

Urocortinergic neurons in the central projecting Edinger-Westphal nucleus contribute to maladaptation in the three hit model of depression in mice

J. Farkas[1], A. Nafz[1], L. Kovács[1] , D. Reglődi[1] , Hashimoto H.[2], B. Gaszner[1]

[1]Department of Anatomy, Medical School, University of Pécs, Pécs, Hungary
[2]Laboratory of Molecular Neuropharmacology, Graduate School of Pharmaceutical Sciences, Osaka University, Osaka Japan

The three hit theory is an accepted concept in the field of mood disorders: genetic predisposition, epigenetic factors and stress together cause depression. Besides several well studied stress-related brain areas, the urocortinergic central projecting Edinger-Westphal nucleus (cpEW) is a neglected center, however it is the main site of urocortin1 (Ucn1) expression.

Our aim was to set up and validate a mouse model for studying depression at behavioral level, moreover, we planned to examine the (mal)adaptive changes in the cpEW.

Offsprings of mice heterozygous for pituitary adenylate cyclase-activating polypeptide (PACAP) (genetic factor) were subjected to severe maternal deprivation (epigenetic factor) and chronic variable mild stress (environmental stress factor) versus controls. The FosB neuronal activity was mapped throughout the brain. We found that mice subjected to all three factors showed increased FosB expression in the cpEW. In a Ucn1-FosB double labeling we saw FosB expression changes taking place specifically in urocortinergic cells. The highest neuronal activity in Ucn1 neurons was found in PACAP KO mice with maternal separation and chronic variable mild stress history. Interestingly, the lowest survival ratio was found in this group, suggesting maladaptation. In contrast, the magnitude of the neuronal activity increase upon stress was blunted in heterozygous mice, accompanied with normal survival but depression-like phenotype.

Based on our findings we conclude that the cpEW plays a role in the pathophysiology of mood disorders. In this experiment we conclude that PACAP heterozygous mice in our three hit model could be a reliable tool to study major depression in mice.

Different activation of the neocortex, hippocampus and mammillary body during acute seizures in young rats

Mónika Fejesné Bakos, Beáta Krisztinné Péva, András Mihály

Department of Anatomy, Histology and Embryology, Faculty of Medicine, University of Szeged, Szeged, Hungary

We examined the 4-aminopyridine (4-AP) induced changes of neuronal activity in the neocortex, hippocampus and mammillary body of developing rats by using c-fos and parvalbumin immuno. We investigated 15, 20, 30 and 60 days old rats. Seizures were induced by intraperitoneal injection of 5 mg/kg 4-AP.

The neocortex of P15 rats showed maximal c-fos expression. The number of activated inhibitory neurons increased significantly with animal age. C-fos expression in the Ammon's horn was maximal at P30 .

The number of activated inhibitory neurons peaked at P20, while c-fos expression of the dentate gyrus was maximal at P30.

The amount of c-fos immunoreactive and activated inhibitory neurons displayed similar alterations during maturation, c-fos expression was significantly higher in P20 animals, while the peak was detected in P60 animals. The number of c-fos positive neurons in the mammillary body showed a positive correlation with the number of activated neurons in the CA1 region of the hippocampus.

According to our results, at early postnatal age (P15) mainly corticothalamic and thalamocortical convulsions predominated. Convulsive treshold of the young animals was significantly lower until P40. This sensibility change may be the consequence of the postnatal maturation of inhibitory interneurons.

Modification of versican expression following unilateral labyrinthectomy is related to functional differences of the individual nuclei in the rat vestibular complex

Botond Gaál, Einar Örn Jóhannesson, Ágnes Magyar, Klára Matesz

Department of Anatomy, Histology and Embryology, University of Debrecen, Debrecen, Hungary

Unilateral lesion of the vestibular system in mammals results in disturbances of eye movements, muscle tone, and posture. Symptoms spontaneously restore within 1-2 weeks, during the vestibular compensation. Studies showed that the extracellular matrix (ECM) has important role in plastic modifications of the central nervous system (CNS). We earlier observed that unilateral labyrinthectomy (UL) is accompanied by the modification of hyaluronan and chondroitin sulfate proteoglycan staining in the perineuronal net (PNN) and neuropil of the lateral vestibular nucleus (LVN) in the rat. PNN reestablishment was parallel with functional restoration, suggesting the role of ECM in the recovery process. The present study examines *versican* expression in each vestibular nucleus following UL.

Experiments were made on adult female rats. The vestibular receptors were mechanically damaged and after 1, 3, 7 and 14 survival days, immunohistochemical reaction against versican was performed on brainstem sections.

In normal animals versican reaction revealed heavily stained dots pericellularly and continuous PNNs were also recognizable in the superior (SVN) and descending vestibular nuclei (DVN). Following UL, changes were seen on 1st postoperative day in the ipsilateral SVN and DVN. The versican staining fainted in the PNN and restored after 3 days. Staining intensity of the neuropil weakened in each nucleus, mostly in the SVN.

Our results suggest that the decreased expression of non-permissive versican in the PNN of the SVN and DVN may be involved in the restoration of vestibular functions within these nuclei.

Support: MTA-TKI 11008.

Morphological and functional integration of grafted embryonic motoneurons into the host rat spinal cord circuitry after ventral root avulsion and reimplantation

László Gál[1,2], Anna Cabaj[1,3], Krzysztof Miazga[1], Gábor Márton[2], Jeremy Chopek[4], Antal Nógrádi[2], Urszula Sławinska[1]

[1]Laboratory of Neuromuscular Plasticity, Nencki Institute of Experimental Biology PAS, Warsaw, Poland
[2]Laboratory of Neural Regeneration, Department of Anatomy, Histology and Embryology, University of Szeged, Szeged, Hungary
[3]Institute of Biocybernetics and Biomedical Engineering PAS, Warsaw, Poland
[4]Spinal Cord Research Centre, Department of Physiology, University of Manitoba, Winnipeg, Canada

Plexus injuries often result in the avulsion of one or more ventral roots, thus leading to irreversible motoneurone loss. Transplantation of embryonic motoneurons into a damaged spinal cord depleted of its own motoneurons is a feasible strategy to replace the lost motor pool and induce functional reinnervation of the denervated limb muscles. Our aim was to investigate the morphological and functional integration of the grafted embryonic motoneurons into the host spinal cord circuit.

Embryonic spinal cord pieces (E13-eGFP rat) was grafted into the lumbar four (L4) spinal segment of Sprague-Dawley rats after L4 ventral root avulsion and reimplantation Three experimental groups have been set: in the control group the ventral root was avulsed and reimplanted without an embryonic graft, animals in the second group received an embryonic graft. In the third group the embryonic tissue received tumor necrosis factor-alpha (TNF-alpha) treatment prior to transplantation. Six months later electromyography was recorded from the ankle flexors and extensors of the hind limbs on the intact and operated sides.

Rhythmic locomotor limb movement could be observed in the treated animals. Two populations of motor unit action potentials (MUAPs) were distinguished in the grafted animals without TNF-alpha treatment. Differences were observed in the firing period, frequency, duration and amplitude of MUAPs. The firing frequency of some MUAPs showed bimodal distribution. Retrograde labelling from the reinnervated muscles proved that both the graft and host neurons contributed to the reinnervation of the denervated hindlimb muscles. Anterograde tracing with Phaseolus vulgaris revealed substantial reciprocal connections between the graft and the host spinal cord. TNF-alpha pretreatment enhanced the number of reinnervating neurons in the spinal cord providing an opportunity to study the integration of the transplanted cells with intracellular recording and labelling.

Our results have provided evidence that grafted embryonic motoneurons are able to survive, differentiate and establish functional connections with the circuitry of the host cord.

Expression of a novel calcium-binding protein, secretagogin, in the mammalian visual system

Anna Gáspárdy[1], János Hanics[1,2], Alán Alpár[1,2]

[1]Department of Anatomy, Histology and Embryology, Semmelweis University, Budapest, Hungary
[2]MTA-SE NAP-B Research Group of Experimental Neuroanatomy and Developmental Biology, Hungarian Academy of Sciences, Budapest, Hungary

Intracellular calcium level is critically regulated by calcium binding proteins. They protect against excess intracellular calcium ion levels or act as sensor proteins thereby regulating downstream cascades. Secretagogin, a recently described calcium sensor protein, has been identified in several organs including forebrain. Here, we show that secretagogin is present throughout the main visual centres of the rat brain. In the diencephalon, immunoreactive neurons were identified in the dorsal and ventral divisions of the lateral geniculate nucleus, and in an outstanding density in the superficial layers of the superior colliculus. *In vivo* tracing experiments suggested that these cells did not belong to the major thalamus-projecting neurons. In contrast to animals developing at standard housing conditions, rat pups born and reared in complete darkness lacked secretagogin expression in the early postnatal period. Human samples showed a largely different distribution pattern. Secretagogin-containing neurons appeared in a very low number both in the superior colliculus and in the lateral geniculate nucleus. The primary visual cortex, however, were densely populated by typically bipolar-shaped immunoreactive neurons that concentrated in supragranular, but excluding the molecular layers. We suggest that secretagogin is a candidate functional and immunohistochemical marker in the mammalian visual system.

Neurons producing melanin-concentrating hormone: regulation of food intake and sleep / awake cycle - a study of the mouse hypothalamus

Balázs Gerics, Péter Sótonyi, Vera Jancsik

Department of Anatomy and Histology, SzIE Faculty of Veterinary Science, Budapest, Hungary

One of the functions of the hypothalamus in mammals is the control of food and water intake. To serve this regulatory task a great number of neuropeptides are produced locally and distributed throughout the brain. Some of these hormones do increase food intake (*i.e.* are orexigenic), while others have the opposite effect, thus are anorexigenic.

One of the orexigenic hormones is the melanin-concentrating hormone (MCH). Somata of MCH-neurons are mainly located in the caudal part of the hypothalamus being predominant in the lateral hypothalamic area (LHA) and the zona incerta (ZI). The anatomy of the MCH-neurons is best known in the rat, interspecific differences of their somata and projections, however, were recorded even in two closely related rodents, like rats and mice. Some possible species-specific function are suggested, *e.g.*, due to the presence and lack of MCH-positive somata within the posterior periventricular nucleus (PVP) in the rat and mouse, respectively. Besides acting as a neuromodulator on both hypothalamic and distant targets melanin-concentrating hormone is involved in regulating the sleep/awake cycle. We have initial recordings of temporal, diurnal differences of the MCH-immuno-positivity of neurons in the mouse hypothalamus.

Ultrasound is a valuable method in cartilage thickness measuring

János Gyebnár[1], Gábor Baksa[2], Péter Mandl[3], Kinga Karlinger[1], Péter Bálint[4]

[1]Department of Radiology and Oncotherapy, Semmelweis University, Budapest, Hungary
[2]Department of Anatomy, Histology and Embryology, Semmelweis University, Budapest, Hungary
[3]Division of Rheumatology, Medical University of Vienna, Vienna, Austria
[4]3rd Department of Rheumatology, National Institute of Rheumatology and Physiotherapy, Budapest, Hungary

Nowadays, the standard protocol in the imaging of the metacarpophalangeal cartilage thickness is plain radiography. It shows the distance between the metacarpal bone and the phalanx, and we can only indirectly estimate the cartilage thicknesses at a cost of radiation exposure.

Our aim is to compare the anatomical cartilage thickness with ultrasound (US) in cadavers to validate ultrasound as a valuable diagnostic modality in cartilage imaging.

Nineteen formalin-fixed metacarpophalangeal (MCP) 2-5 joints (all women, age at death: 65-90 years; mean: 78 years) were examined by measuring the metacarpal cartilage thickness (MCT) with US. High resolution, longitudinal ultrasound images were performed with 7-15 MHz frequency linear transducer. The US MCT measurement was correlated to a single, central anatomical measurement, which, due its position, the most closely corresponds to the ultrasound measurement in flexed joint position.

There was no significant ifference between MCT measured by the anatomical or the ultrasound method (mean±SD; (range) (0.67±0.11; 0.52-0.92 mm) vs. (0.69±0.12; 0.43-0.93 mm)) Pearson correlation was calculated (0.73, CI: 95%).

Sonographic cartilage assessment in MCPs is closely related to anatomical cartilage thickness. Thus, US is a valid and valuable tool for measuring MCT.

Although it requires experience, ultrasound is a fast, cost-effective and repeatable diagnostic method, without any radiation exposure in contrast to plain radiography.

N-methyl-D-aspartate type glutamate receptors influence viability of melanoma cells

Tibor Hajdú, Tamás Juhász, Róza Zákány

Department of Anatomy, Histology and Embryology, Faculty of Medicine, University of Debrecen, Debrecen, Hungary

The NMDA type glutamate receptors (NMDAR) are diheterotetrameric non-selective cationic channels, comprising of NR1, NR2, NR3 subunits and are mostly permeable for Ca^{2+}. NR1 may contain a nuclear localization signal, which binds to importin- , suggesting that nuclear transport of NR1 is conceivable. As NMDARs have been described in some tumors, we aimed to map the expression pattern and potential functions of NMDAR subunits in melanoma cells.

Human melanoma cell lines (A2058, HT199, HT168M1, MEL35/01 and WM35) were used for our experiments. NMDAR subunit mRNAs were detected with RT-PCRs. Western blots of samples from cytosolic, plasma membrane and nuclear fractions of cellular lysates were performed to prove the protein expression of subunits. Subcellular localization was also investigated with fluorescent immunocytochemistry. Cellular viability was measured by MTT assay after treatments with agonists and antagonists.

RT-PCR showed that mRNAs of all types of subunits (NR1, NR2A, NR2B, NR2C, NR2D, NR3A, NR3B) are present in all cell lines. Western blots proved that NR1 and NR3 subunits are present throughout in the cells. NR1-NR3B immunocytochemisty revealed that the two subunits colocalize inside the nuclei rather than the cytoplasm. NR1-NR3 composed NMDARs can function as alternative glycine receptors. MTT assays revealed that treatments with glycine+strychnine (a glycine receptor antagonist) and glycine+strychnine+glutamate significantly increased the metabolic activity and viability in every investigated melanoma cell line.

Our results suggest that NMDAR with unusual composition are present in the nuclei of melanoma cells and may transduce glycine signalling influencing the survival of melanoma cells.

A comparative study of the anatomical and clinical aspects of the female pelvic floor

Tibor Hollósy[1], Dóra Reglődi[1], Pál Tóth[1], Miklós Koppán[2]

[1]Department of Anatomy, Medical School, University of Pécs, Pécs, Hungary
[2]Department of Obstetrics and Gynaecology, Medical School, University of Pécs, Pécs, Hungary

Accordig to the traditional anatomy, the pelvic floor muscles are characterized by their origin, insertion, function and innervation. It seems to be a good way of description at first glance, but it does not give sufficient background for the understanding of gynecological deseases and up-to-date operational methods. Contrary to this, the clinical approach concentrates more on the functional description, *i.e.* the static and dynamic movements, the relation of muscles and fasciae, and the pathological changes caused by their malfunction. The modern, clinically oriented view is that the muscles of the lesser pelvis are the elementary components of „maintaining position of the organs in proper orientation and thereby ensuring their normal function". Therefore, any muscular abnormality may result in dislocation of the organs and/or the loss of the sphincter function of muscles. Most of the anatomical descriptions do not even mention the obvious difference between the shape and consistency of the organs taken out of the body and of those being *in situ*. Our personal experiences clearly show that the understanding of the position of uterus, Fallopian tube, ovary and rectum is frequently beset with difficulties for students, since the organs removed from their original location lack the structures (muscles and fasciae) keeping them in normal position. In our work, we try to reconsile the anatomical descriptions to the clinically important contexts and relations, but only to the degree that serves students in understanding spatial relations and in acquiring firm support for clinical mentality.

Support: TÁMOP-4.1.1.C-13/1/KONV-2014-0001 (Coordinated, practice-oriented, student-friendly modernization of biomedical education in three Hungarian universities (Pécs, Debrecen, Szeged), with focus on the strengthening of international competitiveness).

Effects of PACAP on human trophoblast cells

Gabriella Horvath[1], Reka Brubel[1], Melinda Halasz[2], Aliz Barakonyi[2], Balazs Opper[1], Eszter Fabian[1], Andrea Tamas[1], Gabor Toth[3], Marie Cohen[4], Laszlo Szereday L[2], Dora Reglodi[1]

[1]Departments of Anatomy, PTE-MTA „Lendület" PACAP Research Team, Pécs, Hungary
[2]Medical Microbiology and Immunology, University of Pécs, Pécs, Hungary
[3]Department of Medical Chemistry, University of Szeged, Szeged, Hungary
[4]Department of Gynecology and Obstetrics, University of Geneva, Geneva, Switzerland

Pituitary adenylate cyclase activating polypeptide (PACAP) is a pleiotropic and multifunctional neuropeptide widely distributed throughout the body. The aim of the present study was to investigate the effects of PACAP on invasion, proliferation, cell survival, and angiogenesis of trophoblast cells. Furthermore, cytokine production was investigated in human decidual and peripheral blood mononuclear cells. For in vitro studies, human invasive proliferative extravillous cytotrophoblast (HIPEC) cells and HTR-8/SVneo human trophoblast cells were used. Both cell types were used for testing the effects of PACAP on invasion and cell survival. Invasion was studied by standardized invasion assay. PACAP increased proliferation in HIPEC cells, but not in HTR-8 cells. Cell viability was examined using different methods. Survival of HTR-8/SVneo cells was studied under oxidative stress conditions induced by hydrogen peroxide. PACAP as pretreatment, but not as co-treatment, significantly increased the number of surviving HTR-8 cells. Viability of HIPEC cells was investigated using methotrexate toxicity, but PACAP1-38 could not counteract its toxic effect. Angiogenic molecules

Extracellular matrix expression in the olfactory bulb of the rat

Andrea Hunyadi, Botond Gaál, Szilvia Kecskes, Ibolya van der Wijk, Klára Matesz

Department of Anatomy, Histology and Embryology, University of Debrecen, Debrecen, Hungary

In vertebrates smells are sensed by olfactory sensory neurons in the olfactory epithelium. After binding an odorant, receptors send signals into the olfactory bulb, where information is encoded during a complicated signal processing. The extracellular matrix (ECM) molecules fill the extracellular space. They may aggregate around the neurons forming the perineuronal net (PNN) or they are distributed throughout the neuropil. Hyaluronan (HA) is the backbone of PNNs, and anchors lecticans of the chondroitin sulfate proteoglycan (CSPG) family. The ECM molecules are involved in various forms of plasticity, and its expression is determined by neuronal activity. The aim of our work was to map the distribution of HA and CSPG in the olfactory bulb. Observations were performed on female adult Wistar rats. Olfactory bulbs were removed from anesthetized animals and fixed in St. Marie's fixative. Distribution of HA was detected by biotinylated Hyaluronan Binding Protein histochemistry, and CSPGs by using biotinylated Wisteria floribunda agglutinin (WFA) histochemistry on transverse sections. HA showed diffuse expression throughout the olfactory bulb and sporadic PNNs were accumulated around mitral cells. WFA staining was experienced in the internal plexiform layer and surrounding mitral cells, even forming PNNs. There was great difference between CSPG expressions of glomeruli. Variable WFA labeling in glomeruli suggests ongoing reorganization in synaptic units. The diffuse and high hyaluronan expression corresponds with this argument.

Support: MTA-TKI-11008.

Differential expression patterns of K^+/Cl^- co-transporter (KCC2) in neurons within the superficial spinal dorsal horn of rats

Fariba Javdani[1], Krisztina Holló[1], Krisztina Hegedűs[1], Gréta Kis[1], Zoltán Hegyi[1], Klaudia Dócs[1], Yu Kasugai[2], Yugo Fukazawa[3], Ryuichi Shigemoto[4], Miklós Antal[1,5]

[1]Department of Anatomy, Histology and Embryology, Faculty of Medicine, Medical and Health Science Center, University of Debrecen, Debrecen, Hungary
[2]Department of Pharmacology, Innsbruck Medical University, Innsbruck, Austria
[3]Division of Cell Biology and Neuroscience, Faculty of Medical Sciences, University of Fukui, Yoshida, Japan
[4]IST Austria, Klosterneuburg, Austria
[5]MTA-DE Neuroscience Research Group, Debrecen, Hungary

$GABA_A$ receptor mediated inhibition is associated with a chloride-influx that depends on inwardly directed chloride electrochemical gradient, which is regulated by potassium-chloride co-transporter, KCC2. Here, we investigated the cellular distribution of KCC2 in the superficial spinal dorsal horn of rats by using immunocytochemical methods. We demonstrated that perikarya and dendrites widely expressed KCC2, but axon terminals proved to be negative for KCC2. Studying the somato-dendritic distribution of KCC2, high and low levels of KCC2 expression were equally recovered. In single ultrathin sections we also observed dendritic segments that were negative for KCC2. Investigating KCC2 expression on neurons immunoreactive for NK1 receptor, which allowed us to study a large part of the somato-dendritic compartment of some neurons we found that KCC2 presented a quite heterogeneous distribution along the dendritic membrane. Measuring the distances between gephyrin-IR and KCC2-IR spots on NK1-R-IR dendrites we found that some putative inhibitory postsynaptic membranes keep larger distances from KCC2 than others. In addition, we found that postsynaptic membranes of putative inhibitory synaptic contacts establishing loose association with KCC2 transporters are arranged in clasters along the dendritic membrane. The results suggest that $GABA_A$ receptor mediated synaptic mechanisms may vary at different sites of the somato-dendritic membrane of neurons in the superficial spinal dorsal horn.

This work was supported by the Hungarian Academy of Sciences (MTA-TKI 242) and the Hungarian Brain Research Program (KTIA_NAP_13-1-2013-0001).

Does enriched environment have a neuroprotective effect on Parkinson's disease?

Adel Jungling, Dora Reglodi, Gabor Horvath, Zsofia Nozomi Karadi, Balazs Daniel Fulop, Peter Kiss, Balazs Gaszner, Andrea Tamas

Department of Anatomy, MTA-PTE „Lendület" PACAP Research Team, University of Pécs, Hungary

Environmental enrichment is considered as a strategy of neuroprotection. Its effects have already been shown in traumatic, ischemic and toxic nervous system lesions. The aim of our study was to investigate the effects of early postnatal environmental enrichment in a rat model of Parkinson's disease in adulthood.

We used Wistar rats in our experiment. The animals of the standard group were placed under regular conditions. For environmental enrichment, we placed rats in larger cages, supplemented with toys of different shape and material during the first five postnatal weeks. Three months later rats were treated with unilateral injections of 2 µl 6-OHDA (5 µg/µl) into the left substantia nigra, control animals received 2 µl physiological saline. Behavioral experiments were done preinjury, and 1, 10 days after the operation. After the behavioral testing tyrosine-hydoxylase immunohistolochemistry was performed to label dopaminergic cells of the substantia nigra.

We observed hypokinetic symptoms due to the operation. The 6-OHDA treatment made significant cell loss in the standard group: 24% of dopaminergic cells died, while in rats kept in enriched environment the cell loss was not significant, only 16%.

Our experiments provided evidence for the protective effect of early postnatal environmental enrichment in adulthood, because rats under regular circumstances showed more severe neurological signs and dopaminergic cell loss after 6-OHDA lesion of the substantia nigra compared to animals grew up in environmental enrichment.

Support: NAP (Hungarian National Brain Research Program) KTIA_NAP_13-1-2013-0001, MTA-PTE „Lendület" Program, Arimura Foundation, OTKA K104984.

Multicystic encephalopathy

László Kaiser[1], Kitti Brinyiczki[1], István Bódi[2],

[1]Department of Pathology, Faculty of Medicine, University of Szeged, Szeged, Hungary
[2]King's College Hospital NHS Foundation Trust, London, UK

Multicystic encephalopathy is a rare disorder. This symmetric, multilocular, cystic condition has been named as "hypoxic –ischemic damage of the brain", "multiple cystic emollition", „progressive degenerative encephalopathy", „encephaloclastic porencephaly", „polyporencephaly", „multilocular encephalomalacia". According to our recent knowledge, the cause is attributable to a third trimester noxa, which can be hypoxia, foetal viral infection, toxaemia, maternal anaphylactic shock, maternal traffic accident. The affected area will undergo into a cystic change, on the territory of the basal ganglia and cortical region. Occasionally it is unilateral but most commonly it is bilateral. Histology shows foamy macrophages with reactive glia proliferation in the cystic cavity.

We present two cases with the clinical and pathological findings.

Multicystic encephalopathy is an extremely rare entity. The characteristic findings were described by Aicardi and co-workers (J Neurol Sci 1972, 15:357-373) based on 29 cases available in the international literature. Clinical findings can be paralysis, convulsions, irritability, slow mental development, difficulty of feeding. Although the brainstem, the cerebellum, and the thalamus are relatively unaffected the background remains unknown. Our two presented cases show the characteristic macro and microscopic findings. Histologically cortical and subcortical cysts, gliosis, necrosis, calcification, status spongiosus, and foamy macrophages can be seen.

In the differential diagnosis ependimal, chorioid, colloid, septal and arachnoideal cysts should be considered, as well as Pallister-Hall syndrome, and the congenital polycystic alteration of the brain. Interhemisphaerial cystic corpus callosum agenesis should also be excluded. It is hard to predict the long-term outcome, due to the small number of patients.

Neuronal background of the prey-catching behavior of the frog: sensory-motor integration in the brainstem

Szilvia Kecskés, Klára Matesz, András Birinyi

Department of Anatomy, Histology and Embryology, University of Debrecen, Debrecen, Hungary

The prey-catching behaviour of frogs consists of a sequence of coordinated activity of different muscles. The activity of muscles can be modified via sensorimotor connections. The sensorimotor integration was studied in the ambiguus nucleus which is necessary for gulping and visceromotor functions, and the hypoglossal nucleus responsible for contraction of tongue muscles.

The aim of our experiments was to study whether the afferent fibres establish direct connections with the motoneurons. The nerves were simultaneously labeled with neuronal tracers, and the close appositions between afferent fibers and motoneurons were detected with confocal microscope.

Micrographs showed direct contacts between sensory terminals of trigeminal nerve and ambiguus motoneurons. The contacts were not evenly distributed: two-third of the afferents terminated on the viscero-motoneurons of the stomach, heart and lung, large number of terminals were found on the pharyngo-motoneurons, while the number of connections on the laryngo-motoneurons was insignificant.

We also demonstrated direct connections between trigeminal, vestibular, glossopharyngeal-vagal, hypoglossal and second cervical spinal afferent terminals and hypoglossal motoneurons. Based on the highest number and closest location of the connections, we presume that the glossopharyngeal-vagal afferents can exert the strongest effect on the retractor and protractor motoneurons. The hypoglossal and C2 afferents can modify the retraction of tongue. The monosynaptic influence of trigeminal and vestibular afferents on the hypoglossal motoneurons is probably less important.

We conclude that these monosynaptic connections may serve as one of the neuro-morphological substrates of the fast response during feeding movements of amphibians that gives reflex-like ability of prey-catching behaviour.

Support: MTA-TKI 11008.

Nesfatin-1/NUCB2 mRNA level changes after osmotic challenges

Katalin Könczöl, Rita Matuska, Richard Reichard, Zsuzsanna E. Tóth

Department of Anatomy, Histology and Embryology, Semmelweis University, Budapest, Hungary

Nesfatin-1/NUCB2 (nesfatin) is an anorexigenic peptide, however, besides reducing food intake it also decreases water intake. Nesfatin is highly coexpressed with vasopressin (VP), a main regulator of fluid and osmotic balance, in the supraoptic nucleus (SON). It is a question whether the antidipsogenic effect of nesfatin is independent of its anorectic action. Therefore. we measured nesfatin mRNA expression in the SON after water deprivation (WD) and hypertonic challenge (2% NaCl) and used *ad libitum* fed (Co) and also pair-fed (WD-Co and 2% NaCl-Co) controls. To separate the effect of food intake on fluid homeostasis another group of rats was fasted for 48 h. Body weights, food and water consumption were monitored. Additionally, we investigated whether VP deficiency affects nesfatin mRNA expression in the SON. Nesfatin mRNA levels increased significantly in the treated groups independently of food intake, and these animals consumed less chow than *ad libitum* fed controls. Restricted food intake of pair-fed groups did not change the water intake and nesfatin mRNA levels of these rats. Animals of 2% NaCl group drank more fluid than controls. Body weights of treated animals decreased significantly compared to their controls. Negative energy balance (48h fasting) itself did not influence nesfatin mRNA expression in the SON. VP deficiency resulted in an elevated nesfatin mRNA expression in the SON. Our data show that nesfatin participates in maintaining the osmotic balance, and this action is independent of its role in food intake regulation.

PACAP transgenic mice in the three hit model of depression: the involvement of BNST- CRF, cpEW – Urocortin1

L. Kovács[1], J. Farkas[1], T. Gaszner[1], L. Gaspar[1], G. Bodnár[1],K. Lőrincz[1], H. Hashimoto[2], V. Kormos[3]; B. Gaszner[1]

[1]Department of Anatomy, University of Pécs, Pécs, Hungary
[2]Laboratory of Molecular Neuropharmacology Graduate School of Pharmaceutical Sciences, Osaka Japan;
[3]Department of Pharmacology and Pharmacotherapy, University of Pécs, Pécs, Hungary

According to the three hit theory genetic, epigenetic and stress factors may lead to major depression. The shortage on pituitary adenylate cyclase-activating polypeptide (PACAP) leads to depressive-like symptoms in mice. The importance of hypothalamus-pituitary-adrenal (HPA) axis in etiology of depression is known, but its supra-hypothalamic regulation is largely elusive. The corticotropin releasing factor (CRF) expressing bed nucleus of the stria terminalis [BNST] and central amygdala [CeA], moreover the urocortin1 (Ucn1) producing central projecting Edinger-Westphal nucleus [cpEW] contributes to stress adaptation. We hypothesized that mice carrying all risk factors will show maladaptation in the HPA axis, CRF and Ucn1 systems.

Litters from PACAP heterozygous mice were exposed to maternal separation (MS) vs. controls. Half of adult offspring was subjected to chronic variable mild stress (CVMS). To validate the model, the HPA axis activity was measured by corticosterone radioimmuneassay. The contribution BNST and CeA, in addition urocortinergic neurons in the cpEW were studied.

Results indicate that CVMS most effectively increased adrenal weights and corticosterone titers in MS mice accompanied by increased CRF-cell counts and specific signal density (SSD) in the BNST. In the CeA, the CVMS-induced rise in CRF SSD was observed only in non-MS mice. In MS, the CVMS induced rise of FosB in Ucn1 neurons was abolished.

The increased BNST-CRF and decreased cpEW-Ucn1 neuronal activity suggests that these inverse alterations may contribute to the psychopathology. The three hit theory of depression seems to be applicable in PACAP heterozygote mice to study the pathophysiology of stress-related mood disorders.

Differences in the seizure driven neuronal activity in zebrin II positive and negative cerebellar cortical zones

Beáta Krisztin-Péva, András Mihály

Department of Anatomy, Histology and Embryology, Faculty of Medicine, University of Szeged, Szeged, Hungary

For a long time it was assumed, that the cerebellar cortex is uniform regarding the cytoarchitecture and the microcircuitry. Electrophysiological and immunohistochemical investigations in the past ten years revealed remarkable differences. The differences are in the distinct connection of cerebellar areas the different phenotypes of the Purkinje cells (PC).

We examined the temporal activation pattern of the cortical neurons after 4-aminopyridine induced seizures. The c-Fos protein immunohistochemistry was used as marker of the neuronal activity. The cells were investigated in all cerebellar cortical layers, and a comparison was made between the zebrin II positive (Z+) and the negative (Z-) bands of the vermal lobules and the hemispherium.

In the granular layer the Z+ band displayed a prominent activation peak at 3h after the drug application, as shown by the density of the c-Fos immunoreactive (IR) nuclei. The Z- bands contained significantly fewer IR nuclei, and the maximum c-Fos activation was delayed. The interneurons of the molecular layer (IML) were activated in significantly larger number in the Z+ bands. The PC's, surprisingly, exhibited just scattered c-Fos IR cell nuclei in all bands.

Explaining the surprisingly low activation level of PC's we assume the role of the strong inhibition of IML's during the seizure. To complete our work, we plan further studies in order to evaluate the activation of deep cerebellar nuclei during the acute seizure.

Effect of PACAP on ischaemia-reperfusion-induced kidney injury of male and female rats

Eszter László[1], Ádám Varga[2], Péter Degrell[3], Krisztina Kovács[4], Péter Szakaly[2], Andrea Tamás[1], Dóra Reglődi[1]

[1]Department of Anatomy, PTE-MTA „Lendület" PACAP Research Team
[2]Department of Surgery, University of Pécs, Pécs, Hungary
[3]Department of Internal Medicine 2 and Nephrology Centre, University of Pécs, Pécs, Hungary
[4]Department of Biochemistry and Medical Chemistry, University of Pécs, Pécs, Hungary

Several pathological conditions and operations are accompanied by ischaemia-reperfusion-induced kidney injury. Protective effect of the neuropeptide PACAP (pituitary adenylate-cyclase activating polypeptide) in the kidney has been shown under several circumstances.

The aim of the present study was to investigate the ischaemia-reperfusion-induced kidney injury of male and female rats to reveal the possible gender differences, furthermore to confirm the protective effect of PACAP in the kidney.

Male and female Wistar rats underwent one-sided renal artery clamping followed by 24-hour, 48-hour or 14-day reperfusion. PACAP was administered intravenously before arterial clamping in half of the rats in each group. Histological evaluation of the PAS stained sections was performed with Adobe Photoshop and Scion Image programs. In the focus of our investigation was the tubular damage, that influences the renal function. Cytokine expression pattern and level of oxidative stress markers were also determined following 24-hour reperfusion.

The tubular damage was significantly less severe in the PACAP-treated male and female rats compared to the untreated after 48-hour and 14-day reperfusion. Results of female animals were significantly better in both treated and untreated groups. Investigation of cytokine expression and of oxidative stress markers has confirmed the histological results.

Based on our findings it can be concluded that PACAP is protective in renal ischaemia-reperfusion in both genders. Differences between the results of male and female rats may be due to the stronger effect of PACAP and the presence of further protective factors in females.

Support: TAMOP 4.2.4.A/2-11-1-2012-0001 'National Excellence Program', OTKA K104984, PD109644, Arimura Foundation, PTE-MTA "Lendület" Program.

Neurochemical phenotypes of rat pancreatic spinal and vagal chemosensitive afferent neurons which express the insulin receptor

Bence András Lázár[1,2], Gábor Jancsó[1], Péter Sántha[1]

[1]Department of Physiology, Faculty of Medicine, University of Szeged, Szeged, Hungary
[2]Department of Psychiatry, Faculty of Medicine, University of Szeged, Szeged, Hungary

Spinal and vagal chemosensitive afferents may significantly contribute to the pathogenesis of inflammatory processes affecting both the exocrine and endocrine pancreas. Recent observations indicated functional interactions between the insulin (InsR) and the transient receptor potential vanilloid type 1 (TRPV1) receptor. The aim of this study was to reveal the neurocehmical phenotypes of InsR-expressing spinal and vagal primary afferent nerurons which innervate the rat pancreas. Adult male Wistar rats (n=5) weighing 300-350 g were used. To identify pancreatic afferents biotin-conjugated wheat germ agglutinin (bWGA) was injected into the pancreas. Immunohistochemistry and quantitative morphometry were used to demonstrate TRPV1-, InsR-, substance P (SP)- and calcitonin gene-related peptide (CGRP)-immunoreactivity in neurons of rat spinal (Th8-L4) and nodose ganglia. 287 and 164 neurons were retrogradely labelled in spinal and vagal sensory ganglia. The cross-sectional areas of the labelled neurons amounted to 498,6±114,4 μm^2 in the spinal, and 535,3±149,2 μm^2 in the vagal division. Of the labelled neurons 68% showed TRPV1-, 46% InsR-, 33% SP- and 52% CGRP imunoreactivity in the spinal division, and 64%, 49%, 40% and 22% in the vagal division. Colocalizations of TRPV1 and InsR, SP and InsR, CGRP and InsR immunoreactivities were demonstrated in 23%, 14%, 26% of the labelled neurons in the spinal division, and 35%, 21% and 8% in the vagal division. These findings provide evidence for the colocalizations of TRPV1, InsR and sensory neuropeptides in pancreatic spinal and vagal afferent neurons. We suggest that insulin may modulate TRPV1 activation and subsequent peptide release from spinal and vagal afferents and contribute to inflammatory and nociceptive mechanisms in the pancreas.

Altered expression of insulin-like growth factor binding protein 3 in the maternal brain

András Lékó, Árpád Dobolyi

MTA-ELTE Laboratory of Molecular and Systems Neurobiology, Department of Anatomy, Histology and Embryology, Semmelweis University, Budapest, Hungary

The postpartum physiological and behavioral changes are regulated by a complex neuronal network, which includes parts of the hypothalamus. Lesions of the preoptic area abolish maternal behaviors while the arcuate nucleus plays a role in the regulation of lactation.

In our previous microarray study, significantly increase was described in the anterior hypothalamic areas of mother rat in the expression of insulin-like growth factor binding protein-3 (IGFBP-3) compared to mothers whose litter was taken away immediately after birth. This finding was also validated by RT-PCR. In the blood, IGFBP-3 is the major carrier molecule of insulin-like growth factors (IGFs), it forms a ternary complex with an acid-labile subunit of either IGF-1 or 2. The distribution of the IGF-system including IGFBP-3 has not been described in the brain. Therefore, we developed in situ hybridization probes to map IGFBP-3. IGFBP-3 mRNA was abundant in some nuclei of the hypothalamus and in the choroid plexus as well. We could also confirm the elevation of IGFBP-3 expression in the hypothalamic sites of mothers, but a change was not seen in the choroid plexus suggesting a specific role of hypothalamic IGFBP-3 in the female brain. We also discovered co-localization of IGFBP-3 with tyrosine-hydroxylase (TH) positive neurons using a combination of in situ hybridization and immunohistochemistry. The time course of alterations in the IGFBP-3 mRNA levels during the reproductive cycle was also determined: it is low in control female rats, does not elevate by the end of pregnancy but is markedly induced by the first postpartum day.

Advances of Squamata astroglia to other reptiles: numerous astrocytes and GFAP- free areas

Dávid L Lőrincz[1], Mihály Kálmán[2]

[1]Institute of Biology, Faculty of Veterinary Science, Szent István University, Budapest, Hungary
[2]Department of Anatomy, Histology and Embryology, Semmelweis University, Budapest, Hungary

Squamata are diapsid reptiles. Testudines were positioned formerly to the most ancient group, Anapsida, but it has been challenged and recently they are rather classified as diapsid reptiles, although their position within this group is uncertain. Animals were obtained from breeders, lizards: *Timon tanginatus* (Lacertidae), *Pogona vitticeps* (Agamidae), *Eublepharis macularis* (Gekkota), *Chameleo calypratus* (Chameleonidae), snakes: *Epicrates cenchria maurus* (Boidae), *Python regius* (Pythonidae), *Pantherophis guttata* (Colubridae), and turtles: *Testudo hermanni* (Testudinidae), *Trachemys scripta* and *Ocadia sinensis* (Emydidae), and *Pelomedusa subrufa* (Pleurodira). They were sublethally overanasthetised with Nembutal and transcardially perfused with 4% buffered paraformaldehyde. Coronal sections were processed according to the immunoperoxidase protocoll. As a primary antibody monoclonal mouse anti-GFAP (Novocastra) were used in a dilution of 1:100.

The main astroglial type is the radial ependymoglia. However, there are two principal differences between the two groups. In Squamata a) astrocyte-like elements were frequent in several areas, *e.g.*, in the pallium and the striatum although nowhere predominated; b) considerable GFAP-poor areas were found, *e.g.*, in the dorsal pallium, septum, dorsal ventricular ridge and hypothalamus. They were especially extended in the *Python,* and in the *Pogona* GFAP was almost missing (at least undetectable) throughout the brain.

The Squamata share more astroglial features with the birds than the turtles (and crocodilians: Kálmán and Pritz 2001), although represent separate branch (Lepidosauria *versus* Archosauria). In mammals and birds the GFAP-free areas represent usually advanced, expanded and plastic ones. Note that Squamata display quite complex behavioural phenomena among reptiles.

Connectivity-based segmentation of the brainstem by probabilistic tractography

Adrienn Máté[1], David Kis[1], Andrea Czigner[2], Tamás Fischer[1], Pál Barzó[1]

[1]Department of Neurosurgery, University of Szeged, Szeged, Hungary
[2]Department of Anatomy, University of Szeged, Szeged, Hungary

Investigation of the complex structure of the brainstem is still challanging even with the currently available modern neuroimaging techniques. Mapping of subcortical regions has become possible with connectivity-based segmentation by probabilistic tractography. Our aim was to identify the main functional subregions of the brainstem with the help of this technique.

Twenty healthy volunteers were involved in the study. High-resolution T1-weighted (1 mm^3 isometric voxels) and DTI (60 diffusion directions, 2.4 mm^3 isometric voxels) scans were obtained at 1.5 T. Probabilistic tractography was performed using the fsl software from a pontomesencephalic seed mask to four supratentorial target regions (anterior and posterior limbs of the internal capsule, medial and sensory thalamus on both sides). Then hard segmentation was applied and the resulting connectivity maps were compared to histological sections to verify anatomic correspondance. Quantitative analyses of the connectivity and fractional anisotropy values in the identified subregions were also carried out.

The main brainstem functional subregions identified by the connectivity-based segmentation corresponded well with the known anatomy on group and individual levels as well. A characteristic pattern of connectivity and fractional anisotropy values were detected in the identified subregions along the rostrocaudal axis of the brainstem.

An advantage of connectivity-based segmentation is that it can identify the main fiber tracts in the brainstem without reliance on anatomical ladmarks. Therefore, it may be applied successfully in diseases distorting normal anatomy. Quantitative analyses may be sensitive to the involvement of the main brainstem pathways in certain disease states (traumatic brain injury, demyelinating disorders).

Nesfatin in the arcuate nucleus participates in adaptation to food deprivation

Rita Matuska, Katalin Könczöl, Zsuzsanna E. Tóth

Department of Anatomy, Histology and Embryology, Semmelweis University, Budapest, Hungary

The hypothalamic arcuate nucleus (ARC) is the primary regulatory center of food intake. Anorexigenic neurons like alpha-melanocyte stimulating hormone (α-MSH) containing cells occupy its lateral part; orexigenic neuropeptide Y (NPY) neurons populate the medial subdivision. Food deprivation induces gene expression changes in the ARC, α-MSH expression decreases, while NPY expression increases. Nesfatin-1/NUCB2 (nesfatin) is a recently discovered anorexigenic neuropeptide expressed in the lateral ARC, coexpressed highly with α-MSH. There are no data about nesfatin expression changes in the ARC in response to fasting. Therefore, we investigated 1, 3 and 5 day-long fasted rats compared to controls by immunohistochemistry against nesfatin and also detected activity of the cells (Fos positivity) during this period. Additionally, effect of intracerebroventricularly (icv) injected nesfatin on Fos activity was studied in normal fed rats. In controls nesfatin cells located mainly in the lateral ARC, many of them was double labeled for α-MSH. After 5 days of food deprivation, α-MSH immunpositive cells were undetectable, however the number of nesfatin-positive cells did not decrease. Additionally, nesfatin immunoreactivity increased in the medial ARC. Fasting induced neuronal activity in the medial ARC as well as in the tanycytes along the wall of the 3rd ventricle adjacent to the ARC. Nesfatin injected icv activated the tanycytes - reported to participate in energy homeostasis - similar manner. We suggest that fasting induces nesfatin expression in the medial ARC that may contribute to the activation of the tanycytes. Further studies are needed to elucidate how all this is related to the adaptation process.

Asphyxia and bicuculline-induced seizures reduce connexin 43 (Cx43) expression in the hippocampus and cerebral cortex of neonatal piglets

Adrienne Mátyás[1], Marietta Hugyecz[2], Alíz Zimmermann[2], Eszter Farkas[4], Ferenc Domoki[2], István Balázs Németh[3], Sándor Berczi[1,3], László Siklós[5], Ferenc Bari[2,4]

[1]Department of Anatomy, Histology and Embriology, Faculty of Medicine, University of Szeged, Szeged, Hungary
[2]Department of Physiology, Faculty of Medicine, University of Szeged, Szeged, Hungary
[3]Department of Pathology, Faculty of Medicine, University of Szeged, Szeged, Hungary
[4]Department of Medical Physics and Informatics, Faculty of Medicine, University of Szeged, Szeged, Hungary
[5]Institute of Biophysics, Biological Research Center, Szeged, Hungary

During perinatal asphyxia and subsequent seizures, cerebral blood flow cannot match the metabolic demands of neurons resulting in oxygen and glucose deficiency triggering changes in cerebral protein synthesis. Gap junctions in neurons and astrocytes dominantly express the Cx43 subunit. Our purpose was to determine whether asphyxia/seizures would affect cerebral Cx43 expression in newborn piglets, an accepted large animal model of the human term neonate.

Anaesthetized, room air ventilated, 1-day old piglets of either sex (body weight 1-2 kg, n=30) were divided into four experimental groups: naive controls, sham-operated time controls, seizure animals (bicuculline, 3 mg/kg iv), and asphyxia. During the course of the 8-hour survival, the mean arterial blood pressure, the arterial pH, pCO_2, and pO_2 values were monitored and maintained within their normal physiological ranges.

Cx43 levels were examined with immunoblotting and immunocytochemistry in brain regions most vulnerable to hypoxia: the hippocampus and the cerebral cortex.

The experimental groups did not differ in the monitored physiological parameters. However, seizures and asphyxia decreased significantly Cx43 levels in the hippocampus, but only seizures could reduce Cx43 in the cortex, albeit not in every region assessed compared to the control groups on Western blots. Immunocytochemistry further revealed that the decreased Cx43 levels after seizures and asphyxia are mainly restricted to the molecular layer of the frontal cortex and the stratum lacunosum of the hippocampal CA1 area

The described reduction of cerebral Cx43 expression levels may contribute to the pathomechanism of hypoxic/ischemic encephalopathy of neonates developing after perinatal asphyxia often complicated by seizures.

The anatomy specimen collection of Albert Gellért

András Mihály, Erika Bálint, Roland Weiczner, Zoltán Süle, Andrea Czigner

Department of Anatomy, Faculty of Medicine, University of Szeged, Szeged, Hungary

We describe a more than 70-year-old method, invented by professor Albert Gellért. The human cadavers were carefully prepared and then embedded into paraffin, similarly to tissue blocks in routine histology. Following the embedding, the specimen was stained and covered by a protecting varnish. The specimens were arranged into a collection, which is now known as the „Albert Gellért Anatomical Collection", in the Department of Anatomy, University of Szeged, Hungary. The volume shrinkage of the tissues due to dehydration was 10-40% during the Gellért-method. The „Albert Gellért Anatomical Collection" has syndesmology specimens, a large number of myology specimens, where muscles and muscle groups and some anatomical variations can be studied. We have paraffine-embedded organs: hearts, kidneys, genital organs, alimentary organs, respiratory organs and brains. We have topographical anatomy specimens in which nerves, blood vessels, ganglia are shown together with muscles and organs. The embryology preparations are placentas embedded in paraffine. The collection also includes male-, female- and infant torsos, in order to display the characteristic body shape and proportions. We have one pathology preparation: an infant with hydrocephalus. The present number of preparations stored in the museum of the Department is 500. The preparations are especially suitable for the study of muscles: the attachments, the layers and the fasciculation of the muscles are clearly visible. At present, efforts are directed towards the laser scanning of the specimens. We aim to create a digital/virtual anatomy museum for students, research and postgraduate studies.

Histological structure of the parodontium in Man and Rattus

András Mihály[1], Eszter Mihály[2]

[1]Department of Anatomy, Histology and Embryology, University of Szeged, Szeged, Hungary
[2]Medicover Eiffel Dental Clinic, Budapest, Hungary

Adult human dental tissue and young rat jaws with developing teeth were used. The tissues were fixed by immersion in 4% buffered paraformaldehyde. Decalcified tissues were embedded into paraffin or sectioned on a freezing microtome. Paraffin sections (5 μm) were stained with hematoxylin and eosin. Frozen sections (25 μm) were stained with calcitonin gene-related peptide (CGRP) antibodies using avidin-biotin systems and peroxidase labelling. The histology of the acellular cement and the periodontal ligament were analyzed and the course of the Sharpey-fibers and the epithelial rests of Malassez were described in human samples. We described the epithelial sheath of Hertwig in developing rat maxillae and mandibles (postnatal days 1-11). We describe the layers of the Hertwig-sheath. We observed the numerical increase of CGRP-stained nerve fibers during these postnatal days. CGRP-stained nerve fibers appeared before the development of the dental root indicating the presence of growth factors which guide the sensory axons. We hypothesize, that the epithelial sheath of Hertwig plays essential role in the development of cementoblasts, periodontal fibroblasts and alveolar osteoblasts. We think that the growth factors secreted by the Hertwig-sheath stimulate the axonal growth, too.

Transplantation of human induced pluripotent stem cells into an injured rat spinal cord improves locomotor function

Krisztián Pajer[1], Tamás Bellák[1], Zoltán Fekécs[1], Dénes Török[1], Csilla Nemes[2], András Dinnyés[2], Antal Nógrádi[1]

[1]Laboratory of Neural Regeneration, Department of Anatomy, Histology and Embryology, University of Szeged, Szeged, Hungary
[2]BioTalentum Ltd., Gödöllő, Hungary

Spinal cord injury leads to deficit of motor and sensory functions below the lesion. In this study we investigated whether application of human induced pluripotent stem cells (hiPS) is able to prevent the secondary spinal cord damage and induce functional recovery. hIPS cells were grafted intraspinally or injected intravenously one week after a thoracic (T11 vertebral level) spinal cord contusion injury performed in rats. Control animals received physiological saline one week after injury via the same delivery routes. Locomotor analysis of the injured animals was performed by applying the BBB test and a detailed kinematic analysis system of the hind limb movement to ascertain improvements in locomotor function. The retrograde tracer Fast Blue was injected into the spinal cord two segments caudally to the lesion to determine the extent of propriospinal axonal sparing/regeneration at 9 weeks after the injury.

hiPS cells applied either locally or intravenously induced moderate functional recovery after contusion injury. Morphologically, the contusion cavity at the epicenter was significantly smaller in grafted animals than in controls. The amount of spared white matter was significantly greater in grafted cords compared with controls. Retrograde tracing studies showed statistically significant increase in the number of propriospinal neurons projecting to the distal spinal cord in both intraspinally and intravenously treated rats. The moderate morphological improvement was accompanied by significant functional improvement.

These data suggest that grafted human iPS cells prevent the secondary spinal cord damage and are able to induce a moderate improvement in the outcome of spinal cord injuries.

This work was supported by grants from EU FP7 projects (STEMMAD, PIAPP-GA-2012-324451; EpiHealth, HEALTH-2012-F2-278418; EpiHealthNet, PITN-GA-2012-317146; D-BOARD, FP7-HEALTH-2012-INNOVATION-1-305815).

Demonstrating the anatomy of the canine heart using MRI based 3D reconstruction technology

Dávid Prevics[1], László Reinitz[1], Örs Petneházy[2], Rita Garamvölgyi[2], Gábor Bajzik[2], Péter Sótonyi[1]

[1]Department of Anatomy and Histology, Faculty of Veterinary Science, Szent István University, Budapest
[2]Institute of Diagnostic Imaging and Radiation Oncology, University of Kaposvár, Kaposvár, Hungary

Because of characteristics of the curriculum of the anatomy, the visual demonstration has always had a very important role in its education. The digital tools available today and the increasing demand of the students make it reasonable to develop 3D models as further tools for education. Researches, including recent Hungarian studies, proved that the practical education is more effective than the theoretical lectures and that modern imaging procedures may provide significant help for students in understanding complex 3D structures.

The object of the study was to create and develop a virtual model of the dog's heart wherewith help the students in understanding and learning its anatomy.

We removed the heart from a refrigerated dog cadaver (cross-breed, male, 36 kg body weight). Following a formalin based fixation process, the organ was casted with a two component synthetic resin. This specimen was examined with MRI using a 1 mm slice gap. The sequence was processed with 3D Slicer, using a semiautomatic segmentation method. The resulted model was exported into 3DS Max for further adjustments and the addition of the major vessels.

The final model is rotatable, and the user can create pictures or animations of that using any desired angle or virtual environment. The model is realistic in its proportions.

This model is available for the students to study why the process may be used for modelling further organs.

Localization of CD26/DPP4 enzyme in the rat spinal cord and effects of its inhibitors in inflammatory and neuropathic pain models

Zita Puskár[1], Mark Kozsurek[1], Kornél Király[2], Erika Lukácsi[1], Benjamin Barta[1], Csaba Fekete[3], Gábor Gerber[1]

[1]Semmelweis University, Department of Anatomy, Histology and Embryology, Budapest, Hungary
[2]Semmelweis University, Department of Pharmacology and Pharmacotherapy, Budapest, Hungary
[3]Institute of Experimental Medicine of the Hungarian Academy of Sciences, Lendület Laboratory of Integrative Neuroendocrinology, Budapest, Hungary

CD26/DPP4 is a moonlighting protein existing within and in the membrane of several cell types and acts as a proteolytic enzyme, a receptor and a costimulatory protein. It has a role in immune response and is involved in adhesion and apoptosis. We have shown that DPP4 inhibitors (vildagliptin and the tripeptide isoleucine-proline-isoleucine; IPI) had opioid mediated spinal antihyperalgesic effect in inflammatory conditions. In this study we (1) looked for evidence for the existence of DPP4 enzyme in the spinal cord, (2) examined which opioid receptors are involved in the antihyperalgesic effects of DPP4 inhibitors in carrageenan-induced hyperalgesia and (3) investigated if DPP4 inhibitors are also effective in neuropathic pain.

Dot-like immonolabelleing of the DPP4 appeared in the spinal dorsal horn. DPP4-positivity was found on cell bodies and axon terminals of neurons as well as on the surface of glial cells. DPP4-positive dots were frequently surrounded by mu-opioid receptor immunoreactivity.

In carrageenan-induced hindpaw inflammation antihyperalgesic effect of vildagliptin was completely eliminated by the highly delta-selective antagonist TIPP(psi), while the mu-selective CTAP and kappa-selective gNTI abolished only the 35% and 45% of this effect, respectively. However, IPI-induced antihyperalgesia was fully blocked by CTAP, while TIPP(psi) and gNTI did not alter the nociceptive threshold, suggesting the exclusive involvement of mu-receptors.

In neuropathic pain model of Seltzer produced by partial sciatic nerve injury both DPP4 inhibitors reduced nociceptive thresholds significantly, but this effect was found to be opioid independent.

These data suggest that DPP4 enzyme exists in the spinal cord and interacts with the endogenous opioid system in a very complex manner especially in inflammatory pain.

Transient Receptor Potential Vanilloid ion channels expressed on human chondroprogenitor cells

Csilla Szűcs Somogyi[1], Csaba Matta[1,2], Tamás Juhász[1], Ádám Finta[1], Péter Bánáthy[1], Nicolai Miosge[3], Róza Zákány[1]

[1]Department of Anatomy, Histology and Embryology, Faculty of Medicine, University of Debrecen, Debrecen, Hungary
[2]Department of Preclinical Sciences, School of Veterinary Medicine, Faculty of Health and Medical Sciences, University of Surrey, Guildford, Surrey GU2 7XH, United Kingdom
[3]Tissue Regeneration Group, Medical Faculty, Department of Prosthodontics, Georg August University, Goettingen, Germany

Chondroprogenitor cell (CPC) population, characterized by a multipotent differentiation capacity, was recently described in human osteoarthritic cartilage. These cells show a strong commitment especially towards chondrogenic lineage. Accumulating evidence indicates that Transient Receptor Potential Vanilloid ion channels (TRPV) have novel functions, such as regulating cell migration and differentiation in various cell types. Therefore, our aim was to find out whether TRPVs have any role in cell migration or chondrogenic differentiation in these chondroprogenitor cells.

All six TRPV ion channels were present at mRNA level in CPCs cultured in monolayer; TRPV1 and TRPV4 were monitored also at the protein level. After treating the CPCs with TRPV1 agonist (10 μM capsaicin) and antagonists (10 μM capsazepine, 10 μM ruthenium red) we evaluated their proliferation rate, monitored gene expression of certain genes possibly involved in migration, and also examined their migration potential with Boyden chamber assay. The TRPV1 agonist and antagonists exerted a concentration-dependent influence on the proliferation rate of chondroprogenitor cells. The mRNA expression of hyaluronidases (especially HYAL2) significantly decreased, while CD44 and hyaluronan synthase 2 (HAS2) expressions elevated after capsaicin treatments. While capsaicin promoted, the TRPV1 antagonists attenuated the migration of CPCs. These findings suggest that TRPV1 may stimulate the migration via influencing hyaluronan production and formation of precartilage cell aggregations in CPCs during chondrogenesis.

Subthreshold dendritic impulse propagation in neocortical layer II/III principal cells of an animal model for Alzheimer's disease

Attila Somogyi, Zoltán Katonai, Ervin Wolf

Department of Anatomy, Histology and Embryology, University of Debrecen, Debrecen, Hungary

Alzheimer's disease (AD) is the most frequent neurological degenerative disorder. The amyloid hypothesis suggests that amyloid-beta accumulation induces or at least related to neurodegeneration, disrupts synaptic transmission and neural networks and leads to dementia. We investigated the dendritic impulse propagation in morphologically realistic computational models of layer II/III pyramidal neurons of the somatosensory cortex from human amyloid precursor protein over expressing Tg2576 transgenic and control mice. In passive segmental cable models of these cells (n=58), within the NEURON (Duke University, USA) simulation environment, current was injected to various dendritic points of mutant and healthy neurons to simulate local activity of synapses and to study attenuations and delays of PSPs during subthreshold dendritic impulse propagation towards the soma. Effects of degree of soma-dendritic membrane inhomogeneity on dendritic impulse propagation were also studied by utilizing three membrane models (uniform, leaky soma and leaky dendrite models, where somatic and dendritic membrane resistances were equal or either the membrane resistance of soma or dendrites was smaller than that of the other compartment). Neuron input resistances and membrane time constants were fitted to electrophysiological measurements in all models.

Despite the severe morphological degeneration detected in dendrites of transgenic neurons, features of subthreshold dendritic impulse propagation remained relatively unaltered in the uniform and leaky dendrite models. However, current transfers in apical dendrites of transgenic neurons got significantly bigger in the leaky soma model. This alteration may be related to increased excitability of neocortical pyramidal neurons found in AD-related transgenic mice and also in humans with AD.

Induction of maternal amylin in the preoptic area depends on TIP39-containing posterior thalamic neurons

Éva R. Szabó[1,2], Melinda Cservenák[1,2], Edina Udvari[2], Árpád Dobolyi[1,2]

[1]Laboratory of Neuromorphology, Department of Anatomy, Histology and Embryology, Semmelweis University, Budapest, Hungary

[2]Laboratory of Molecular and Systems Neurobiology, Institute of Biology, Eötvös Loránd University and the Hungarian Academy of Sciences, Budapest, Hungary

Amylin, a peptide previously known as a pancreatic hormone, was found to be expressed in the preoptic area of mother rats in our previous microarray study. The increase in mRNA expression was validated by RT-PCR and the appearance of the peptide was detected by immunohistochemistry. Amylin is not expressed in the brain before and during pregnancy but its significant increase was observed in rats and mice immediately after parturition in the preoptic area, the center of maternal behaviors. Amylin-positive neurons, in the medial preoptic nucleus, parts of the medial preoptic area, and the ventral part of the bed nucleus of the stria terminalis were activated by pup exposure in dams. Since our previous studies suggested that suckling effect on maternal motivation may be mediated by posterior thalamic neurons expressing tuberoinfundibular peptide of 39 residues (TIP39), we examined the relationship of amylin and TIP39. Fiber terminals containing TIP39 and the parathyroid hormone 2 receptor (PTH2 receptor; the receptor of TIP39) have the same distribution as amylin neurons in the preoptic area. TIP39 terminals closely apposed amylin neurons suggesting their innervation by TIP39 neurons. The maternal induction of amylin was markedly reduced in mice lacking the PTH2 receptor suggesting a functional relationship between amylin and TIP39. These results imply that amylin is a novel neuropeptide with maternal functions, and its maternal induction is driven by posterior thalamic TIP39-containing neurons that have been suggested to convey suckling information.

Support: Bolyai János Fellowship of the HAS, OTKA K100319 research grant, and the NAP_B Program.

The human thoracolumbar fascia: anatomy, histology and immunohistochemistry

Csaba Szigeti, András Mihály

Department of Anatomy, Histology and Embryology, University of Szeged, Szeged, Hungary

The thoracolumbar fascia (TLF) is a complex myofascial and aponeurotic girdle around the lower back, which stabilizes the lumbosacral spine. The TLF has significant role in maintaining posture, transmitting and balancing tension and shear force between the active muscle and passive bony compartments. It has strong connections with the superficial fascial layers in the lower limb, the abdomen and the thorax, thus building a complex biomechanical protecting system. The presence of SP, CGRP, PGP 9.5 and S-100 immunopositive signals and the numerous sympathetic vasomotor fibers in the TLF prove its dense sensory and autonomic innervation, respectively. Although the proprioceptive innervation of TLF is not fully determined yet, evidences show that reduced proprioception activity of the fascia results in increased pain sensitivity.

The present study utilized fixed cadavers, paraffin-plastinated TLF preparations in order to elucidate the fascia layers of the TLF. The intrafascial nerve endings were studied on fresh human tissue samples through silver impregnation and immunohistochemistry.

The role of septins in store operated Ca^{2+} entry (SOCE) during chondrogenesis of human mesenchymal stem cells (hMSC)

Roland Takács[1], Csaba Matta[1], Tamás Juhász[1], Judit Vágó[1], Csilla Szűcs[1], János Fodor[2], László Csernoch[2], Róza Zákány[1]

[1]Department of Anatomy, Histology and Embryology, Faculty of Medicine, University of Debrecen, Debrecen, Hungary
[2]Department of Physiology, Faculty of Medicine, University of Debrecen, Debrecen, Hungary

Septins belong to a highly conserved family of proteins in eukaryotes and are increasingly recognized as components of the cytoskeleton. All septins bind GTP and form hetero-oligomeric complexes and higher-order structures, including filaments and rings. Septins form plasmamembrane domains juxtaposed to the endoplasmic reticulum membrane punctae which are important in the STIM1-ORAI1 signalling. The knock down of certain septin types or the inhibition of their remodeling inhibits SOCE and related downstream events. Septins have no previously described role in chondrogenesis and their role in other differentiational processes is also sparsely described.

Previous results of our laboratory indicate that SOCE is necessary for chondrogenesis, therefore we aimed to link septin function to chondrogenesis.

Our studies were carried out in hMSC differentiated as high density cultures (HDC). We verified the expression of the SOCE-associated septin types and the components of SOCE at the mRNA and protein level. HDC were treated with the inhibitor of septin remodeling, forchlorfenuron. We performed transient gene silencing of the discussed septin types with an shRNA vector, examined SOCE functions using cells loaded with the calcium-sensitive dye Fura-2 with a set-up measuring single cell calcium levels. Eventually, we compared chondrogenesis in control to forchlorfenuron-treated cultures by chondrogenic marker analysis and histological stainings.

Our results demonstrate the link between SOCE and chondrogenic processes in hMSC. Our present findings, although further experiments are needed, provide a novel function of the septin protein family.

This work was sponsored by the grant GOP-1.1.1-11-2012-0197.

Determination of the essential number of motoneurons required to produce functionally useful hindlimb locomotion

Dénes Török[1], Zoltán Fekécs[1], László Gál[1,2], Antal Nógrádi[1]

[1]Laboratory of Neural Regeneration, Department of Anatomy, Embryology and Histology, Faculty of Medicine, University of Szeged, Szeged, Hungary
[2]Laboratory of Neuromuscular Plasticity, Nencki Institute of Experimental Biology PAS, Warsaw, Poland

An avulsion injury of one or more spinal ventral roots induces a critical loss of motoneurons followed by irreversible locomotor function impairment. Recent peripheral nerve surgery techniques result in the improvement of limb function, however, the question remains how many motoneurons are needed to achieve sufficient muscle reinnervation. The aim of this study was to determine the minimum motoneuron numbers, required to reinnervate the denervated muscles of the limb and produce a functionally useful locomotor pattern. In order to determine the threshold of satisfactory functional reinnervation we have developed a sensitive movement recording and analysis system as none of the commercially available methods/equipment were able to provide in-depth data about the motor pattern of the whole hind limb. Therefore we combined the use of video-based footprint and hind limb motion analyses to achieve a reliable assessment. Rats that underwent a lumbar 4-5 (L4-5) ventral root avulsion had their L4 ventral root reimplanted and received different doses of riluzole in order to rescue incremental numbers of the damaged motoneuron pool. Control animals received no treatment. Lateral and rear-view parameters of the hind limb movement pattern were evaluated by measuring specific joint angles, footprints and gait parameters in single video frames. Four months postoperatively we carried out retrograde tracing in order to label and count the reinnervating motoneurons. A correlation between the numbers of the reinnervating motoneurons and the functional improvement was made and a strong relationship between functional restoration of the original movement pattern and morphological reinnervation has been proven.

Immunohistochemistry of cerebellar seizures: mossy fiber afferents play important role in seizure spread and initiation in the rat

Zoltán Tóth[1], Gergely Molnár[1], András Mihály[1], Beáta Krisztin-Péva[1], Marietta Morvai[1], Zsolt Kopniczky[2]

[1]Department of Anatomy, Faculty of Medicine, University of Szeged, Szeged, Hungary
[2]Department of Neurosurgery, Faculty of Medicine, University of Szeged, Szeged, Hungary

Clinical reports suggest the participation of the cerebellum in epilepsy. Mossy fibers are the main excitatory afferents of the cerebellar cortex; most of them use glutamate and strongly excite granule cells through NMDA- and AMPA receptors. The role of the pontocerebellar mossy fibers in cerebellar neuronal hyperactivity was investigated in the present study. We detected neuronal hyperactivity through the expression of the glutamate induced c-fos protein, by means of immunohistochemistry and immunoblotting in the vermis and in the hemispheres. Generalized seizures were induced by means of intraperitoneal 4-aminopyridine injections. Following the 4-aminopyridine seizures, the c-fos expression of cerebellar granule cells was significantly elevated at 1.5 h in every lobule. Maximum c-fos expression was seen at 3 h. The role of the pontocerebellar mossy fiber afferents in the induction of c-fos expression was examined after the transection of the middle cerebellar peduncle on the left side. Immunohistochemical analysis 14 days after the surgery revealed that the synapsin I immunoreactivity was significantly reduced in the cerebellar cortex on the operated side, compared to the sham operated controls and to the non-operated cerebellar hemisphere of the operated animals; indicating the degeneration of mossy fiber terminals. Transection of the middle cerebellar peduncle suppressed cerebellar c-fos expression in the vermis and in the hemispheres significantly. These findings suggest the strong involvement of the middle cerebellar peduncle and the pontocerebellar mossy fibers in the pathophysiology of cerebellar epilepsy.

Early phenomena following cryogenic lesions of rat brain

László Tóth[1], Dávid Szöllősi[1], Katalin Kis-Petik[2], Erzsébet Oszwald[1], Mihály Kálmán[1]

[1]Department of Anatomy, Histology and Embryology, Semmelweis University, Budapest, Hungary
[2]Department of Biophysics and Radiation Biology, Semmelweis University, Budapest, Hungary

The cerebrovascular laminin becomes detectable following lesions, whereas the immunoreactivity of the lamina basalis-receptor beta-dystroglycan disappears. These alterations are supposed to be indirect markers of the *post-lesion* glio-vascular detachment which may have role in the impairment of blood-brain-barrier. The aim of the present study is to estimate the temporal and territorial correlations between the *post-lesion* exudation and the aforementioned phenomena.

Cryogenic lesions were performed in deep ketamine-xylazine anaesthesia with a copper rod cooled with dry ice. Immediately, or in 5 or 10 min brains were removed and immersed in buffered 4% paraformaldehyde, and immunohistochemical reactions were performed in floating sections. *Post-lesion* exudation due to blood-brain-barrier impairment was estimated with immunohistochemical detection of plasma-fibronectin and immunoglobulins. Gliovascular connections were investigated with immunohistochemistry (GFAP, S100, glutamine synthetase, and (applying perfusion) electron microscopy.

Laminin immunoreactivity appeared already at immediate fixation. Exudate was found around the laminin-immunopositive vessels but not in a confluent territory. B-dystroglycan was still detectable. At five-ten minutes the territory of exudate became confluent and dystroglycan disappeared. Some but not all vessels were free of astrocytes. Electron microscopy demonstrated wide perivascular spaces.

'In vivo' monitoring was attempted with a Femtonics Femto2D-Inverted multiphoton microscope in the Department of Biophysics of Semmelweis University. Astrocytes were labeled supravitally with sulforhodamine 101 smeared on the brain surface so some gliovascular connections were visible. However, within the investigated *post-lesion* period (20 min) no astrocyte motility was observed.

Unilateral labyrinthectomy modifies the tenascin-R expression in the perineuronal nets of the vestibular nuclei in the rat

Ildikó Wéber[1], Ágnes Magyar[3], Einar Örn Jóhannesson[1], Botond Gaál[1], Szilvia Kecskes[1], András Birinyi[1], Klara Matesz[1,2]

[1]Department of Anatomy, Histology and Embryology, University of Debrecen, Debrecen, Hungary
[2]MTA-DE Neuroscience Research Group, Debrecen, Hungary
[3]Department of Pediatrics, University of Debrecen, Debrecen, Hungary

The vestibular system or system of balance provides information about the motion, equilibrium, and spatial orientation of the body. Lesion of vestibular system results in various static and dynamic symptoms which are restored spontaneously during the vestibular compensation. Vestibular compensation involves multiple, parallel mechanisms in the vestibular nuclei and in various parts of vestibular networks. We have previously observed modification of hyaluronan and chondroitin sulfate proteoglycan expression in the perineuronal net (PNN) of the lateral vestibular nucleus (LVN) during the vestibular compensation suggesting the role of extracellular matrix in the compensatory mechanisms.

In the present work by using immunohistochemical method, we studied the modification of TN-R expression in the superior (SVN), medial (MVN), lateral (LVN), and descending (DVN) vestibular nuclei of the rat following UL. On the first postoperative day, the perineuronal nets (PNN) disappeared on the side of UL in the SVN, LVN, MVN, and rostral part of DVN. At survival day 3, the staining intensity of PNNs recovered in the operated side of the MVN, whereas they are restored by the time of seventh postoperative day in the SVN, LVN and rostral part of DVN. The staining intensity of TN-R reaction remained unchanged in the caudal part of DVN, bilaterally.

Our results showed that the UL is accompanied by the modification of TN-R staining pattern in the vestibular nuclei. The time course of re-establishment of PNN is being attained parallel to the improvement of vestibular symptoms.

Support: MTA-TKI 11008.

Diagnostic value of histological findings in cases of advanced putrefaction and autolysis

Roland Weiczner, Beáta Havasi, Réka Anita Tóth, Éva Kereszty

Department of Forensic Medicine, Faculty of Medicine, University of Szeged, Szeged, Hungary

Performing autopsies without available medical data in the cases of "unattended death" with advanced autolytic and putrefactive changes is not exceptional in the forensic pathology. The macroscopically inconclusive autopsies increase the significance of the supplementary diagnostics, not forgetting the relevance of good old routine pathohistology.

The myocardial scarring after ischaemia, the chronic congestive heart failure-related haemosiderin deposits in ghost remnants of macrophages, the lamellar fibroelastosis of muscular arteries suggesting hypertension or the hyalinised glomeruli in the kidney, altogether, if not accompanied by signs of external inflicts, may support the diagnosis of natural cardiovascular death *(Case #1: a male corpse found in his flat with running heating after at least four days)*. The multiplex myocardial scars with different age, signs of oedema and chronic congestion (haemosiderin deposits) in the lungs, the remnants of granulation tissue from organising pneumonia or the fatty degeneration of the liver could be decisive by demonstrating the medical history if such data would be later available *(Case #2: an unidentified female corpse found in the River Tisza)*.

The medical history, the circumstances of death, the time elapsed and the environment surrounding the body after death, largely influence the diagnostic value of histology. For corpses with unknown identity, the careful evaluation of "time-resistant" histological findings could even contribute to the personal identification. The histological specimens after processing for routine haematoxylin-eosin stained light microscopic slides can be surprisingly informative and sometimes even decisive, even if we are taken aback by the macroscopical appearance of the organs at first sight.

Secretagogin labels the noradrenergic axis in the rat brain stem

Péter Zahola[1,2], János Hanics[1,2], Alán Alpár[1,2]

[1]MTA-SE NAP-B Research Group of Experimetal Neuroanatomy and Developmental Biology, Hungarian Academy of Sciences, Budapest, Hungary;
[2]Department of Anatomy, Histology and Embryology, Semmelweis University, Budapest, Hungary

Secretagogin, a recently described calcium binding protein, has been identified in several organs including brain. Being a calcium sensor it is believed to regulate downstream cascades after a conformational change upon activation. Here, we show that secretagogin is present in the rat brainstem with a distinct distribution pattern largely concentrated in noradrenergic centres, especially locus coeruleus. Additionally, secretagogin-containing neurons were identified in rather heterogeneous fields including, but not restricted to, superior colliculus, dorsal nucleus of vagus, medial vestibular nucleus or interpeduncular nucleus. Tyrosine hydroxylase-containing neurons typically co-expressed secretagogin both in their somata and axonal fibres. In stress, secretagogin and tyrosine hydroxylase levels in brain stem samples elevated in parallel as shown by select brain stem serial section- or micropunch-technique based protein analysis. Knock-down of secretagogin expression using small interfering RNA in primary neuronal brain stem cultures resulted in reduced tyrosine hydroxylase expression. We suggest that secretagogin is a useful neurochemical marker to identify neuronal subsets in the mammalian brain stem and could play a role in stress reactions.

Case presentation: Six-year-old child with schizencephaly

Tamás Zombori[1] Kitti Brinyiczki[1], Adrienn Máté[2], László Sztriha[2], László Kaiser[1], István Bódi[3]

[1]Department of Pathology, Faculty of Medicine, University of Szeged, Szeged, Hungary
[2]Paediatric Clinic, Faculty of Medicine, University of Szeged, Szeged, Hungary
[3]Clinical Neuropathology Department, King's College Hospital NHS Foundation Trust, London, UK

Childhood epileptic conditions, based on the patophysiological mechanisms, can be classified into three main groups:

(a) The cause of epilepsy is well characterised, it is definitive;

(b) The cause is not known, however there is a high suspicion of certain background condition;

(c) The cause is entirely unknown.

Based on the above criteria, (a) symptomatic, (b) cryptogenic and (c) idiopathic epileptic groups can be identified.

Due to the development of diagnostic methods, there is an increased proportion of diagnosed neonatal and childhood symptomatic epilepsy cases, mainly those which are attributable to developmental defects. Focal cortical dysplasia, the cortical dysgenesis and the impaired developmental migratory conditions are more frequently diagnosed, due to diagnostic improvements. In our case report, we present the morphological findings of a patient, suffering from schizencephaly.

Bilateral schizencephaly with microcephaly is a severe psychomotor retardation with spastic tetraparesis. Unilateral schizencephaly is dominated by impaired motor function with one sided disability and spastic hemiparesis. Clinical symptoms show a wide range of variation. Unilateral schizencephaly is frequently diagnosed when an epileptic focus is looked for. The most important differential diagnostic condition is porencephaly, where loss of brain parenchyma is due to a previous damage, most commonly due to vascular damage during the third trimester. It should be emphasized that in porencephaly the noxa affects the brain after the neuronal migration has already ceased, there is no glia reaction in the immature brain. Porencephaly is usually associated with sever neurological and mental impairment.